คุณลักษณะและสมบัติของตัวเร่งปฏิกิริยาแพลทินัมบนตัวรองรับไทเทเนียที่เติมไนโตรเจนในปฏิกิริยาไฮโดรจิเนชันแบบเลือกเกิดของสามไนโตรสไตรีน

นายกัมปนาท นุตทะบัติ

จุฬาลงกรณ์มหาวิทยาลัย
Chulalongkorn University

บทคัดย่อและแฟ้มข้อมูลฉบับเต็มของวิทยานิพนธ์ตั้งแต่ปีการศึกษา 2554 ที่ให้บริการในคลังปัญญาจุฬาฯ (CUIR)
เป็นแฟ้มข้อมูลของนิสิตเจ้าของวิทยานิพนธ์ ที่ส่งผ่านทางบัณฑิตวิทยาลัย
The abstract and full text of theses from the academic year 2011 in Chulalongkorn University Intellectual Repository (CUIR)
are the thesis authors' files submitted through the University Graduate School.

วิทยานิพนธ์นี้เป็นส่วนหนึ่งของการศึกษาตามหลักสูตรปริญญาวิศวกรรมศาสตรมหาบัณฑิต
สาขาวิชาวิศวกรรมเคมี ภาควิชาวิศวกรรมเคมี
คณะวิศวกรรมศาสตร์ จุฬาลงกรณ์มหาวิทยาลัย
ปีการศึกษา 2558
ลิขสิทธิ์ของจุฬาลงกรณ์มหาวิทยาลัย

CHARACTERISTICS AND CATALYTIC PROPERTIES OF Pt/N-DOPED TiO_2 IN THE LIQUID-PHASE SELECTIVE HYDROGENATION OF 3-NITROSTYRENE

Mr. Kampanat Nuttabut

A Thesis Submitted in Partial Fulfillment of the Requirements
for the Degree of Master of Engineering Program in Chemical Engineering
Department of Chemical Engineering
Faculty of Engineering
Chulalongkorn University
Academic Year 2015

Copyright of Chulalongkorn University

Thesis Title	CHARACTERISTICS AND CATALYTIC PROPERTIES OF Pt/N-DOPED TiO_2 IN THE LIQUID-PHASE SELECTIVE HYDROGENATION OF 3-NITROSTYRENE
By	Mr. Kampanat Nuttabut
Field of Study	Chemical Engineering
Thesis Advisor	Associate Professor Joongjai Panpranot, Ph.D.

Accepted by the Faculty of Engineering, Chulalongkorn University in Partial Fulfillment of the Requirements for the Master's Degree

.....Dean of the Faculty of Engineering

(Professor Bundhit Eua-arporn, Ph.D.)

THESIS COMMITTEE

.....Chairman

(Associate Professor Bunjerd Jongsomjit, Ph.D.)

.....Thesis Advisor

(Associate Professor Joongjai Panpranot, Ph.D.)

.....Examiner

(Chutimon Satirapipathkul, D.Eng.)

.....External Examiner

(Assistant Professor Okorn Mekasuwandumrong, D.Eng.)

กัมปนาท นุตทะบัติ : คุณลักษณะและสมบัติของตัวเร่งปฏิกิริยาแพลทินัมบนตัวรองรับไทเทเนียที่เติมไนโตรเจนในปฏิกิริยาไฮโดรจิเนชันแบบเลือกเกิดของสามไนโตรสไตรีน (CHARACTERISTICS AND CATALYTIC PROPERTIES OF Pt/N-DOPED TiO_2 IN THE LIQUID-PHASE SELECTIVE HYDROGENATION OF 3-NITROSTYRENE) อ.ที่ปรึกษาวิทยานิพนธ์หลัก: รศ. ดร. จูงใจ ปั้นประณต, 99 หน้า.

เตรียมไทเทเนียมไดออกไซด์ด้วยวิธีโซลโวเทอร์มอลและดัดแปรด้วยนอร์มอลเมทิลไพโรลิโดน (NMP) นำไทเทเนียที่ดัดแปรด้วยสารประกอบไนโตรเจน ไปใช้เป็นตัวรองรับตัวเร่งปฏิกิริยาแพลทินัม และทดสอบในปฏิกิริยาไฮโดรจิเนชันแบบเลือกเกิดของสามไนโตรสไตรีนเป็นสามไวนิลอนิลีน ภายใต้ความดันไฮโดรเจน 2 เมกะปาสคาล และ อุณหภูมิ 40 องศาเซลเซียส วิเคราะห์คุณลักษณะของตังเร่งปฏิกิริยาด้วยเทคนิคการกระเจิงรังสีเอ็กซ์ การดูดซับทางกายภาพด้วยแก๊สไนโตรเจน เอ็กซเรย์โฟโตอิเล็กตรอนสเปกโตรสโกปี ฟูเรียร์ทรานฟอร์มอินฟราเรดสเปกโตรสโกปี ยูวี-วิสิเบิลสเปกโตรโฟโตมิเตอร์ กล้องจุลทรรศน์อิเล็กตรอนแบบส่องผ่าน รีดักชันของไฮโดรเจนด้วยการโปรแกรมอุณหภูมิ อินฟราเรดสเปกโตรสโกปีของการดูดซับด้วยแก๊สคาร์บอนมอนอกไซด์ และการดูดซับทางเคมีด้วยแก๊สคาร์บอนมอนอกไซด์ ตัวเร่งปฏิกิริยาแพลทินัมบนตัวรองรับไทเทเนียที่เติมไนโตรเจน ด้วยวิธีโซลโวเทอร์มอล ในอัตราส่วนไนโตรเจนต่อไทเทเนียเท่ากับ 0.1 ให้ค่าร้อยละผลได้ของสามไวนิลอนิลีนสูงที่สุด ที่ร้อยละ 86 ภายใต้สภาวะที่กำหนด ซึ่งเป็นผลมาจากอันตรกิริยาที่แข็งแรงระหว่างโลหะแพลทินัมและตัวรองรับ นอกจากนี้การมีไนโตรเจนอยู่บนตัวเร่งปฏิกิริยาอาจช่วยส่งเสริมปฏิกิริยาเกิดไฮโดรจิเนชันของหมู่ไนโตรผ่านการถ่ายทอดอิเล็กตรอนจากตัวรองรับที่เติมไนโตรเจนไปยังโลหะแพลทินัมอีกด้วย

จุฬาลงกรณ์มหาวิทยาลัย
Chulalongkorn University

ภาควิชา วิศวกรรมเคมี ลายมือชื่อนิสิต .....

สาขาวิชา วิศวกรรมเคมี ลายมือชื่อ อ.ที่ปรึกษาหลัก .....

ปีการศึกษา 2558

5670119521 : MAJOR CHEMICAL ENGINEERING

KEYWORDS: LIQUID PHASE SELECTIVE HYDROGENATION, 3-NITROSTYRENE, SOLVOTHERMAL, IMPREGNATION, PLATINUM CATALYST, N-DOPED TITANIA

KAMPANAT NUTTABUT: CHARACTERISTICS AND CATALYTIC PROPERTIES OF Pt/N-DOPED TiO_2 IN THE LIQUID-PHASE SELECTIVE HYDROGENATION OF 3-NITROSTYRENE. ADVISOR: ASSOC. PROF. JOONGJAI PANPRANOT, Ph.D., 99 pp.

The titanium dioxide (TiO_2) was prepared by the solvothermal (SV) and modified with N-metylpyrolidone (NMP). The N-doped TiO_2 was used as the supports for preparation of Pt/TiO_2 catalysts. The catalytic performances were investigated in the liquid-phase selective hydrogenation of 3-nitrostyrene (NS) to 3-vinylaniline at H_2 pressure 2 MPa and 40 ^{o}C. The catalysts and supports were characterized by X-ray diffraction (XRD), N_2 physisorption, X-ray photoelectron spectroscopy (XPS), Fourier transform infrared spectroscopy (FT-IR), temperature program reduction (TPR), UV-visible spectrophotometer (UV-vis), infrared spectroscopy of adsorbed CO (CO-IR), CO chemisorption, and transmission electron microscopy (TEM). The highest yield of vinyl aniline (86%) was obtained over the Pt/0.1N(SV)-TiO_2 under the conditions used and was attributed to the stronger metal-support interaction. In addition, the N-doped TiO_2 supported Pt catalyst may promote the hydrogenation of the NO_2 group via electron transfer from N-doped TiO_2 to Pt metal.

จุฬาลงกรณ์มหาวิทยาลัย
Chulalongkorn University

Department: Chemical Engineering Student's Signature .....

Field of Study: Chemical Engineering Advisor's Signature .....

Academic Year: 2015

ACKNOWLEDGEMENTS

This thesis was absolutely completed with the kindness and thesis would not have been completed without all the support from my thesis advisor, Assoc. Prof. Dr. Joongjai Panpranot by her help, teaching, and advice. I would like to sincere thanks to her throughout the duration of this research.

I would like to grateful for my committee members, Associate Professor Dr. Bunjerd Jongsomjit as the chairman, Dr. Chutimon Satirapipathkul as the examiner, and Assistant Professor Dr. Okorn Mekasuwandumrong as the external examiner, for comments and suggestions in my thesis. And finally, this research was financial supported from the Thailand Research Fund (BRG5780010-Joongjai Panpranot) are gratefully acknowledged.

จุฬาลงกรณ์มหาวิทยาลัย
Chulalongkorn University

CONTENTS

Page

จุฬาลงกรณ์มหาวิทยาลัย
CHULALONGKORN UNIVERSITY

Page

จุฬาลงกรณ์มหาวิทยาลัย
CHULALONGKORN UNIVERSITY

Page

CHAPTER 1

INTRODUCTION

1.1 Motivation

Liquid phase selective hydrogenation of nitro group in aminostyrene produces important intermediates in many industrial for pharmaceuticals, herbicides, and other fine chemicals. Heterogeneous catalyst development is necessary for this reaction. Recently, Pt and Au supported on TiO_2 have been employed in the liquid phase selective nitro styrene hydrogenation and high conversion (100%) and selectivity (89%-100%) can be obtained [1-5]. Yoshida et al. [6] synthesized Pt supported on TiO_2 by impregnation method. Complete conversion of nitrostyrene was achieved to 100% with low VA selectivity. The pressurization with CO_2 resulted in the decrease in hydrogenation rate. Matthias, J.B. et al. [7] used different supported platinum catalysts for the liquid phase selective hydrogenation. TiO_2 was found to improve the selectivity and reaction rate compared to the other supports. Furukawa S. et al. [8] presented Pd- and Rh-Based intermetallic compounds for the liquid phase selective hydrogenation of nitrostyrene. The addition of metal element with higher electronegativity provides polar sites and enhances the activation hydrogen donor, resulting in an improved the yield of aminostyrene.

Titanium dioxide (TiO_2) is one of the most frequently used supports that promoted active metal for hydrogenation reaction. TiO_2 exhibited a strong metal-support interaction (SMSI) with group VIII noble metals. The SMSI effect has shown to affect the rate of reaction and led to hydrogenation of NO_2 group to amine [7]. Comsup et al. [9, 10] synthesized TiO_2 by solvothermal method with controlled particle size and found that dispersion of metal (Ag/TiO_2) increased by doping Ag on TiO_2. $Pt/N\text{-}TiO_2$ was synthesized for photocatalytic reaction. The photocatalytic activities were improved. N-doped TiO_2 was led to generation electron–hole pairs and the photogenerated conduction band electrons can transfer to electron acceptor, H^+. Pt on N-doped TiO_2 can rapidly traps electrons and hydrogen can be produced [11-14].

จุฬาลงกรณ์มหาวิทยาลัย
CHULALONGKORN UNIVERSITY

In this work, Pt/TiO_2 catalysts were synthesized by incipient wetness impregnation method for the liquid phase selective hydrogenation of 3-nitrostyrene. N-doped TiO_2 was prepared by solvothermal synthesis and impregnation method. The effects of preparation methods and N-doped TiO_2 on the properties of Pt/N- TiO_2 catalysts were investigated by means of several characterization techniques.

1.2 Research objectives

To investigate the characteristics and catalytic properties of the N-doped TiO_2 supported Pt catalysts in the liquid-phase selective hydrogenation of 3-aminostyrene to 3-vinylaniline.

1.3 Research scopes

1) Synthesis of the TiO_2 supports by using the solvothermal method.

2) Synthesis of the N-doped TiO_2 supports by using various amounts of NMP solution as the nitrogen source using solvothermal and incipient wetness impregnation methods.

3) Synthesis of the Pt/TiO_2 and the Pt/N-doped TiO_2 catalysts by using the wet impregnation method withan aqueous solution of 0.5% wt$H_2PtCl_6H_2O$.

4) Catalyst calcination in air at 300°C for 2 h and followed by reduction in H_2 flow at different temperatures 200°C.

6) Reaction study of the Pt/TiO_2 and the Pt/N-doped TiO_2 catalysts in the liquid-phase selective hydrogenation of 3-aminostyrene to 3-vinylaniline by using the stirred batch reactor under H_2 pressure of 4 MPa and temperature of 40°C for 5, 10, 20, 40 and 60 min.

จุฬาลงกรณ์มหาวิทยาลัย
Chulalongkorn University

7) Characterization of the TiO_2 support, the N-doped TiO_2 supports, the Pt/TiO_2 and the Pt/N-doped TiO_2 catalysts by using various techniques:

- X-ray diffraction (XRD)
- N_2 physisorption
- X-ray photoelectron spectroscopy (XPS)
- UV-vis spectrophotometer (UV-vis)
- Fourier transform infrared spectroscopy (FT-IR)
- Transmission electron microscopy (TEM)
- CO chemisorptions
- H_2 temperature program reduction
- Infrared spectroscopy of adsorbed CO (CO-IR)

จุฬาลงกรณ์มหาวิทยาลัย
Chulalongkorn University

1.4 Research methodology

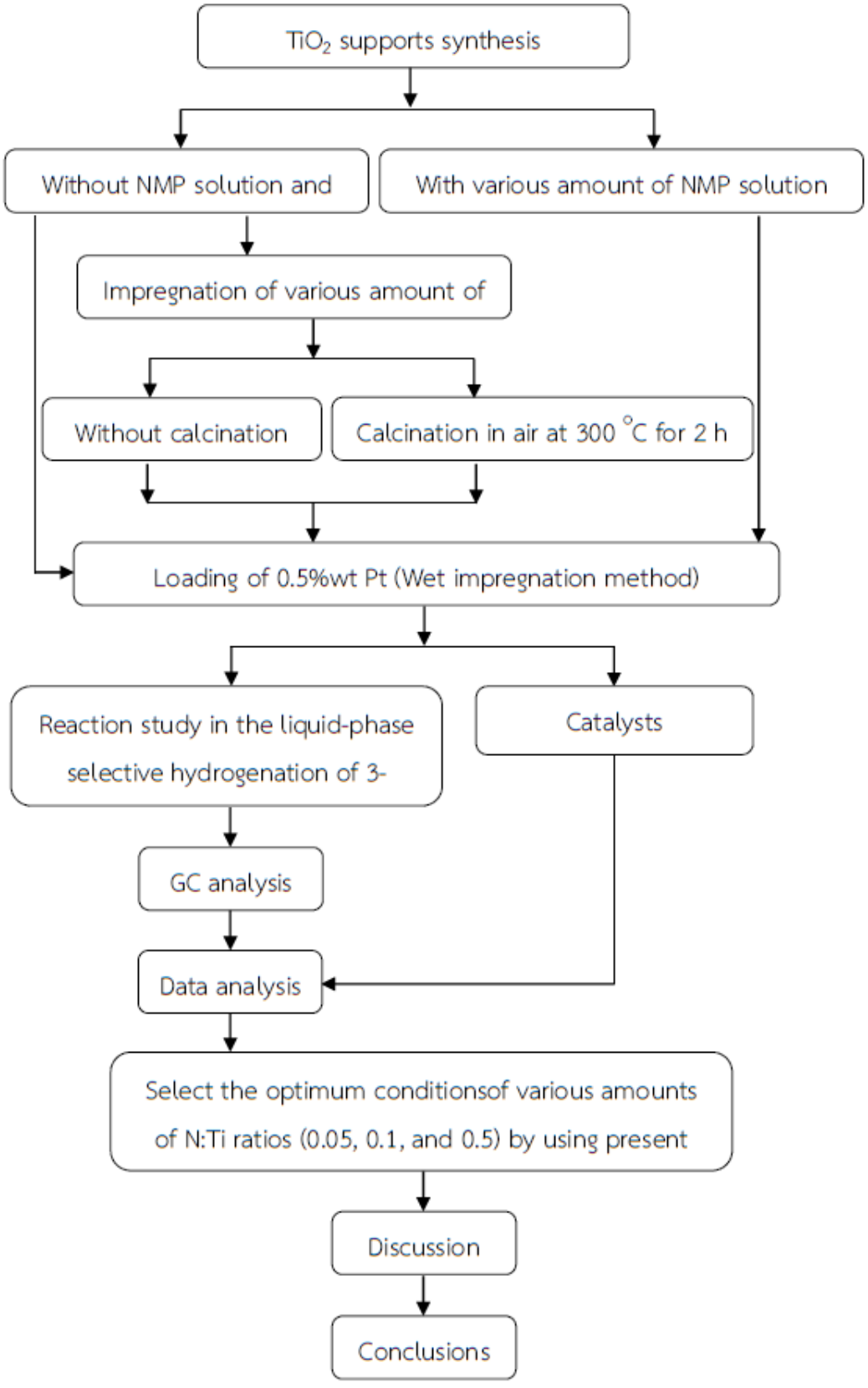

CHAPTER 2

THEORY

In this chapter, the necessary information of preparation of catalyst for liquid phase selective hydrogenation such as solvothermal method, incipient wetness impregnation method, path way of reaction, catalyst metal and support, and Nitrogen doping are provided.

2.1 Titanium dioxide (TiO_2)

Titanium dioxide or titania is occurring oxide of titanium. Its chemical formula is TiO_2 and has been used in heterogeneous catalysis such as white pigment, corrosion protective coating, especially catalyst support (increase catalyst surface area, interactions between the catalyst, TiO_2 lead to changes in reactivity and selectivity, and change in catalytic properties has been attributed to the strong-metal support interaction effect (SMSI)) [15] and photocatalysts (TiO_2 can carry out hydrolysis and generate electricity when transparent and under the influence of light) as a famous application and it is an improvement for catalytic reaction, which is the main driving force for surface investigations on titanium dioxide. The crystalline structures are consisting of three major crystalline structures as anatase (tetragonal), rutile (tetragonal) and brookite (orthorhombic). Their crystalline structures are illustrated in **Figure 2.1** andproperties of rutile, anatase and brookite $TiO_2$are shown in **Table 2.1.** Rutile is the most thermally stability form. Anatase and brookite tend to be more stable at lower temperatures and they transformed to rutile with upon heating [16-19].

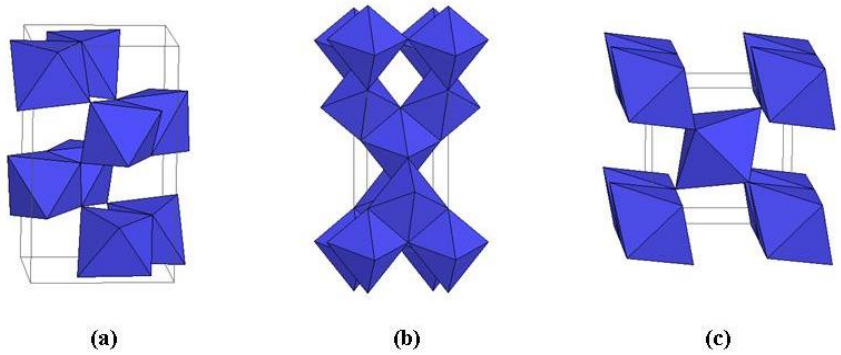

Figure2. 1 Crystal structures of (a) anatase, (b) brookite, and (c) rutile

Table 2.1 Properties of the three main polymorphs of TiO_2 (anatase), rutile, and brookite)

Crystal structure	System	Density (kg/m^3)	Lattice parameters (nm)				Band gap (eV)
			a	b	c	c/a	
Rutile	Tetragonal	4240	0.4584	-	0.2953	0.644	3.05
Anatase	Tetragonal	3830	0.3733	-	0.937	2.51	3.26
Brookite	Rhombohedral	4170	0.5436	0.9166	-	0.944	-

However, the physical and chemical properties of titanium dioxide such as the crystal structure, particle size, morphology, and properties are dependent on the preparation methods which including of hydrothermal, Sol-gel, Chemical vapor deposition and physical vapour, Solvothermal, Electrochemical approaches, Solution combustion, Microemulsion technique, Micelle and inverse micelle, and Sonochemical reactions [16, 17, 20-22].

2.2 Nitrogen doping

Non-metal doped TiO_2 has been used as a catalyst for many reactions and improved to be an effective approach to adsorption of TiO_2 such as N, C, F and S which N-doped TiO_2 has been decreased band gap energy of TiO_2 when compared with pure TiO_2antase phase. Especially in photocatalytic reaction, non-metal doped was extended the light adsorption of TiO_2 toward to the visible light region and increase photocatalytic activity. N-doped TiO_2 has two main advantages: first, it was increased the cystallinity, increased electric field formation, and promoting electron transfer. Second, N-doped TiO_2 was formed new band gap energy from localized of N2p states to the conduction band of TiO_2 [18, 23-26]. It would be improved rate of photogenerated electron-hole pairs which shown in **Figure 2.2**.

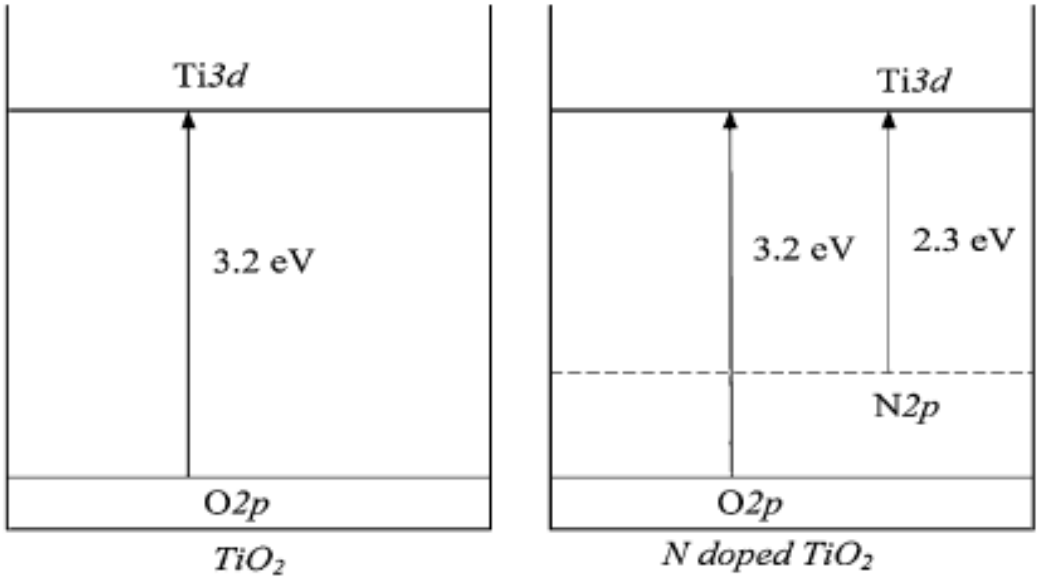

Figure 2.2 Proposed band structure of pure and nitrogen doped TiO_2.

2.3 Hydrogenation reaction

Selective hydrogenation of a C=C double bond and nitro group (NO_2) is an addition of hydrogen to a carbon-carbon double bond or N=O double bond in order to produce nitro group product. The simplest source of two hydrogen atoms is molecular hydrogen (H_2), but mixing nitrostyrene with hydrogen does not result in any discernible reaction. However, a careful hydrogenation proceeds is very rapidly hydrogenated to a nitro group product. Although the overall hydrogenation reaction is exothermic, high activation energy prevents it from taking place under normal conditions. This restriction may be circumvented by the use of a catalyst, as shown in the following diagram [3, 6, 27, 28].

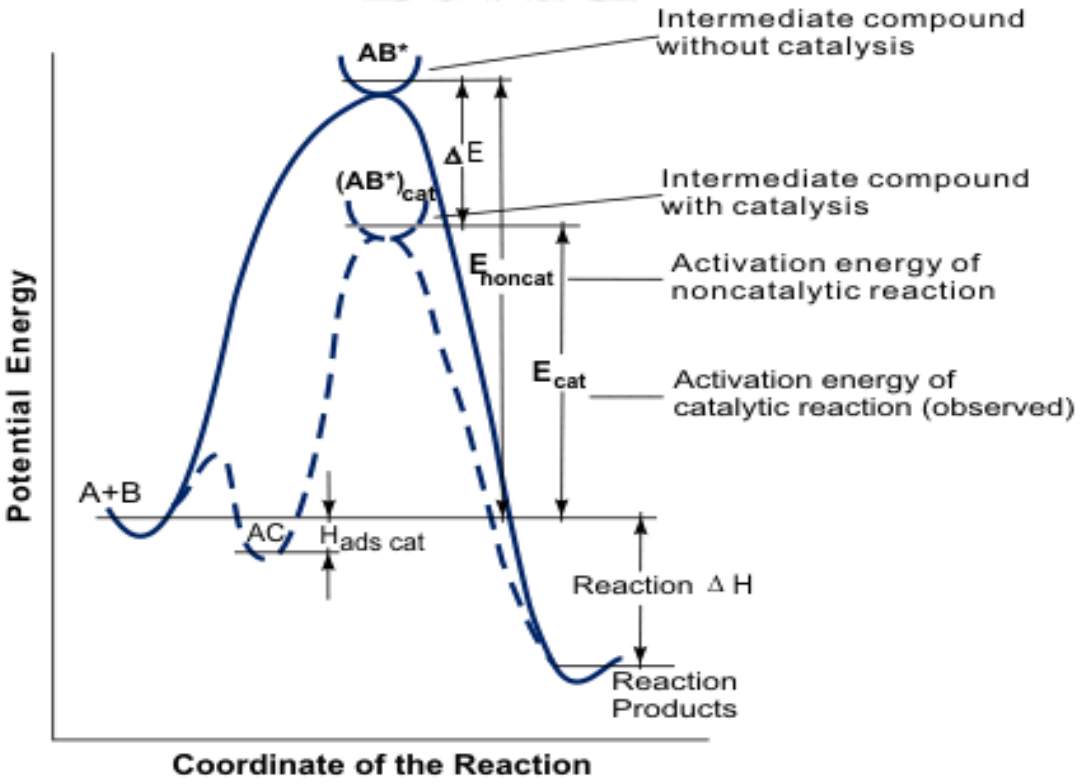

Figure 2.3 Potential energy profiles for with catalysis and without catalysis reactions [4, 29]

Platinum metal has been used as a conventional active metal in liquid phase selective hydrogenation of nitroaromatic compounds by promoting or using as a co-catalyst and bimetallic with other metal such as Pd, Au, Zn and Rh. Preparation of Pt catalysts have been reported. And it was doped on TiO_2, SiO_2, Al_2O_3, MgO, carbon and polymer. For examples: impregnation, deposition-precipitation, colloid deposition, embedded during polymerization, and ionic liquid method [2-10, 27-30].

In this research, liquid phase selective hydrogenation of nitrostyrene is an important in intermediates production for pharmaceuticals, find chemical, pigments, and dyes [31]. Hydrogenation is the addition of hydrogen to two functional groups as a C=C double bond and nitro group (NO_2) are flowing at **Figure 2.2** and show in the mechanism. Reaction path way of 3-nitrostyrene can be produced tree main products as a vinilaniline or aminostyrene (VA or AS), ethylnitrobenzene (ENB), and ethylaniline (EA). VA and ENB are formed simultaneously in reaction and then both of products will be EA. The mechanism of a C=C double bond in reaction can be described in four steps [4, 5, 7, 29, 32] :

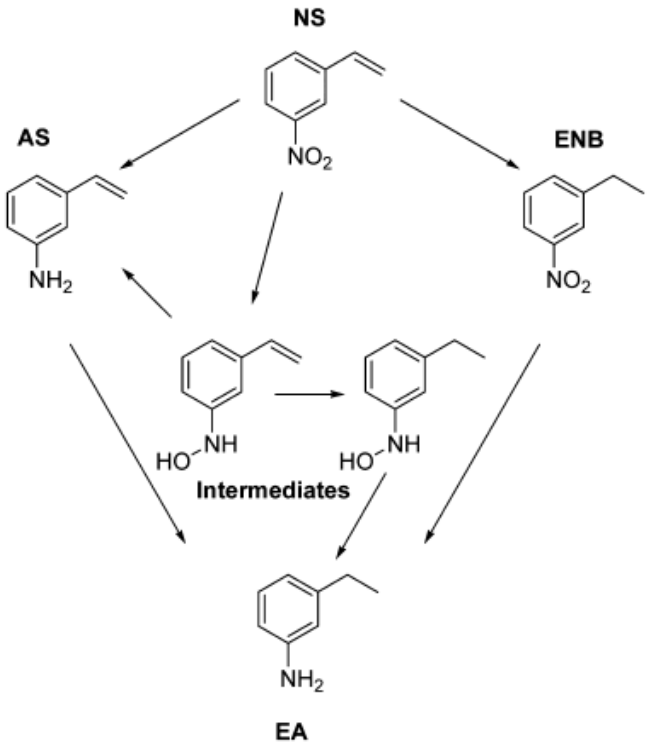

Figure 2.4 Hydrogenation pathway of 3-nitrostyrene based on the C=C bond or the NO_2 group hydrogenation [7]

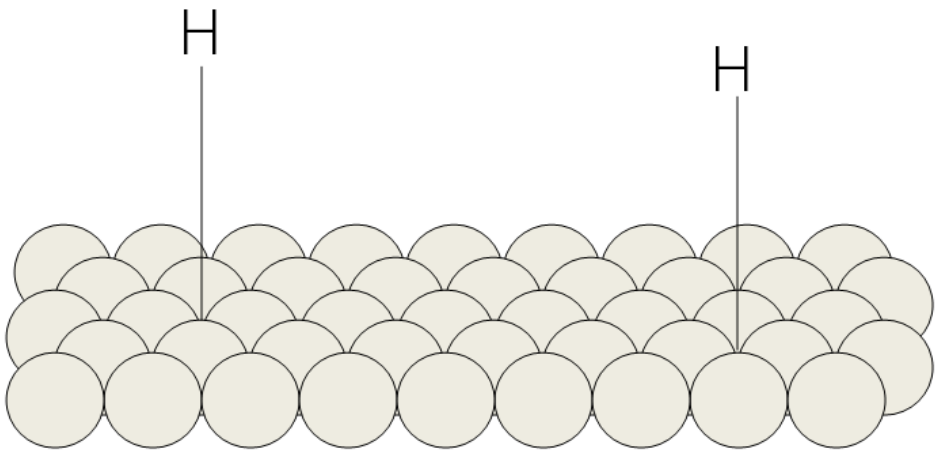

Step 1: Hydrogen molecules react with the metal atoms at the catalyst surface. The relatively strong H-H sigma bond is broken and replaced with two weak metal-H bonds.

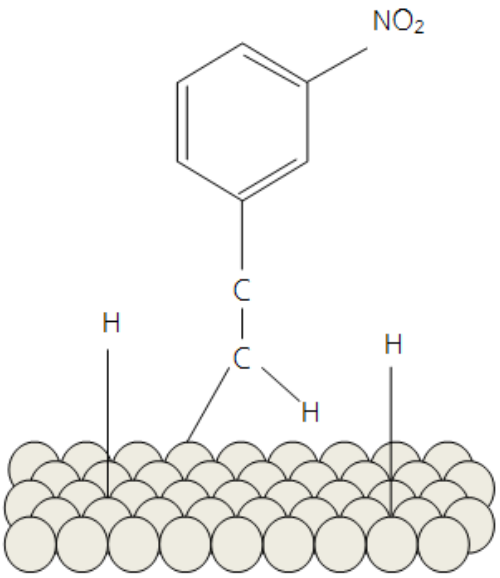

Step 2: The pi bond of a C=C double bond interacts with the metal catalyst weakening the bond. A hydrogen atom is transferred from the catalyst surface to one of the carbons of the double bond.

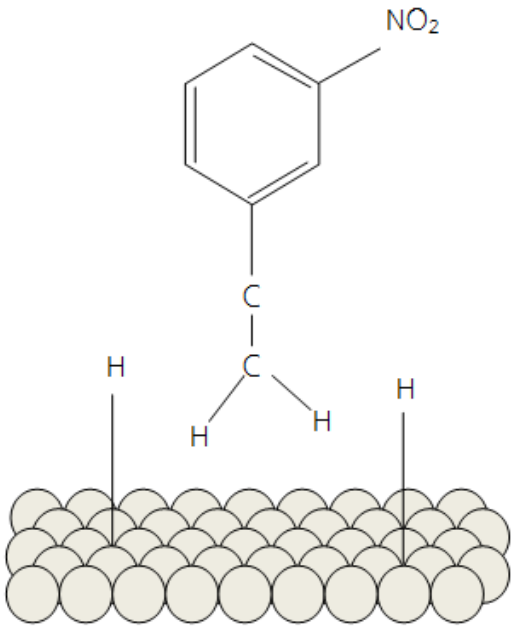

Step 3: The pi bond of a C=C double bond interacts with the metal catalyst weakening the bond. A second hydrogen atom is transferred from the catalyst surface forming nitrostyrene product.

Step 4: A C=C double bond is released from the catalyst's surface allowing the catalyst to accept additional hydrogen and ethylnitrobenzene molecules.

จุฬาลงกรณ์มหาวิทยาลัย

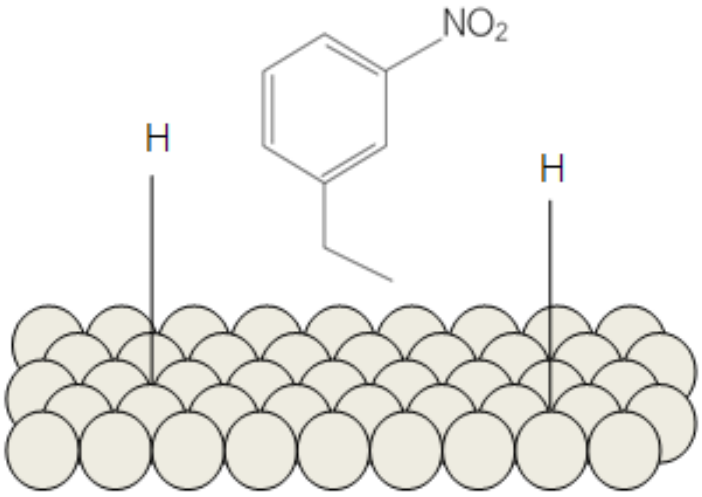

Step 4: A C=C double bond is released from the catalyst's surface allowing the catalyst to accept additional hydrogen and ethylnitrobenzene molecules.

The mechanism of a nitro group (NO_2) in reaction can be described in five steps:

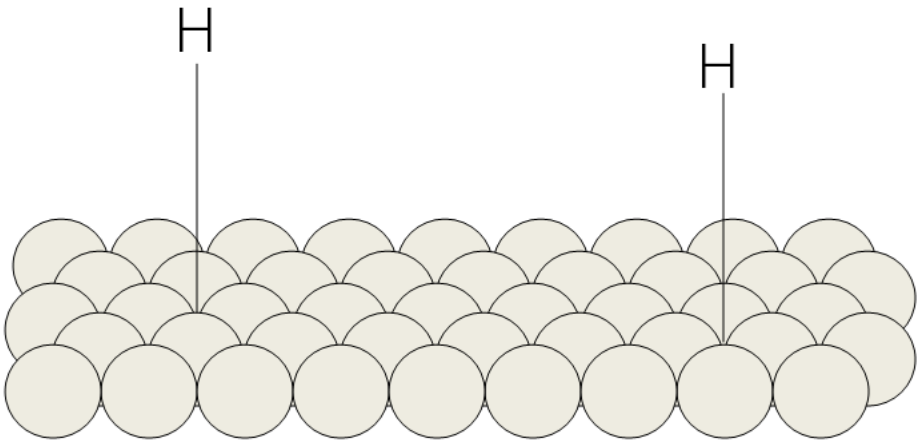

Step 1: Hydrogen molecules react with the metal atoms at the catalyst surface. The relatively strong H-H sigma bond is broken and replaced with two weak metal-H bonds.

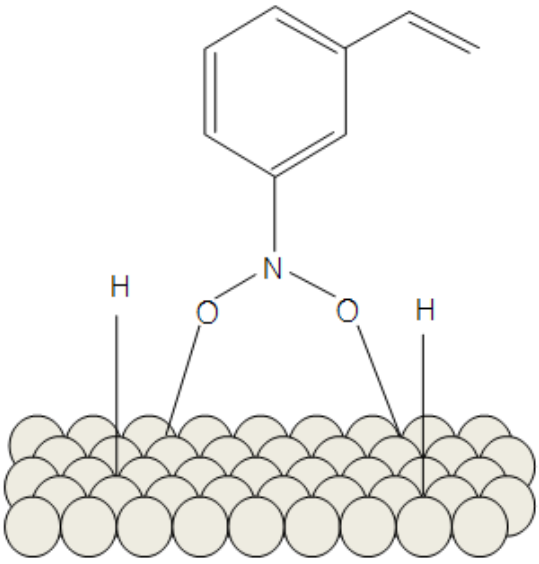

Step 2: A nitro groupinteracts with the metal catalyst weakening the bond as a nitrostyrene adsorbed on metal catalyst

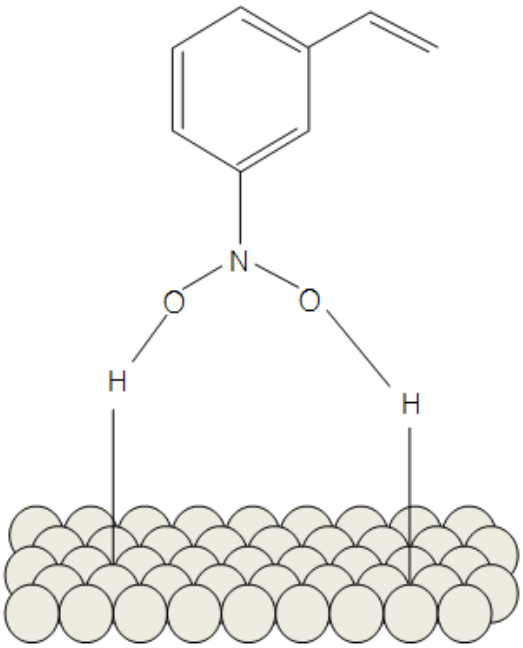

Step 3: A hydrogen atom is transferred from the catalyst surface to one of the N=O double bond and interacts with the metal catalyst weakening the bond. Hydrogen atom and hydrogen species ($H^{\delta-}$) on metal atom were release an electron through nitro group to support.

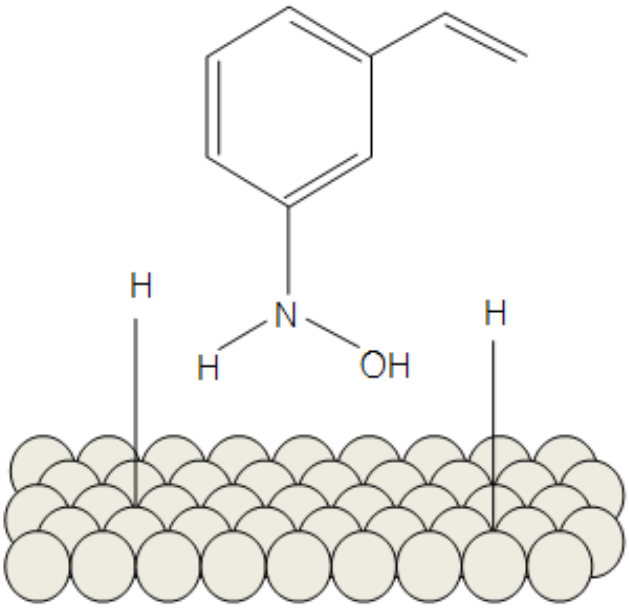

Step 4: A second hydrogen atom is interact with the catalyst surface. Then oxygen atom is interacting with hydrogen atom forming water and reactants on the catalyst surface become intermediate species.

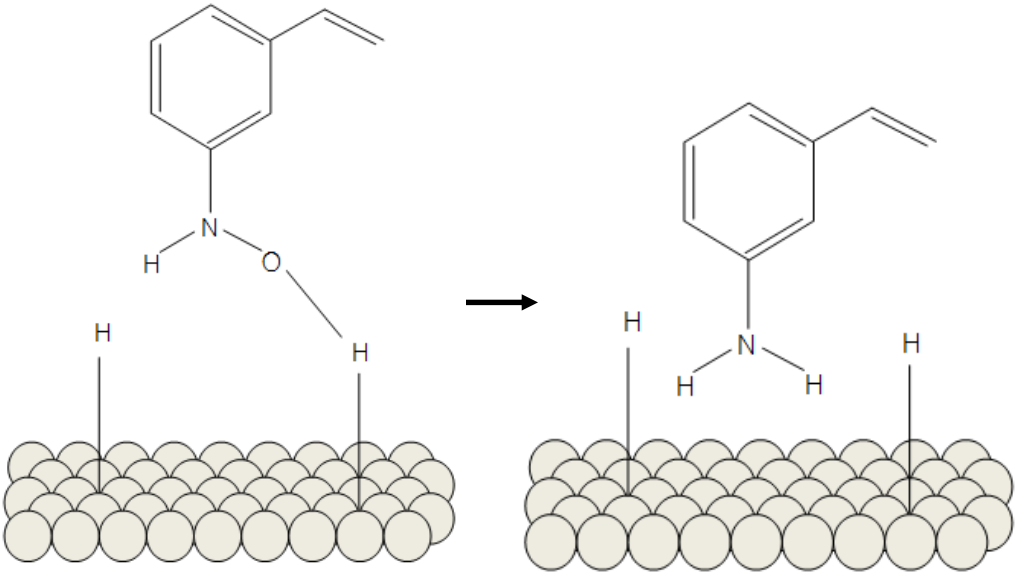

Step 5: Oxygen atom on intermediate species is interact hydrogen atom on the catalyst surface and electron transfer from metal to support. Vinylaniline was formed.

จุฬาลงกรณ์มหาวิทยาลัย
Chulalongkorn University

CHAPTER 3

LITERATURE REVIEWS

Pt/N-doped TiO_2 catalysts were used in liquid phase hydrogenation of 3-nitrostyrene to vinylaniline. Platinum metal was used as active metal on the catalyst support. Non-metal based promoter, nitrogen (N), was promoted on TiO_2 and it improved particle properties of the TiO_2 such as band gap energy and enhanced electron transfer. Therefore, the synthesis method and characterization of these Pt/N-doped TiO_2 catalysts for selective in reaction are important to be studied.

3.1 Selective hydrogenation of nitrostyrene using different catalysts

Boronat, M., et al (2007) reported that Au/TiO_2 had higher liquid phase hydrogenation of nitroaromatics activity than Pt/TiO_2 and Pd/TiO_2 but Pt metal showed activity for liquid phase the C=C hydrogenation. The supported gold catalysts catalyzed the liquid phase selective hydrogenation of 3-nitrostyrene. TiO_2 support showed higher activity (98% conversion and 96% selectivity of vinylaniline in 6 h.) than other support. Metal oxides such as TiO_2 and Fe_2O_3 enhanced role of reducing the nitro group which cannot be in inert support (SiO_2 or C). In present of H_2 dissociated on gold while nitrostyrene was weakly adsorbed on metallic [1].

Serna, P., et al (2009) studied kinetic model and synthesized gold catalyst by deposition precipitation. The catalytic tests for the hydrogenation of 3-nitrostyrene using different Au and Pt catalysts show that 0.2% Pt/TiO_2 exhibited the best catalytic activity (95% conversion and 70% vinylaniline selectivity) at0.25 h but in a long time (6 h) 1.5% Au/TiO_2 showed highest activity (98.5% conversion and 96% vinylaniline selectivity). While bimetallic Au and Pt were synthesized and used in reaction, catalytic activity was very excellent to 94% conversion and 93% vinylanilineselectivity by 0.52 h. And then increasing Pt loading, affected to increase 3-nitrostyrene hydrogenation and Pt metal can be improved the H_2 dissociation on metal support [4].

Shimizu, K., et al (2009) showed the use of supported Au nanoparticles (NPs) prepared by colloid deposition method for chemoselective reduction of a nitro group of substituted nitroaromatics by H_2. The Au/Al_2O_3 catalyst with Au particle size of 2.5 nm selectively hydrogenates a nitro group in the presence of various other reducible functional groups, and it shows higher intrinsic activity than the state-of-the-art catalyst (Au NPs on TiO_2). The rate of reaction and selectivity of Au/Al_2O_3 were closed to Au/TiO_2. The Au/TiO_2behaviour was explained by H_2 dissociated occurring on low coordinated at corner or edges Au atom and nitrostyrene was adsorbed the oxide surface between Au and TiO_2 through the nitro group. For the hydrogenation of C=C or C=N with catalyst, H_2 addition to produced H^+ and H^- in a OH or NH ligand and metal, respectively. The H^+/H^- pair transferred to the polar bonds and released an electron from support to metal [5].

Shimizu, K., et al (2010) showed that the silver clusters on θ-Al_2O_3 prepared by impregnation method, were a catalytic to highly chemoselective reduction of a nitro group for the reduction of substituted nitroaromatics and proposed mechanism of interaction substrate with catalyst support to electron transfer. Cooperation of the acid–base pair site on Al_2O_3 and the unsaturated Ag sites on the silver cluster was responsible for the rate-limiting H_2 dissociation to yield of H^+/H^- pair at metal/support interface, while the basic site on Al_2O_3 acts as an adsorption site of nitroaromatics. High chemoselectivity can be attributed to a preferential transfer of H^+/H^- to the polar bonds in the nitro group [32].

Serna, P., et al (2011) studied the deposition–precipitation of Au/TiO_2 catalyst for hydrogenation of 3-nitrostyrene. The results show the relationship between the activities of Au/TiO_2 in reaction and the concentration of low coordinated Au site with H_2 dissociation. While increased amount of Au atom, it affected to decrease particle size. The highest yields were obtained on small particles of 3.8 and 5.8 nm and it was suggested that the particular shape may be important which conform in the selectivity toward 3-vinylaniline that was dependent on gold particle size. The highest activity consisted with 3-5 nm range of Pt particle but did not selective in nitro group

hydrogenation. When increased Pt terraces with increasing Pt particle size, the rate of styrene hydrogenation was increased. Thus the catalytic of 3-nitrostyrene hydrogenation was improved by small Pt particle and has been selection of support with higher specific surface area as an effect of strong metal support interaction (SMSI). The SMSI reflected in change of electronic density and generated or decorated special active site on the support while Pt/TiO_2 can be decorated with TiO_x species by treatment under H_2 at above 400 ^{o}C. Under this condition, Pt catalyst led to hydrogenation of nitro group [33].

Yoshida, H., et al (2011) showed that selectivity of 3-nitrostyrene hydrogenation in ethanol occurring in the order vinylaniline (VA) >ethylnitrobenzene (ENB) >ethylaniline (EA) allow conversion around 20%. Then the total conversion was continued that the selectivity of VA did not change while the selectivity of ENB was decreased but that EA was increased. When the CO_2 pressure was raised to 2 MPa, ENB selectivity was increased while that VA selectivity was decreased. The effect of CO_2 pressure were significant at 10 MPa, the ENB much higher the VA and EA and the product distribution changed in toluene as a nonpolar solvent but not in ethanol as a polar solvent. And the rate of hydrogenation of three products were widly and different in the rate of VA hydrogenation in ethanol [6].

จุฬาลงกรณ์มหาวิทยาลัย
Chulalongkorn University

J.Beier et al (2012) has reported platinum metal synthesized by an ionic liquid method and used for chemoselective hydrogenation of 3-nitrostyrene. The reaction mediums (acidic or basic) have an effect in reaction. Acidity inhibited the activity of 3-nitrostyrene hydrogenation. The effect of solvents such as a toluene, tetrahydrofuran, ethyl acetate, $CHCl_3$, trifluoroacetic acid, 1,2-Dichlorobenzene, and ethanol were investigated. Ethanol using with Pt@IL base catalyst led to higher an activity (100% conversion, 96% selectivity of ethtlnitrobenzene) but SiO_2 represented higher aminostyrene selectivity with ethanol solvent. The effect of support on the selectivity and reaction rate in the hydrogenation of NS at high conversion (95–98%) was reported. It was found that ethylnitrobenzene selectivity was higher with SiO_2 support. On the other hand, for higher aminostyrene selectivity, TiO_2 was the best support [7].

Makosch, M., et al (2012) synthesized Pt/TiO_2 catalysts by incipient wetness impregnation method and presented a simple surface modification method by organic thiols for the liquid phase selective hydrogenation of 4-nitrostyrene. In these different organic thiols modification on selectivity and activity during the liquid phase hydrogenation of 4-nitrosytrene, the rate at 40% conversion of the unmodified Pt/TiO_2 catalyst was the highest observed than all the catalysts. The thiols were blocked part of the surface of the Pt nanoparticles and thus active sites. The structure modifications have an affected the selectivity: the modifiers containing polar groups (thioglycerol, 1,6-hexanedithiol and **α**-lipoic acid) yielded 100% selectivity toward 4-aminostyrene whereas an unpolar modifier (1-dodecanethiol) yielded only 88% selectivity. This trend was observed at conversion levels close to 100%. The **α**-lipoic acid modifier was the best catalyst modified which confirmed by 100% yield followed by 1,6-hexanedithiol (98%) and thioglycerol (97%). When compared with the rate, 1, 6-dithiolhexane was gave the best result that 0.01 $mmolgcat^{-1}$ s^{-1}, 100% conversion, and 98% selectivity. The catalyst stability was shown 3 cycles and slightly decreased activity of catalyst in reaction [2].

Campos, C., et al (2013) synthesized Ir/ZrO_2 catalyst by impregnation method for chemoselective hydrogenation of substituted nitroarenes. The catalyst has different behaviour dependent on the kind of substituent groups in meta position, withdrawing or donating electron density in ability to supply/withdraw electrons to/from the reaction site. For m-nitrostyrene hydrogenation, the formation of methylnitrobenzeneand the total hydrogenation product m-ethylanilinewas hydrogenated between the NO_2 and $CH = CH_2$ group. In this case the active phase showed a higher selectivity to the desired product m-vinylaniline at conversion higher than 90%. At the beginning the selectivity towards the desired product is very low, prevailing the hydrogenation of $CH = CH_2$ due to the activation that the NO_2 group provides to the polarization of the doble bond. Delocalization of positive charge in the benzene ring promotes the C2 electrophilicity and at the same time stabilized the NO_2 group disfavoring the hydrogenation and the formation of m-vynilaniline. At 120 min

m-ethylaniline product of totalhydrogenation was incresed and decreased m-ethylnitrobenzene [34].

Furukawa, S., et al (2014) presented Pd- and Rh-based intermetallic compounds supported on silica that were prepared by pore-filling impregnation, and studied their catalytic properties in reactions of nitrobenzene and nitrostyrene (NS). The formation of the intermetallic compounds have been made the platform for the chemoselective hydrogenation of NS: two metal elements are coadjacent at the atomic level on the surface of the nanoparticles. An increase in the electronegativity of the second metal element provides polar sites and enhances the activation of methanol as a hydrogen donor, which accelerates the hydrogenation of the nitro group of NS and improves the yield of aminostyrene. Over Rh catalysts, aminostyrene(AS) selectively was formed as a result of the absence of 4-methyl-1-cyclohexene activation ability. Pd13Pb9 exhibits the highest chemoselectivity in the conversion of NS to AS (92%) among Pd catalysts. Moreover, RhPb2 did not only exhibit high selectivity toward AS (93%) but also exhibited the highest NS conversion (94%). This catalyst was given high selectivity toward AS (91%) [8].

Ishida, T., et al (2014) used Pd/CMPs for hydrogenation of 4-nitrostyrene under the H_2 flow 0.3 MPa, 50 ^{o}C and 1 h. Pd/CMPs were prepared by Pd-catalyzed polymerization. The catalytic reaction with Pd/CMP-1-H_2 has shown 99% conversion and 99% selectivity of 4-vinylaniline [30].

Pisduangdaw, S., et al (2014) synthesized Pt/TiO_2 catalysts by single-step flame spray pyrolysis method for the liquid-phase selective hydrogenation of 3-nitrostyrene. The catalyst performances of the FSP-made catalysts (F-Pt/Ti) in both of hydrogenation activity and selectivity to vinylaniline (VA) improved from 61 to 66% and 40 to 73% by reduction at high temperature. While as compared to the F-Pt/Ti, the Pt/TiO_2 obtained by impregnation (I-Pt/Ti) on a sol-gel TiO_2 the result contained higher amount of rutile phase and exhibited lower Pt dispersion and hydrogenation activity (5% after reduction at 200^{o}C and 50% at 500^{o}C). The rutile occurred after reduction at 600 and 700 ^{o}C for

the I-Pt/Ti and F-Pt/Ti, respectively, leading to excessive decoration of Pt by the reducible TiO_x species and poor catalytic performances [3].

Pisduangdaw, S., et al (2014) studied the Pt–Co/TiO_2 catalysts prepared by single step flame spray pyrolysis with Pt at 0.5 wt.% and Co loadings varying at 0, 0.1, 0.2, and 0.5 wt.%. They were used for the liquid-phase selective hydrogenation of 3-nitrostyrene. When reduced at 200 °C, the addition of cobalt resulted in an increased ratio of CO adsorbed on Pt terrace to corner atoms, hence the ENB selectivity increased with the maximum at 0.2 wt. % Co. However, the nitrostyrene conversion and VA selectivity of Pt–Co/TiO_2 were more increased than the monometallic FPt/Ti and the Pt–Co/TiO_2 reduced at 200 °C, suggesting the modification of the electronic properties of Pt by Co and the formation of Pt–TiOx sites [27].

Yarulin, A., et al (2015) reported the Pt/HPS catalysts prepared by impregnation method and bimetallic Pt–Zn/HPS prepared within the hypercross-linked polystyrene (HPS) support for liquid-phase hydrogenation of 3-nitrostyrene (3-NS) to 3-vinylaniline (3-VA). In addition of Zn to Pt, a significant increase in 3-VA selectivity (from 16% up to 97%) was attained at close to full 3-NS conversion. Pt–Zn/HPS shows high performance over repeated reaction runs without detectable catalyst deactivation or metal leaching. Therefore, HPS was suitable for modification of Pt catalyst in selective hydrogenation [35, 36]

Table 3.1 Summery of the selective hydrogenation of nitrostyrene with various catalysts and conditions.

No.	Years	Researchers	Catalysts	Preparation method	Reaction conditions
1	2007	Boronat, M., et al.	Au/TiO_2, Pt/TiO_2, Pd/TiO_2 ,Au/SiO_2, Au/Fe_2O_3, Au/C	Impregnation	0.9 MPa and 120 °C
2	2009	Serna, P., et al.	Au/TiO_2 Pt/TiO_2	Deposition precipitation	0.8 MPa and 120, 80, 40 °C
3	2009	Shimizu, K., et al.	Au/γ-Al_2O_3, Au/SiO_2, Au/ montmorillonit, Au/ MgO, Au/C, Au/TiO_2, Pt/ γ-Al_2O_3	Colloid deposition	8 MPa and 40 °C
4	2010	Shimizu, K., et al.	Ag/MgO, Ag/CeO_2, Ag/ZrO_2, Ag/TiO_2, Ag/SnO_2, Ag/WO_3, Ag/Al_2O_3,	Impregnation	3 MPa and 160 °C
5	2011	Serna, P., et al.	Au/TiO_2, Pt/TiO_2	Deposition – precipitation	0. 9 MPa and 120 °C
6	2011	Yoshida, H., et al.	Pt/TiO_2	Impregnation	4 MPa and 50 °C
7	2012	J.Beier, M., et al.	Pt/TiO_2, Pt/SiO_2, Pt/Al_2O_3, Pt/C	Ionic liquid	0.1 MPa

No.	Years	Researchers	Catalysts	Preparation method	Reaction conditions
8	2012	Makosch, M., et al.	Pt/TiO_2	Impregnation	1 MPa amd 80 ℃
9	2013	Campos, C., et al.	Ir/ZrO_2	Impregnation	2 MPa and 25 °C
10	2014	Furukawa, S., et al.	Pd/ SiO_2, Rh/ SiO_2 Intermetallic catalysts, Pd–M/SiO_2 (M = Cu, Ga, Pb, and Zn) and Rh–M′/SiO_2 (M′ = Fe, Ni, Pb, Sb, Sn, and Ti)	Impregnation	350 °C under the H_2 flow
11	2014	Ishida, T., et al.	Pd/CMPs	Pd-catalyzed polymerization	0.3 MPa and 50 °C
12	2014	Pisduangdaw, S., et al.	Pt/TiO_2	Flame spray pyrolysis	4 MPa and 50 °C
13	2014	Pisduangdaw, S., et al.	Pt–Co/TiO_2	Flame spray pyrolysis	4 MPa and 50 °C
14	2015	Yarulin, A., et al.	Pt–Zn/HPS	Impregnation	1 MPa and 75 °C

3.2 Nitrogen doping

Sathish, M., et al (2005) synthesized N-doped TiO_2 nanocatalyst with spherical shape and homogeneous size. The results show that light adsorption were shift to the vesible light region and decrease the band gap energy of catalyst. The valance band was took place by new valance of N 2p state on N-doped TiO_2. The cystallinity of nanocatalyst became to anatase TiO_2 lattice. A higher photocatalytic activity for the decomposition of methylene blue in the visible region has been obtained for the N-TiO_2 sample compared to Degussa P25 and pure TiO_2 [37].

Yin, S., et al, Jagadale, T., et al (2008), Du, J., et al (2013) show that nitrogen doping leads to a narrowing of the band gap through formation of an N 2p state above the O 2p state. This consequently induces visible light responsive photocatalytic activity. It was also predicted that other kind of anions such as C, S, and F would cause a similar effect to that of nitrogen. Photocatalytic activity is also strongly related to crystallinity as well as the specific surface area of a prepared powder. Well-crystallized photocatalysts with a fine particle size usually exhibit excellent photocatalytic activity. Some solution processes such as hydrothermal and solvothermal processes have been utilized for the synthesis of well-crystallized nano size photocatalysts with high photocatalytic activity [25].

จุฬาลงกรณ์มหาวิทยาลัย
Chulalongkorn University

Cheng, X., et al (2011) has synthesized N-doped TiO_2 by hydrolysis–precipitation process using ammonia water as the doping species for photocatalytic reaction. The XRD pattern shown that the cystallinity of catalysts increased anatase and nitrogen doping has an affected from anatase to rutile. The advantage on N-doped TiO_2 followed by enhanced electric field strength, led to the decrease in the recombination chance of photogenated charge carriers, promoted charge and electron transfer. In other hand, the new energy level was formed by that the photoinduce electrons can be transfer from N2p states to the conduction band of TiO_2 and improved the rate of photogenate electron hole pair. Under the visible light irradiation with 120 min, a 65.3% degradation rate of phenol could be achieved. The photocatalytic activity of nitrogen

doped TiO_2 was 2.08 and 1.97 times than that of pure TiO_2 and P25 TiO_2, respectively. The enhanced visible light activity was attributed to the well anatase crystallinity, small crystallite size, intense light absorbance edge in visible region, more content of surface hydroxyl groups and high separation efficiency of photogenerated charge carriers [38].

Zhang, X., et al (2008), has reported that the TiO_2 material, when doped with non-metal elements such as N, and it exhibited red-shifted absorption edge. TiO_2 could be doped with nitrogen by various physical and chemical methods. Both substituted and interstitial nitrogen dopants were responsible for the red-shifted absorption. However the band gap energy on N-doped TiO_2 was not strong when interact with support in photocatalytic reaction. Pt metal has been used to improve activity of photocatalytic reaction with solar irradiation and was believed to improve the charge separation of TiO_2 photocatalysts, which are primarily important for photocatalytic reactions. Photogenerated electrons can be captured efficiently by Pt nanoparticles and there they are transferred to dioxygen to produce superoxide, hydrogen peroxide or water [26].

จุฬาลงกรณ์มหาวิทยาลัย
Chulalongkorn University

CHAPTER 4

EXPERIMENTAL

This chapter explains about the research methodology of all supports and catalysts preparation, catalyst characterization techniques including x-ray diffraction (XRD), N_2physisorption, x-ray photoelectron spectroscopy (XPS), UV-vis spectrophotometer (UV-vis), fourier transform infrared spectroscopy (FT-IR), and CO chemisorptions, infrared spectroscopy of adsorbed CO (CO-IR) and the equipment used for analysis reaction products.

4.1 Catalyst preparation

4.1.1 Synthesis of the supports

TiO_2 were prepared and modified by the solvothermal and incipient wetness impregnation method. The chemicals that were used to synthesize the TiO_2 support and N-doped TiO_2 supports are shown in **Table 3.1.** [9, 10]

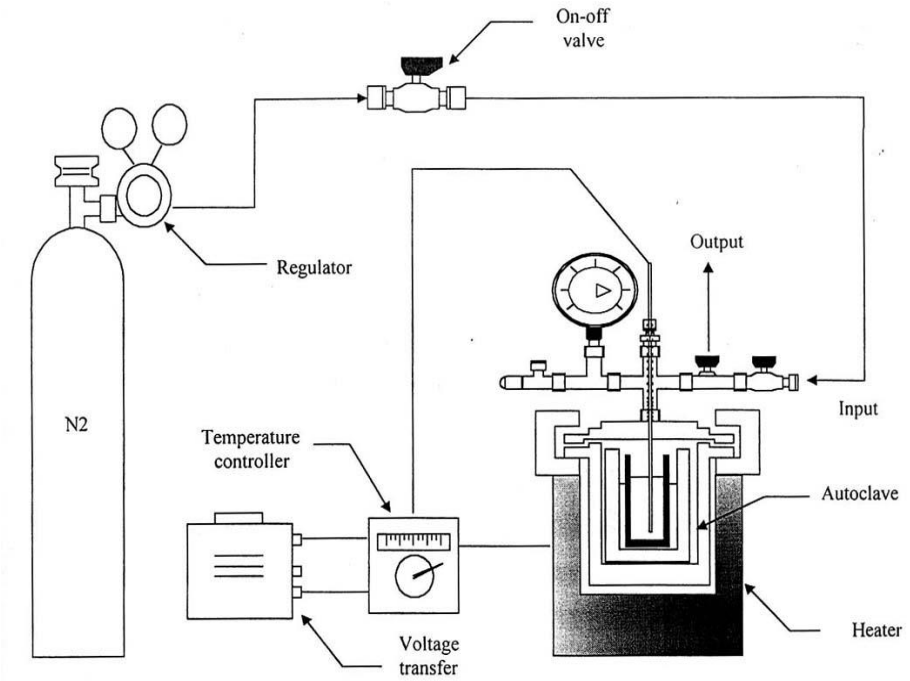

Figure 4.1 Diagram of the reaction equipment for the synthesis of titanium dioxide

The TiO_2 supports were prepared and modified by using the solvothermal method. TNB and 1,4-butanediol were used as TiO_2 precursor and organic solvent, respectively. Firstly, 25 g of TNB was dissolved in 100 cm^3 of 1,4butanediol. Then mixed solution in the test tube and 30 cm^3 1,4-butanediol was filled into the out tube and putted them into 300 cm^3 autoclave. The nitrogen gas was purged into the autoclave reactor before heating up to 300 ^oC at a rate of 2.5 ^oC/min and held constant at that temperature for4 h. The N-doped TiO_2 was prepared by addition amount of NMP into the mixed solution before setting up in the autoclave. The molar ratios of N/Ti were 0.05, 0.1, and 0.5. After cooling to room temperature, the products were washed with methanol and dried in air [9, 10].

Synthesis of the N-doped TiO_2 supports by incipient wetness impregnation method using N-metylpyrrolidone (NMP) as the nitrogen source. NMP solution was equal to the pore volume of the TiO_2 support was added drop-wise to the support during mixing with various N/Ti molar ratios (0.05, 0.1, and 0.5).Then first part was dried in air and second part was dried in air and followed by calcined at 300 ^oC for 2 h.

Table 4.1 The chemicals used for synthesis of the TiO_2 support and N-doped TiO_2 supports

Chemicals	Supplier
Titanium (IV) n-butoxide 97%; (97% $Ti(OCH_2CH_2\ CH_2CH_3)_4$)	Aldrich
1,4-butanediol 99% ($HO(CH_2)_4OH$)	Aldrich
N-metylpyrrolidone 99.5% (99.5% C_5H_9NO)	Merck
Methanol (CH_3OH)	Aldrich

4.1.2 Synthesis of the Pt/TiO_2 and Pt/N-doped TiO_2 catalysts by incipient wetness impregnation method

The TiO_2 supported Pt catalysts were prepared by the incipient wetness impregnation method. An aqueous solution of $H_2PtCl_66H_2O$ equal to the pore volume of the TiO_2 support was added drop-wise to the support during mixing with 0.5 wt % loadings. After impregnation, the catalysts were dried at room temperature for 6 h and then at 110 ℃ overnight in an oven. The dried catalysts were calcined in air at 300 ℃ for 2 h. The series of catalysts are denoted by the nitrogen content in the TiO_2 supports. This catalyst was reduced under H_2 flow during 3 h at 200 ℃ before its use in the reaction [3, 27].

4.2 Catalytic reaction in the liquid-phase hydrogenation of 3-nitrostyrene

The chemicals and reagents that used in the catalytic reaction in the liquid phase hydrogenation of 3-nitrostyrene are shown in Table 3.2. Themagnetically stirred 50 ml of teflon container stainless steel autoclave reactor was loaded with 20 mg of reduce catalyst at 200 ^{o}C, 10 ml ethanol, and 0.4 ml of 3-nitrostyrene (3.6 mmol) were obtained into 50 ml autoclave and reaction carried out isothermally at 40 ^{o}C and 4 MPa of H_2. Then the purged with hydrogen to remove the air for 3-5 times. The experiment of reaction mixture was stirred with a magnetic stirrer. After the reaction, the reactor was carefully depressurized and cooled it below room temperature by ice water at 2 min and. The product was then analyzed by a gas chromatograph attached with a flame ionization detector which the operating conditions are shown in Table 3.3. And stirred continuously for 5, 10, 20, 40, and 60 min which the schematic diagram of the liquid phase hydrogenation of 3-nitrostyrene is shown in Figure 3.1. The stability of catalysts was studied by separated catalysts from the reaction mixture by centrifugation. The separated catalyst was washed with ethanol (5 mL) and distilled water (5 mL), followed by drying at 100 ℃ for 30 min and calcining in air at 300 ℃ for 30 min [3, 6, 27].

จุฬาลงกรณ์มหาวิทยาลัย
Chulalongkorn University

Table 4.2 The chemicals and reagents are used in catalytic reaction and catalysts stability

Chemicals and reagents	Supplier
High purity grade hydrogen (99.99%)	Thai industrial gases limited
3-nitrostyrene ($C_8H_7NO_2$)	Aldrich
3-vinylaniline ($C_8H_9NH_2$)	Aldrich
3-ethylaniline ($C_2H_5C_6H_4NH_2$)	Aldrich
Absolute ethanol 99.8% (CH_3CH_2OH)	Merck
Methanol	Merck
Toluene	Aldrich
Distillate water (H_2O)	Center of Excellence on Catalysis and Catalytic Reaction Engineering

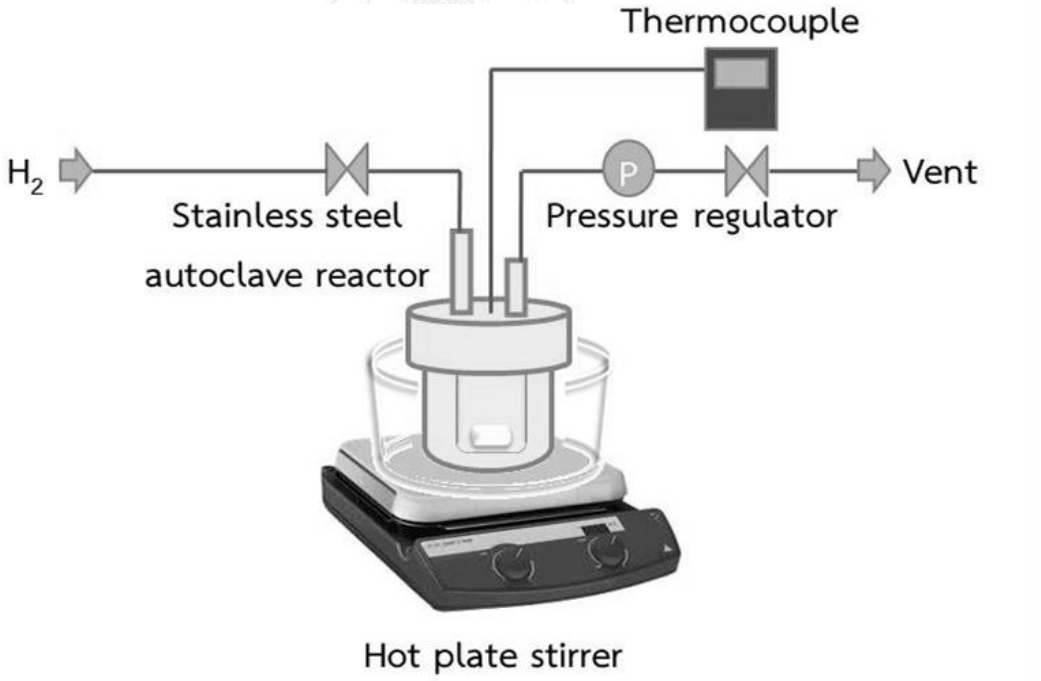

Figure 4.2 The schematic diagram of the liquid-phase hydrogenation [15]

Table 4.3 The operating conditions for gas chromatograph

Gas chromatography	Shimadzu GC-2014
Detector	FID
Packed column	Rtx®5
Carrier gas	Helium (99.99 vol.%)
Make-up gas	Air (99.9 vol.%)
Column temperature	140°C
Injector temperature	270°C
Detector temperature	310°C
Time analysis	30 min

4.3 Catalyst characterization

4.3.1 X-ray diffraction (XRD)

The x-ray diffraction (XRD) was used determined XRD patterns of all the supports and all the catalysts by using the SIEMENS D5000 x-ray diffractometer connected with a computer with Diffract ZT version 3.3 programs for fully control of the XRD analyzer. The experiments were carried out by using Cu K_α radiation with Ni filter in the 2θ range of 20° to 80° and resolution 0.04°. This technique is use for specify TiO_2anatase and crystalline size of supports and catalysts.

4.3.2 N_2 physisorption

The specific surface area (using the stand BET method), average pore volume, average pore size (using the BJH desorption analysis) and hyteresis loop (using the adsorption-desorption isotherms) of catalysts and TiO_2 support were measured by using the Micromeritics Pulse ChemiSorb 2750 instrument. Prior to analysis, all the catalysts and TiO_2 support were thermally treated at 150ºC for 1 h. Then, nitrogen adsorption-desorption isotherms were obtained at -196ºC under liquid nitrogen.

4.3.3 X-ray photoelectron spectroscopy (XPS)

The XPS spectra, the blinding energy, full width at half maximum (FWHM) and the composition of the Pt catalysts on the surface layer of the catalysts were performed by using the Kratos Amicus x-ray photoelectron spectroscopy. The experiment was operated with the x-ray source at 20 mA and 12 kV (240 W), the resolution at 0.1 eV/step and the pass energy of the analyzer was set at 75 eV under pressure approximately $1x10^{-6}$ Pa. For calibration, the blinding energy was referenced to C 1s line at 285.0 eV. The blinding energy of O 1s, Ti 2p, N 1s, and Pt 4f are determined. Particularly, it is maintain nitrogen on TiO_2 support.

4.3.4 UV-visible spectrophotometer (UV-vis)

The absorbance spectrums of all the supports were recorded by using the Perkin Elmer Lambda 650 spectrophotometer in the wavelength range from 200-700 nm. This technique can confirm nitrogen occurring on TiO_2 support.

4.3.5 Fourier transforms infrared spectroscopy (FT-IR)

The FT-IR spectra of all the supports were recorded by using the Nicole 6700 of the IR spectrometer in the wavelength range from 500-4000 cm^{-1}. The Ti-O stretching vibration, the OH groups on the hydroxyl, the C-H stretching, C=O and C-N absorption are discover by this technique.

4.3.6 Transmission electron microscopy (TEM)

The Pt particles size and particles size distribution of all the catalysts were observed by using the JEOL-JEM 2100 transmission electron microscope operated at 120 kV at Scientific and Technological Research Equiment Centre, Chulalongkorn University.

4.3.7 CO-Pulse Chemisorption

The Pt active sites and the relative percentages dispersion of Pt supported catalysts were determined by CO-pulse chemisorption technique using Micromeritics ChemiSorb 2750 (pulse chemisorption system). Approximately 0.05 g of catalyst was filled in a u-tube, incorporated in a temperature-controlled oven and connects to a thermal conductivity detector (TCD). Then, helium (He) was pursed into the reactor with a flow rate 30 ml/min in order to remove remaining air. Prior to chemisorption, the catalyst was reduced in H_2 flow rate 30 ml/min) at 200 ^{o}C for 1 h. After that cooled down to room temperature under Helium flow, then CO is plus into the catalyst bed at 30 ^{o}C. The non-adsorbed CO was measured using thermal conductivity detector. Pulsing was continued until no further CO adsorption is observed. The amount of Pt metal active sites and the relative percentage dispersions of Pt were calculated from CO adsorbed based on CO:Pt ratio of 1:1.

4.3.7 H_2 temperature program reduction

The H_2-TPR measurements were carried out in a U-tube reactor. Prior to these measurements, all the catalyst samples were pretreated with a N_2 flow (25 mL/min, 1 h, 200^{o}C). The TPR profiles were obtained by passing carrier gas (10% H_2 in nitrogen) through the catalyst samples (25 mL/min, ramping from 30 to 500 oC at 10 ^{o}C/min) using a Micromeritics AutochemiSorb 2910 system attached with ChemiSoft TPx software.

จุฬาลงกรณ์มหาวิทยาลัย
Chulalongkorn University

4.3.8 Infrared spectroscopy of adsorbed CO (CO-IR)

The CO adsorbed species on the Pt/TiO_2 catalysts were measured using an FTIR-620 spectrometer (JASCO) with an MCT detector at a wavenumber resolution of 2 cm^{-1}. He gas was introduced into the sample cell in order to remove the remaining air. The system was switched to hydrogen and heated to 200–500 °C. The temperature was kept constant for 60 minutes and then cooled down to the room temperature with He gas. After that, carbon monoxide was made to flow to the system for 15 minutes. The IR spectrum of CO adsorbed onto the catalyst was recorded in the 1800–2200 cm^{-1} range after the gaseous CO had been removed from the cell by He flow.

จุฬาลงกรณ์มหาวิทยาลัย
Chulalongkorn University

CHAPTER 5

RESULTS AND DISCUSSION

The results and discussion in this chapter are consisted of two parts including the effect of synthesis conditions of the N-doped TiO_2 supports and the effect of various amounts of the N-doped TiO_2. The characteristics of catalysts were investigated by N_2-physisorption, XRD, XPS, FTIR, CO-IR, and SEM analysis. The catalytic properties of Pt catalysts supported on N-doped TiO2 supports were investigated in the liquid-phase selective hydrogenation of 3-aminostyrene to 3-vinylaniline.

5.1 The effect of synthesis conditions on the N-doped TiO_2 supported Pt catalysts

The N-doped TiO_2 supports were prepared by solvothermal and incipient wetness impregnation methods with and without calcination method and were labeled as N(SV)-TiO_2, N(Cal)-TiO_2 and N(IM)-TiO_2, respectively. The molar ratios of N/Ti were 0.05, 0.1, and 0.5. The Pt catalysts were prepared by the incipient wetness impregnation method by using an aqueous solution of $H_2PtCl_66H_2O$ equal to the pore volume of the TiO_2 support with 0.5 wt % Pt loading. The catalysts were labeled as Pt/TiO_2, Pt/N(SV)-TiO_2, Pt/N(Cal)-TiO_2 and Pt/N(IM)-TiO_2.

จุฬาลงกรณ์มหาวิทยาลัย
Chulalongkorn University

5.1.1 Catalysts characterization

5.1.1.1 N_2 physisorption

The results from N_2 physisorption technique show the BET surface area, pore volume, average pore size and N_2 adsorption-desorption isotherm of TiO_2. **Table 5.1** shows the physical properties of the N-doped TiO_2 supports prepared by different routes. The results show that the different N-doped synthesis conditions affected the BET surface area and average pore size of TiO_2 support. All the samples were prepared by solvothermal method and nitrogen could be added to TiO_2 structure via N-Ti formation. This method resulted in no significant changes in surface area, pore volume, and average pore size. However, when nitrogen was added by impregnation on both

0.1N(IM)-TiO_2 and 0.1N(Cal)-TiO_2 the BET surface area increased and the average pore size decreased as compared to the 0.1N(SV)-TiO_2. The results could be implied that nitrogen covered on TiO_2 surface in 0.1N(IM)-TiO_2 and inserted into TiO_2 lattice in 0.1N(Cal)-TiO_2. Which it confirmed by the absorbance of Pt/0.1N(IM)-TiO_2 shifted higher than the absorbance of 0.1N(IM)-TiO_2 in **Figure 5.7** and **Figure 5.6**, respectively. **Figure 5.1** shows the N_2 adsorption-desorption isotherm of TiO_2 and N-doped TiO_2 supports, it was type IV isotherm with a hysteresis loop at relative high pressure range (P/P_0). These results indicated the characteristics of mesoporous material with pore diameter in the range of 2 to 50 nm. The solvothermal method produced mesoporous TiO_2 [39].

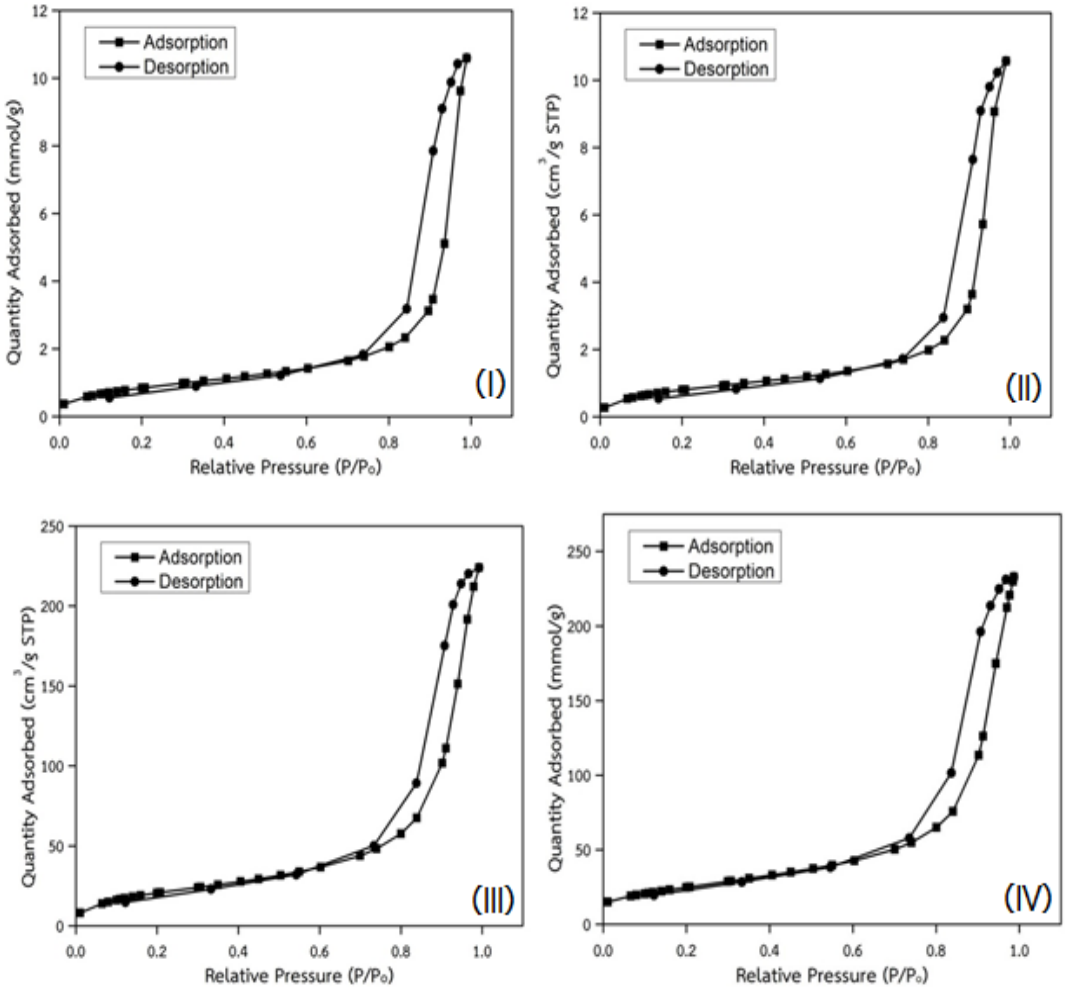

Figure 5.1 N_2 adsorption-desorption isotherm of TiO_2 supports as a follow by TiO_2 (I), 0.1N(SV)-TiO_2 (II), 0.1N(IM)-TiO_2 (III), and 0.1N(Cal)-TiO_2 (IV)

Table 5.1 Physical properties of TiO_2 supports

Catalysts	BET Surface Area (m^2/g)	Pore Volume (cm^3/g)	Average Pore Size (nm)
TiO_2	72.7	0.36	20.2
0.1N(SV)-TiO_2	70.3	0.36	20.9
0.1N(IM)-TiO_2	80.1	0.35	17.3
0.1N(Cal)-TiO_2	90.7	0.35	15.7

5.1.1.2 XRD

The chemical phase and crystal structure of TiO_2 supports and catalysts prepared by different methods were characterized by X-ray diffraction technique at the diffraction angles (2θ) between 20° and 80°. The crystallite size was estimated from the diffraction peaks at 25° (2θ) by using Scherrer Equation.

Figure 5.2 and Figure 5.3 show the XRD patterns of TiO_2 supports and catalysts prepared by different method. The anatase phase TiO_2 was confirmed by the XRD characteristic peaks at 25° (the major of anatase phase), 36°, 49°, 54°, 63°, 69° and 75° without other phases of TiO_2. The presence of pure anatase phase suggested that amorphous TiO_2 could be converted into crystalline anatase through the solvothermal method [9, 10]. The peak position of anatase (101) TiO_2, d-spacing, and the lattice parameters for TiO_2 and N-doped TiO_2 supports are given in **Table 5.2**. The peaks position of anatase (101) of TiO_2, 0.1N(SV)-TiO_2, 0.1N(IM)-TiO_2, and 0.1N(Cal)-TiO_2 were found at 2θ=25.39°, 25.45°, 25.22°, and 25.18°, respectively. The distance between crystals planes (d-spacing), which according to the lattice parameters of 0.1N(IM)-TiO_2 and 0.1N(Cal)-TiO_2 were increased when compare with TiO_2. It was suggested that impregnation method could be inserted nitrogen in the TiO_2 lattice and it covered on the TiO_2 surface which it was related to decreasing crystallite sizes and the peak position of anatase TiO_2. But the d-spacing of 0.1N(SV)-TiO_2 was decreased which related to nitrogen covered on the TiO_2 surface.

In **Table 5.3** show similar results in the crystallite sizes and peak position of Pt/N-TiO_2 which confirmed nitrogen doped in TiO_2 lattice. The d-spacing was asynchronous resulted with N-doped supports in **Table 5.2** owing to affected from synthesis conditions. The increasing of d-spacing confirmed nitrogen inserted into TiO_2 lattice. The XRD patterns show anatase phase TiO_2 and the Pt diffaction peak was not appeared. These results shows that in addition of Pt loading was not an effected to TiO_2 lattice and XRD diffraction peak.

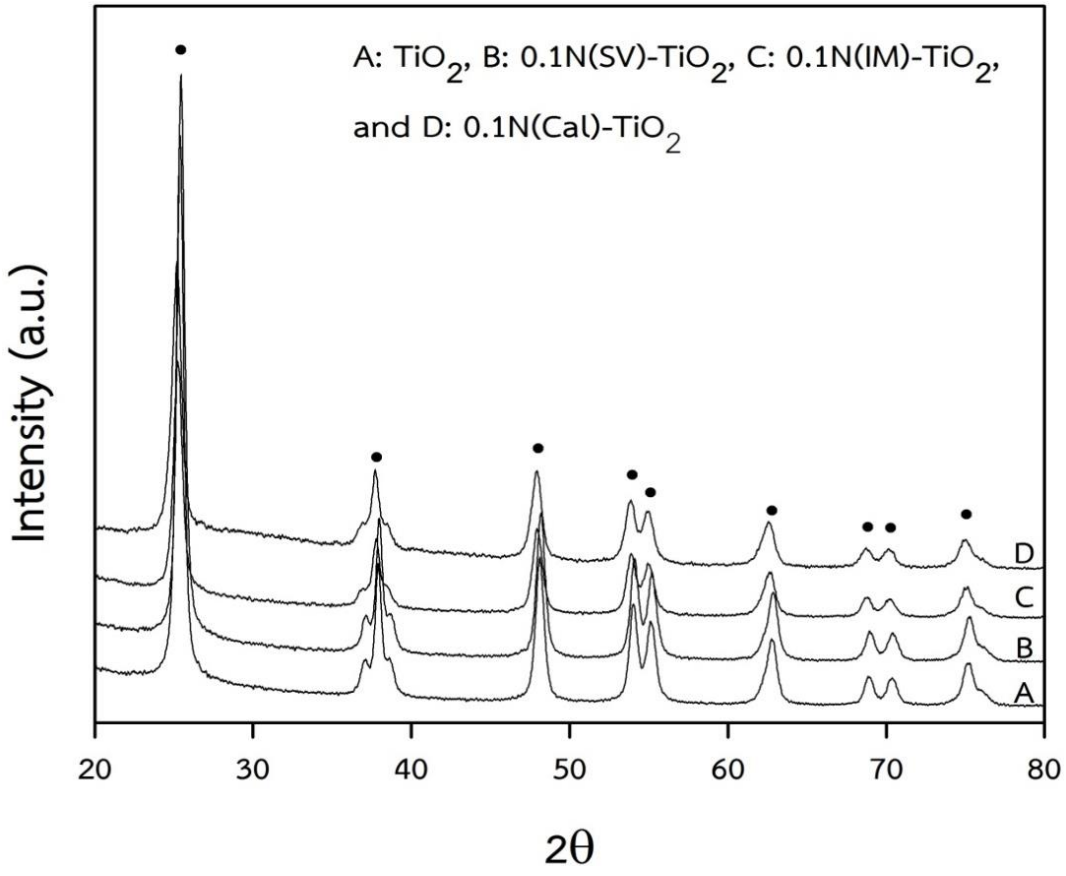

Figure 5.2 XRD patterns of the N-doped TiO_2 supports with different synthesis method

Table 5.2 The peak position of anatase (101) TiO2, d-spacing and the lattice parameters of the N-doped TiO_2 supports with different synthesis method

Catalysts	Crystallite size (nm)	Peak position of anatase (101) (2θ, degree)	d-spacing (nm)	Lattic parameter[a] (A^0)		
				a (=b)	c	c/a
TiO_2	14.0	25.39	0.3505	3.7779	9.2421	2.45
0.1N(SV)-TiO_2	14.4	25.45	0.3497	3.7734	9.3095	2.47
0.1N(IM)-TiO_2	11.0	25.22	0.3528	3.7932	9.6022	2.53
0.1N(Cal)-TiO_2	10.2	25.18	0.3534	3.7947	9.7441	2.57

[a] calculated from Bragg's law using the diffraction peaks of anatase (101) TiO_2.

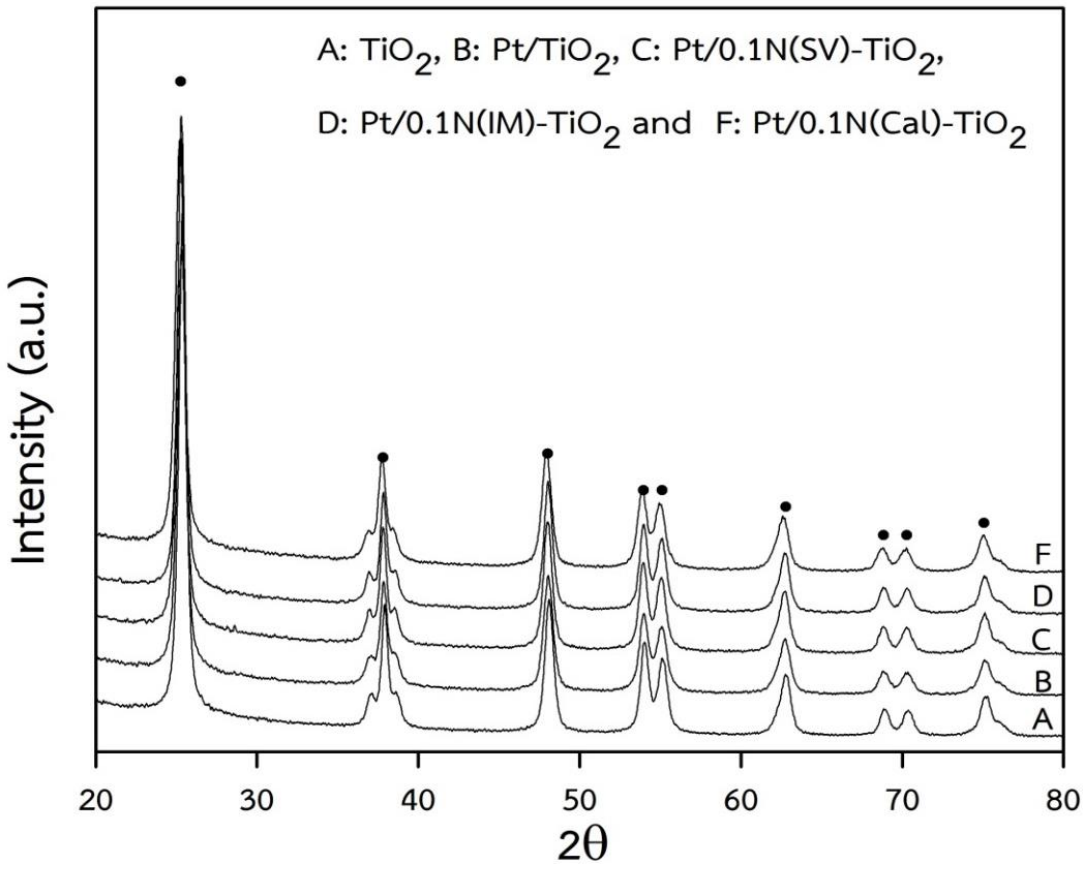

Figure 5.3 XRD patterns of the Pt catalysts supported on different N-doped TiO_2 supports

Table 5.3 The peak position of anatase (101) TiO2, d-spacing and the lattice parameters of the Pt catalysts supported on different N-doped TiO_2 supports

Catalysts	Crystallite size (nm)	Peak position of anatase (101) (2θ, degree)	d-spacing (nm)	Lattic parameter[a] (A^0)		
				a (=b)	c	c/a
Pt/TiO_2	12.3	25.33	0.3514	3.7832	9.4818	2.51
$Pt/0.1N(SV)-TiO_2$	13.9	25.26	0.3522	3.7886	9.5068	2.51
$Pt/0.1N(IM)-TiO_2$	11.8	25.28	0.3519	3.7825	9.6049	2.54
$Pt/0.1N(Cal)-TiO_2$	11.8	25.20	0.3531	3.7947	9.6345	2.54

[a] calculated from Bragg's law using the diffraction peaks of anatase (101) TiO_2.

5.1.1.3 Fourier transforms infrared spectroscopy (FT-IR)

The FT-IR spectra (tran smittance mode) of TiO_2 supports and Pt/TiO_2 catalysts with different of N-doping synthesis methods are shown in **Figure 5.4 and Figure 5.5**, respectively. The Ti-O stretching vibration in the TiO_2 lattice was found at 710 cm^{-1} and the hydroxyl of Ti-OH bonds appeared as broad band around wavenumbers 3350 cm^{-1}. The bending vibration of O-H and N-H was found at 1640 cm^{-1}. The IR peaks corresponding to the C-H stretching, vibration of surface adsorbed NO_3 and Ti-N were indicated at 2350 cm^{-1}, 1420 cm^{-1} and 1280 cm^{-1}, respectively [21, 24, 38, 40-43].

The incorporation of N-species in the N-doped TiO_2 sample is confirmed by the Ti-N and NO_3 bands which were not found in the un-doped ones. The IR peaks 2350 cm^{-1}, 1420 cm^{-1} and 1280 cm^{-1} with different support synthesis methods were detected and illustrated to the characteristic of the C-H stretching, vibration of surface adsorbed NO_3 and Ti-N. The highest peaks in **Figure 5.5** were appeared for the $N(Cal)-TiO_2$.

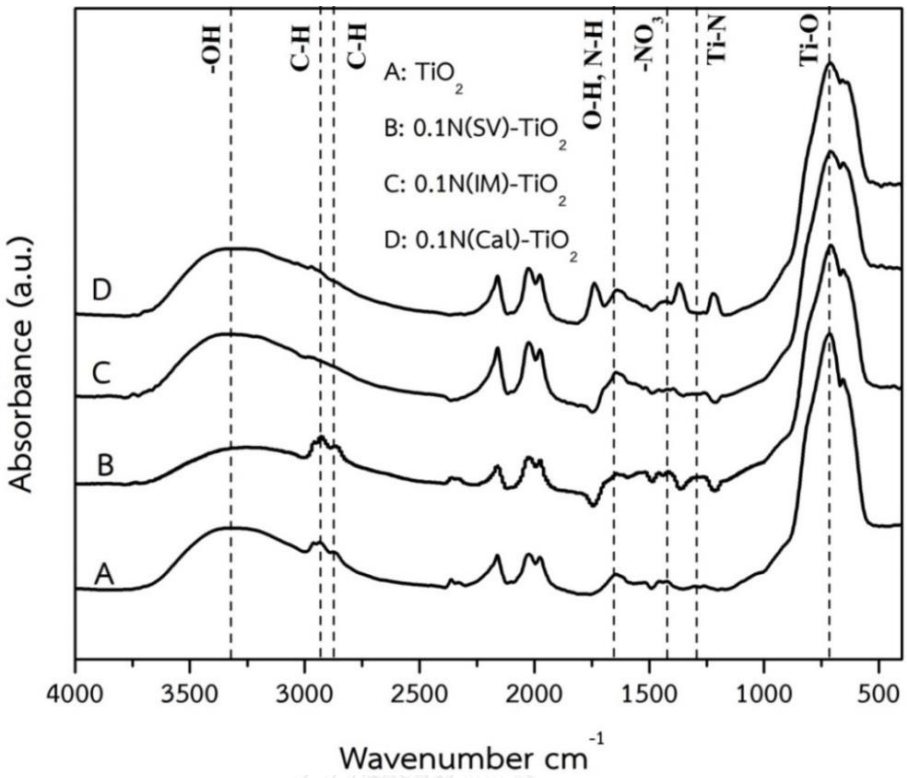

Figure 5.4 FT-IR spectra of different N-doped TiO_2 support synthesis

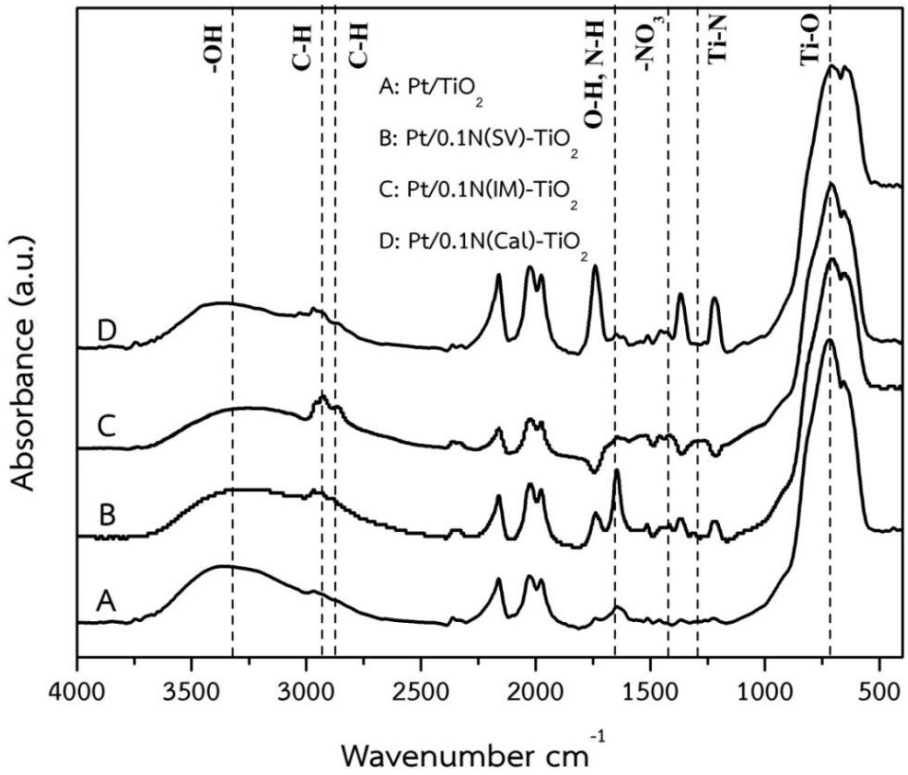

Figure 5.5 FT-IR spectra of the Pt catalysts with different N-doped TiO_2 support synthesis

5.1.1.4 UV-visible spectrophotometer (UV-vis)

The presences of nitrogen in the N-doped TiO_2 structure were investigated by the UV-visible spectroscopy. The UV–visible light absorption spectra results of TiO_2 support and Pt/TiO_2 catalysts with different of N-doping synthesis methods are shown in **Figure 5.6 and Figure 5.7**. The TiO_2 absorbance was in the region of 400-500 nm. A significantly shift of the absorbance to the visible-light region implied that the nitrogen was doped and inserted into the TiO_2 so that they exhibited the strong visible-light absorbance ability. The absorbance of visible light has been improved after the doping of the nitrogen in TiO_2, which is of great importance for its practical application [11-13, 17, 18, 23, 37, 38, 41, 43-45].

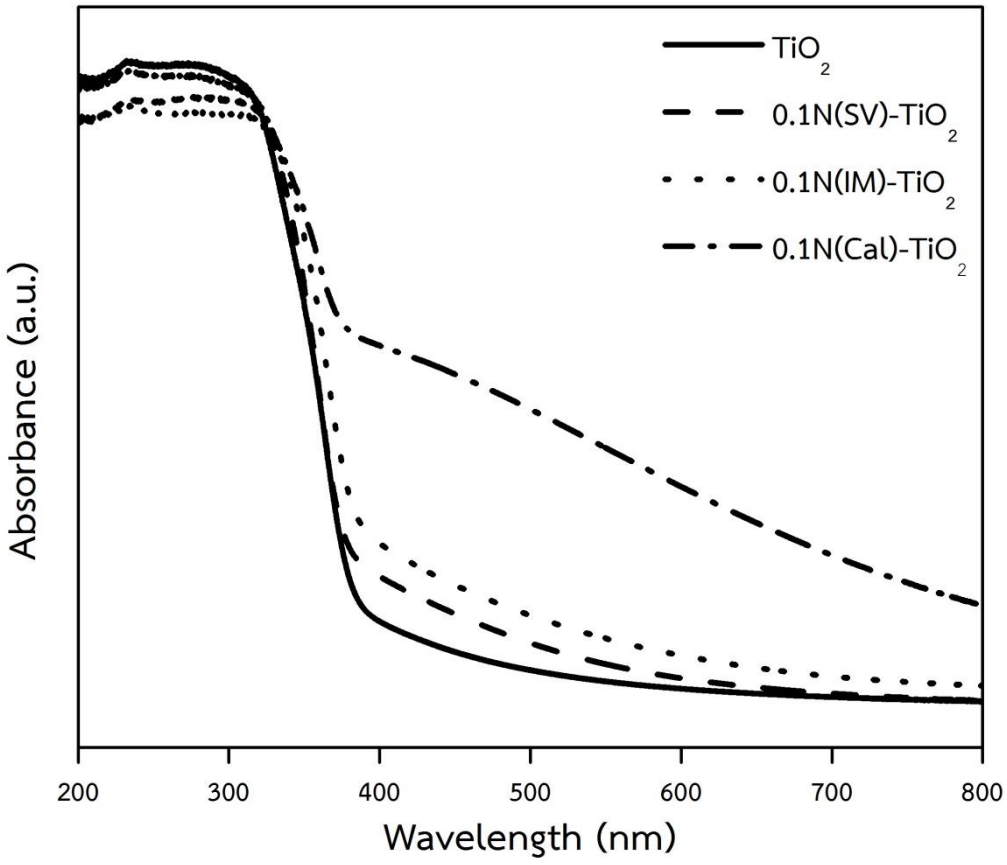

Figure 5.6 UV–visible of different N-doped TiO_2 supports synthesis

The results can be concluded that all the absorbance of samples was shifted base on TiO_2 and Pt/TiO_2 absorbance which it was confirmed nitrogen in the support. At the absorbance edge of supports, the 0.1N(Cal)-TiO_2 was observed with obviously higher than the 0.1N(SV)-TiO_2 and the 0.1N(IM)-TiO_2. The degree of nitrogen doping strongly affected the visible light absorption of TiO_2 when observed at the absorbance edge of catalysts. It is implied that impregnation method resulted in higher amount of nitrogen inserted into TiO_2 lattice than the solvothermal method. The shifting of Pt/0.1N(IM)-TiO_2 absorbance as a resulted of calcination temperature. Which it was also strongly affected the nitrogen doped on TiO_2 to the visible light absorption and the nitrogen inserted into TiO_2 lattice

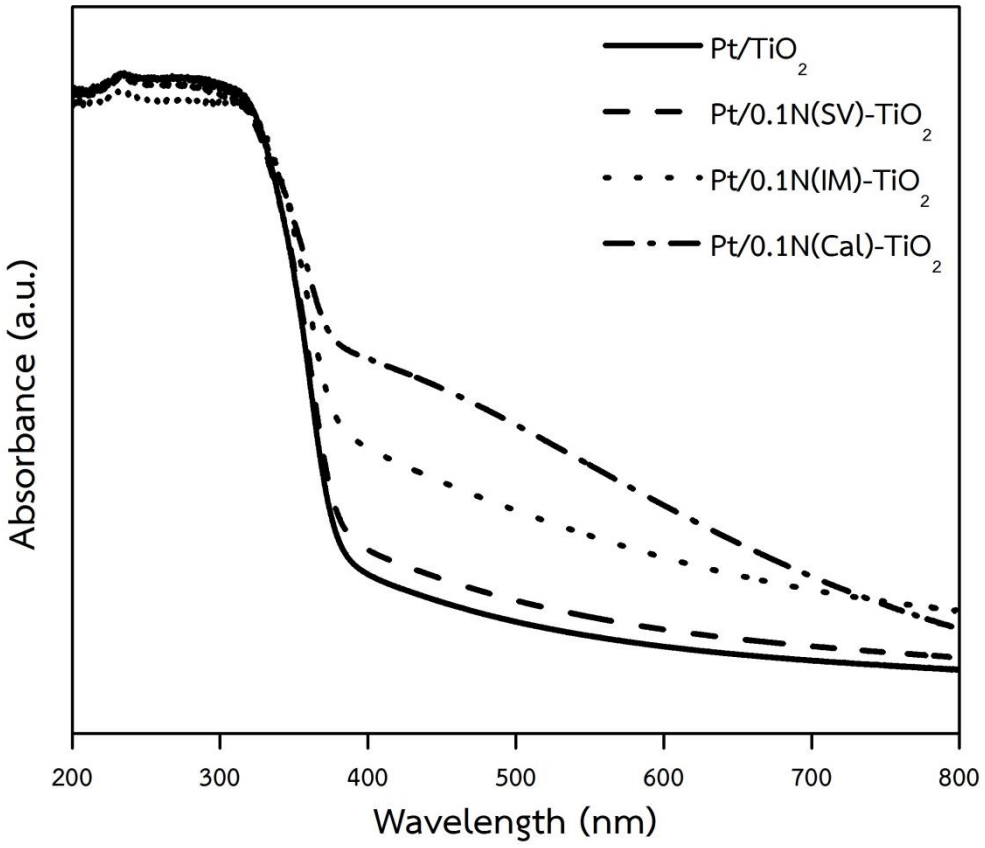

Figure 5.7 UV–visible of the Pt catalysts with different N-doped TiO_2 supports synthesis

5.1.1.5 X-ray photoelectron spectroscopy (XPS)

The electronic states of Pt catalysts were investigated by X-ray photoelectron spectroscopy to describe the relation between nitrogen and TiO_2 support and to understand the characteristics of platinum, nitrogen, and titania species on the samples.

The XPS binding energy of N 1s peak is shown as a broad peak around 400 eV which could be originated from the nitrogen species bound to various surface oxygen sites (**Figure 5.8**). The first major peak around 400-401 eV was attributed to presence of interstitial N state and the oxidized nitrogen of Ti-O-N which were chemically adsorbed on the catalysts surface [12, 14, 23, 24, 26, 45]. The second peak around 404-406 eV was assigned to nitrogen species bound to various surface oxygen sites either NO or NO_2. And the broad peak around 395-397 eV can be attributed to N replacing oxygen in the TiO_2 to form Ti-N bond TiO_2 [12, 14, 23, 24, 26, 28, 37, 38, 40, 43, 45].

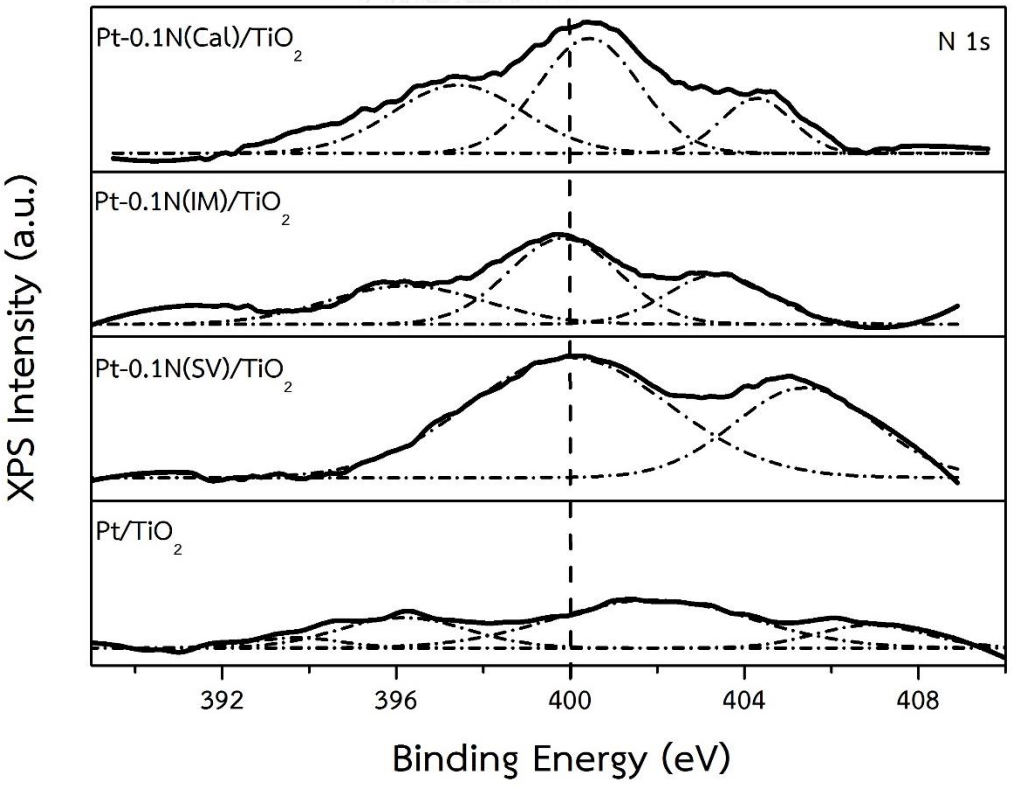

Figure 5.8 XPS spectra for N1s of Pt catalysts with different N-doped TiO_2 support synthesis

The results confirmed that the N-doped TiO_2 prepared by impregnation and solvothermal method had amount of nitrogen incorporated in the TiO_2 surface. The binding energy of Pt/0.1N(SV)-TiO_2 had higher amount of nitrogen accumulated on TiO_2 surface. It corresponded to the absorbance of Pt/0.1N(SV)-TiO_2 in **Figure 5.7.** The absorbance of Pt/0.1N(IM)-TiO_2 and Pt/0.1N(Cal)-TiO_2 slightly shifted which related to low amount of nitrogen on the surface but it implied that nitrogen inserted into TiO_2 lattice. The binding energy of Pt/TiO_2 of N 1s peak present around 402 eV. It was defined to decomposition or oxidation of Nitrogen compound precursor. [46] . In **Table 5.4** show surface atomic concentration of different catalyst synthesis. And the XPS binding energy of N 1s based on 400 eV. The results confirmed that Pt/0.1N(SV)-TiO_2 had higher N/Ti ratio which it represented to Ti-O-N species on the surface and not showed in Pt/TiO_2 catalyst.

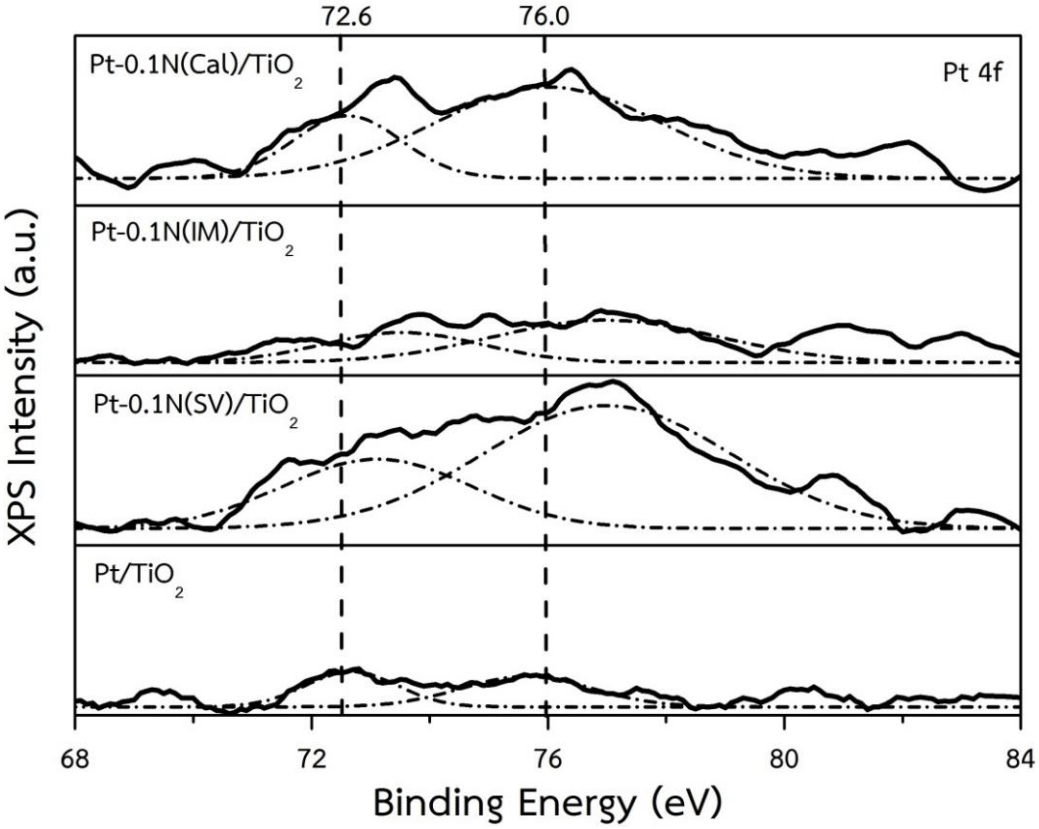

Figure 5.9 XPS spectra for Pt 4f of Pt catalysts with different N-doped TiO_2 support synthesis

The oxidation state of platinum can be determined by XPS technique. Generally, the metallic platinum binding energies were consisted two main peaks which represented Pt^0, Pt^{2+}, and Pt^{4+} as follows by first peak was assigned to $4f_{7/2}$ electrons around 70–71, 72–73 and 74–75 eV , respectively. The second peak was related to $4f_{5/2}$ electrons around 74, 76, and 77–78 eV, respectively [12-14, 35, 47].

The platinum catalysts with and without N-doped TiO_2 supports are illustrated in **Figure 5.9**. All the catalysts were not treated by H_2 before characterization. The XPS binding energy of Pt 4f peak was presented for Pt/TiO_2 at around 74.2 eV and 77.8 eV, for Pt/0.1N(SV)-TiO_2 at around 72.8 eV and 76.9 eV, for Pt/0.1N(IM)-TiO_2 at around 74.6 eV and 77.4 eV, and for Pt/0.1N(Cal)-TiO_2 at around 72.7 eV and 76.0 eV. These peaks were obviously assigned to oxidized platinum and Pt^{2+} species. Ramos-Fernandez et al. [48] have shown the oxidation state of platinum catalysts reduced (at 200 °C) and unreduced under H_2 condition. The Pt^{2+} species was changed and the XPS binding energy were shifted to around the range of Pt^0 species when the catalyst was fully reduced after the reduction treatment. Thus, N-doped TiO_2 synthesis affected to the formation of the Pt species on the sample. Which this conclusion confirm by decreasing of N/Ti ratio in **Table 5.4** when compared with Pt/TiO_2.

Table 5.4 The surface atomic concentration of Pt catalysts with different N-doped TiO_2 support synthesis

Catalysts	Atomic concentration (%)[a]				
	O 1s	Ti 2p	N 1s	Pt 4f	N/Ti ratio
Pt/TiO_2	78.33	21.35	0.00	0.32	0.00
Pt/0.1N(SV)-TiO_2	77.45	19.68	2.57	0.30	0.13
Pt/0.1N(IM)-TiO_2	60.01	37.24	2.54	0.21	0.07
Pt/0.1N(Cal)-TiO_2	78.11	20.42	1.31	0.16	0.06

[a] The calculation based on the XPS binding energy of N 1s at 400 eV

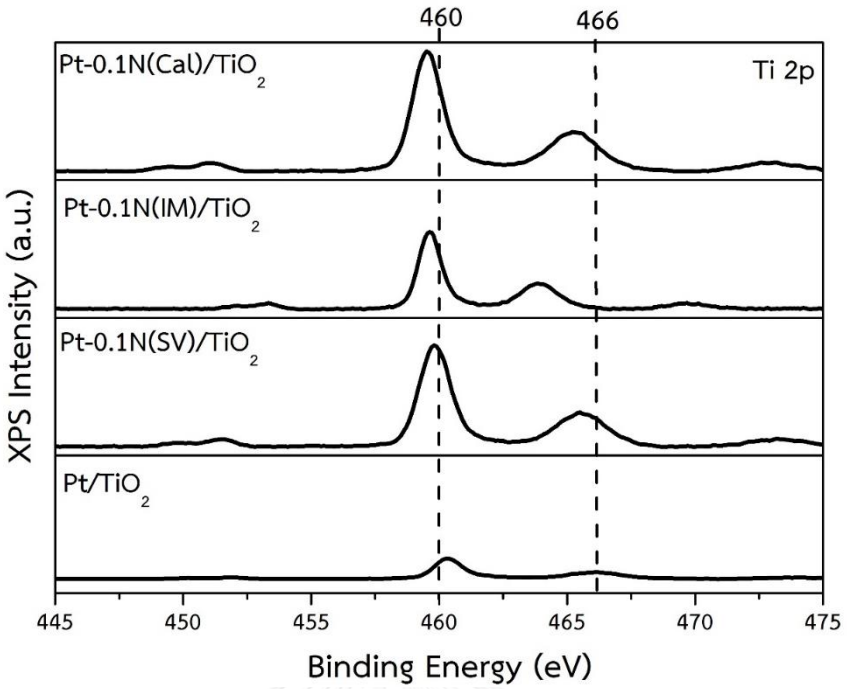

Figure 5.10 XPS spectra for Ti 2p of Pt catalysts with different N-doped TiO_2 support synthesis

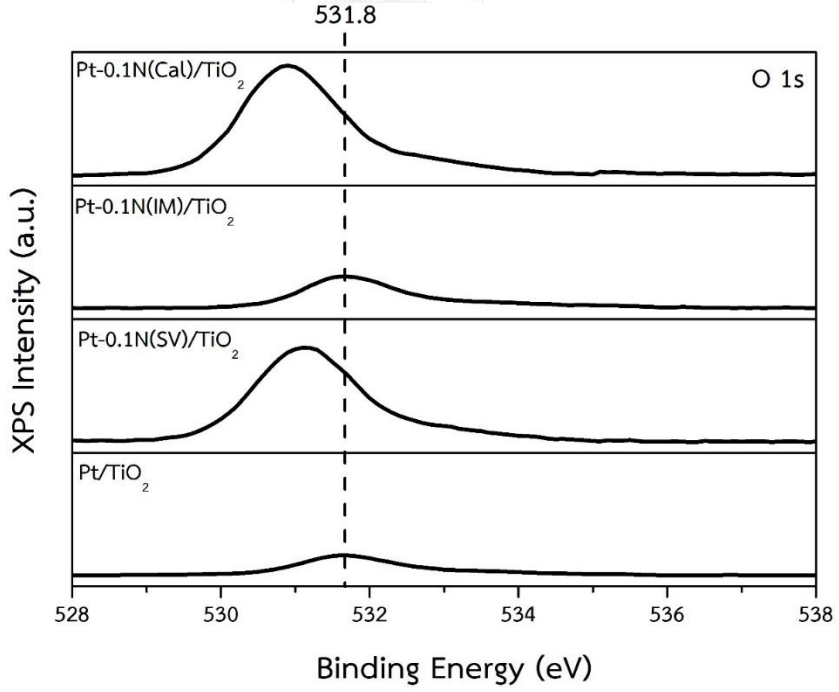

Figure 5.11 XPS spectra for O 1s of Pt catalysts with different N-doped TiO_2 support synthesis

Figure 5.10 and **Figure 5.11** illustrate the XPS spectra of Ti 2p and O 1s of Pt catalysts with different N-doped TiO_2 support synthesis methods. The XPS spectra of Ti 2p consisted of two major peaks around 459 and 465 eV were indicated to the binding energies of Ti $2p_{3/2}$ and Ti $2p_{1/2}$, respectively which were suggested that the Ti^{4+} species in anatase TiO_2. The XPS binding energy of Ti 2p peak was presented for Pt/TiO_2 at around 460.4 eV and 466.0 eV, for Pt/0.1N(SV)-TiO_2 at around 459.8 eV and 465.5 eV, for Pt/0.1N(IM)-TiO_2 at around 459.5 eV and 465.2 eV, and for Pt/0.1N(Cal)-TiO_2 at around 459.5 eV and 465.2 eV. All the binding energies of Pt/N-doped TiO_2 catalysts decrease when compared with Pt/TiO_2 catalyst and suggest that Ti interaction with anions. It relate to electron transfer from N to Ti. The results relate to nitrogen incorporated into the TiO_2 lattice and substituted for oxygen. The XPS spectra of O 1s peak at 531 eV was attributed to the crystal lattice oxygen (Ti-O) in TiO_2 [14, 23, 24, 37, 38, 42, 43, 45]. The XPS binding energy of O 1s peak was presented for Pt/TiO_2 at around 531.8 eV, for Pt/0.1N(SV)-TiO_2 at around 531.0 eV, for Pt/0.1N(IM)-TiO_2 at around 531.8 eV, and for Pt/0.1N(Cal)-TiO_2 at around 531.0 eV. The lower peak suggested that oxygen and nitrogen occurred in the same TiO_2 lattice.

5.1.1.6 H_2-temperature-programmedreduction (H_2-TPR)

The temperature-programmed reduction was determined by H_2-TPR measurements. The catalysts exhibited two hydrogen consumption peaks around 350 and 450 °C. The first peak was the reduction of Pt oxide particles and the second peak was attributed to reduction of Pt species interacting with the TiO_2 support in the form of Pt-TiO_x interface sites [3, 27].

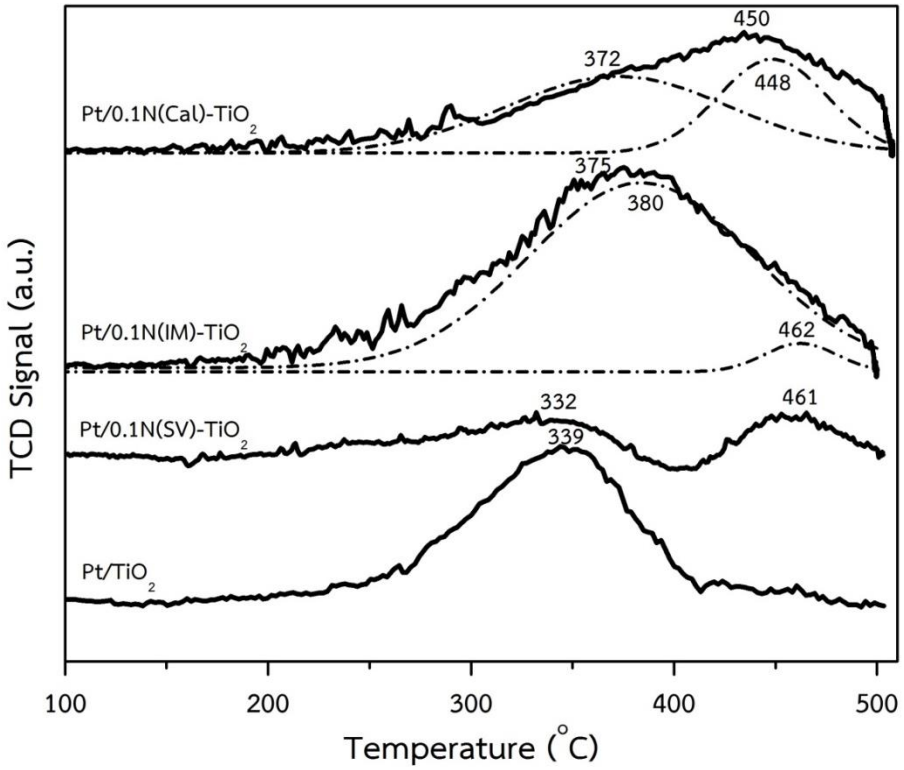

Figure 5.12 H_2-TPR profiles of Pt catalysts with different N-doped TiO_2 supports synthesis

The reduction profiles of catalysts are shown in **Figure 5.12**. The Pt/0.1N(SV)-TiO_2 showed stronger metal-support interaction as they exhibited higher reduction temperature peaks at 461 °C. The 1st reduction peak of Pt/0.1N (IM)-TiO_2 and Pt/0.1N(Cal)-TiO_2 also shifted toward higher temperature. It is suggested that increasing amount of nitrogen on the TiO_2 resulted in the formation of more difficult to reduce Pt-TiO_x species. The reduction profiles of Pt/0.1N (IM)-TiO_2 and Pt/0.1N(Cal)-TiO_2 could be deconvoluted into two peaks at 384, 462 °C and 372, 448 °C, respectively. The H_2 consumption of catalyst was calculated from the main peak area as illustrated in **Table 5.5**. The lower reduction ratio of Pt oxide particles and H_2 consumption ratios of Pt/Pt–TiO_x was confirmed that Pt/0.1N(SV)-TiO_2 exhibited the stronger metal-support interaction than the other catalysts.

Table 5.5 H_2 consumption ratios of Pt/Pt–TiOx from H_2-TPR profiles with different catalysts

Catalysts	Reduction ratio of Pt oxide particle	Pt/Pt-TiO_x
Pt/TiO_2	1	-
Pt/0.1N-TiO_2	0.20	1.65
Pt/0.1N(IM)-TiO_2	1.34	14.71
Pt/0.1N(Cal)-TiO_2	0.66	1.67

5.1.1.7 Infrared spectroscopy of adsorbed CO (CO-IR)

The characteristics of the surface of dispersed Pt particles were examined by the FT-IR spectra of adsorbed CO on the platinum catalysts are shown in **Figure 5.13**. The CO absorbance was presented in the range of frequency of 2,000–2,100 cm^{-1} on the investigated catalysts. The type of CO linearly adsorbed on low-coordination Pt atom (such as kink, edge, and corner) on edge sites was characterized by the adsorption bands at around 2,050 cm^{-1} which assigned to linear-type adsorbed CO formed mainly on small Pt particles [28]. The Pt terrace was decreased while the number of Pt–TiO_x sites increased and the Pt on corner occurred with small Pt particles. It was reported by Pisduangdaw et al. [3, 27] and Yoshida et al. [28] that Pt nanoparticle supported on small TiO_2 crystallites exposed low coordinated Pt sites which promoted the electron donation from the TiO_2 support to Pt particles.

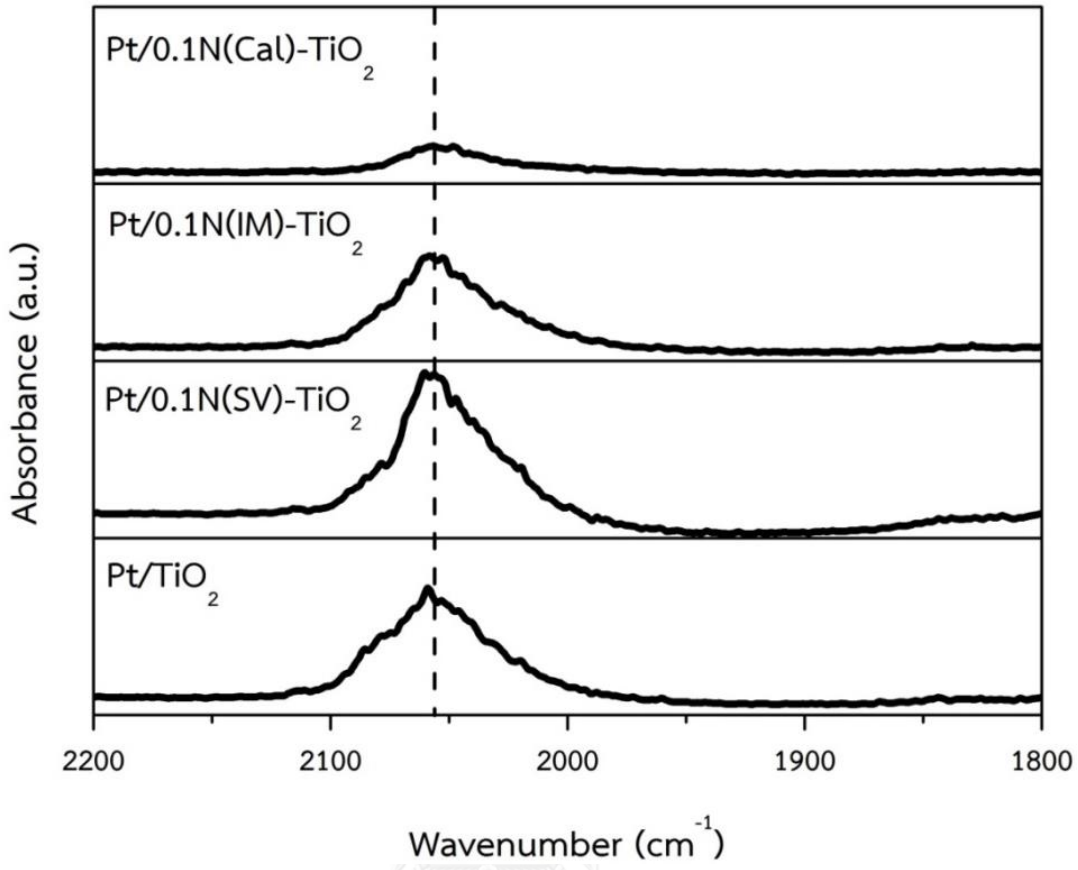

Figure 5.13 CO-IR absorption bands of Pt catalysts with different N-doped TiO_2 supports synthesis

จุฬาลงกรณ์มหาวิทยาลัย
Chulalongkorn University

In this work, the absorption band of catalysts appeared at 2,055, 2,053, 2,052, and 2,051 cm^{-1} as Pt/TiO_2, Pt/0.1N (SV)-TiO_2, Pt/0.1N (IM)-TiO_2, and Pt/0.1N (Cal)-TiO_2, respectively. At the absorption band of the CO adsorbed on Pt is red-shifted to extended on support follow by Pt/0.1N (SV)-TiO_2 > Pt/TiO_2 > Pt/0.1N (IM)-TiO_2 > Pt/0.1N (Cal)-TiO_2. All the catalyst absorption bands were attributed to only CO linearly adsorbed on Pt atom, small TiO_2 crystallites, electron transfer from TiO_2 support, and could be implied the Pt corner presented on the catalyst. The results of these geometrical and electrical factors affected the adsorption of the nitro group on catalyst surface.

5.1.1.8 CO chemisorption

The amounts of active Pt particles on the Pt/TiO_2 catalyst surface were calculated from the CO chemisorption results based on the assumption that one carbon monoxide molecule adsorbs on one Pt site and the results are shown in **Table 5.6**. The metal dispersion was in the range of 13-68 % as determined by CO chemisorption. The Pt dispersion decreased in the order: Pt/0.1N (SV)-TiO_2 > Pt/0.1N (IM)-TiO_2 > Pt/0.1N (Cal)-TiO_2, which were consistent to the results of Pt nanoparticles from CO-IR absorption bands and average particles size. The highest Pt dispersion was obtained on the solvothermal method. Nitrogen doped into TiO_2 structure led to nitrogen covered and the inhibition of Pt particle interacted with TiO_2 surface [3, 27].

Table 5.6 Pt Dispersion (%) of Pt catalysts with different N-doped TiO_2 supports synthesis

Catalysts	Pt Dispersion (%)
Pt/TiO_2	68.5
Pt/0.1N(SV)-TiO_2	64.1
Pt/0.1N(IM)-TiO_2	53.5
Pt/0.1N(Cal)-TiO_2	13.5

จุฬาลงกรณ์มหาวิทยาลัย
Chulalongkorn University

5.1.1.9 Transmission electron microscopy (TEM)

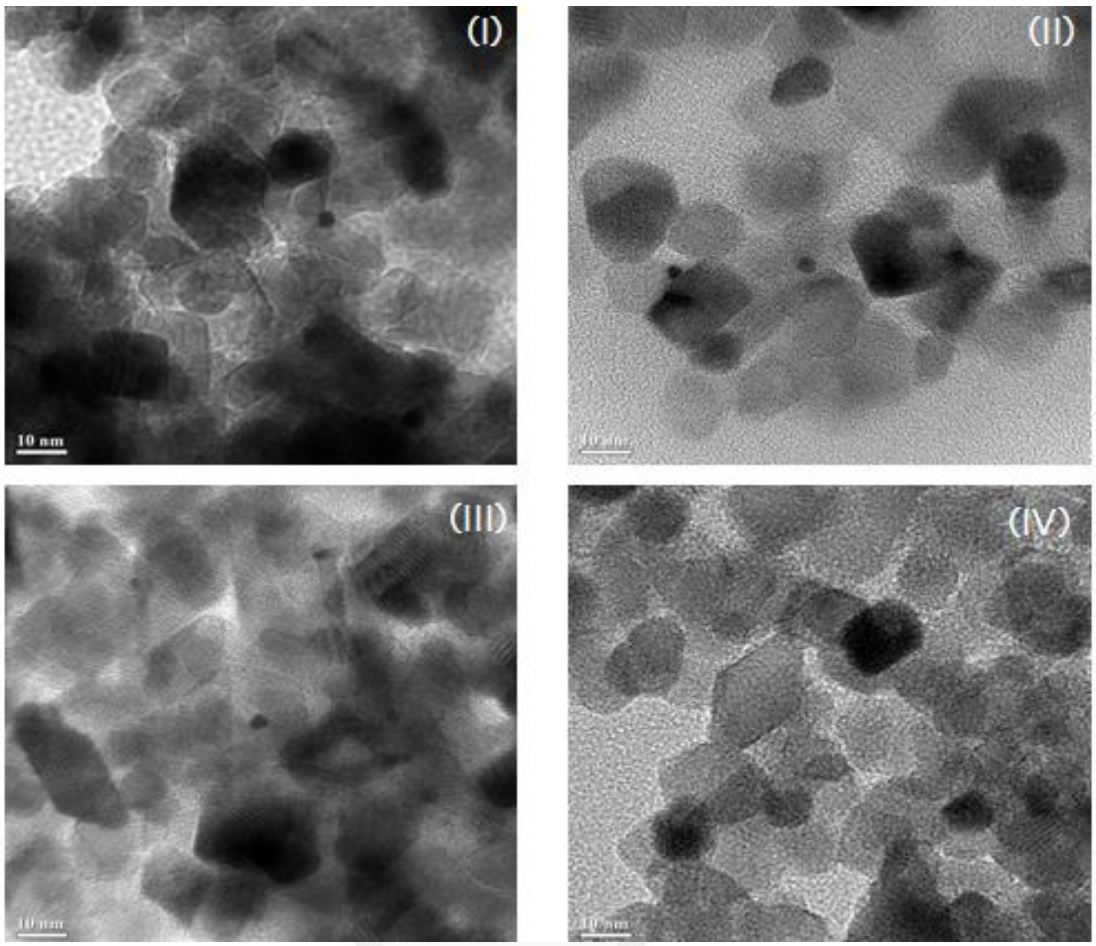

Figure 5.14 TEM micrographs of Pt catalyst as a follow by Pt/TiO_2(I), Pt/0.1N(SV)-TiO_2(II), Pt/0.1N(IM)-TiO_2(III), and Pt/0.1N(Cal)-TiO_2(IV)

The morphology of the Pt/TiO_2 catalysts with different N-doped TiO_2 supports were characterized by transmission electron microscope and the results are shown in **Figure 5.14**. The nearly spherical particles shape were found on catalyst samples and the average particles size of Pt/TiO_2, Pt/0.1N(SV)-TiO_2, Pt/0.1N(IM)-TiO_2 as shown in **Table 5.7** was found in the range of 3.3-3.8 nm. They were not significantly different and Pt/0.1N(Cal)-TiO_2 not found Pt particle. These results were confirmed that small Pt nanoparticles occurred on TiO_2 supports. However, low amount of Pt particles were observed in TEM micrographs owing to low amount of metal loading (0.5 wt% Pt) [3, 7, 33, 35, 36, 49].

Table 5.7 Average particles size of Pt catalyst with different N-doped TiO_2 support synthesis

Catalysts	Average particles size
Pt/TiO_2	3.51
$Pt/0.1N(SV)-TiO_2$	3.33
$Pt/0.1N(IM)-TiO_2$	3.83
$Pt/0.1N(Cal)-TiO_2$	-

5.1.2 Catalytic activity

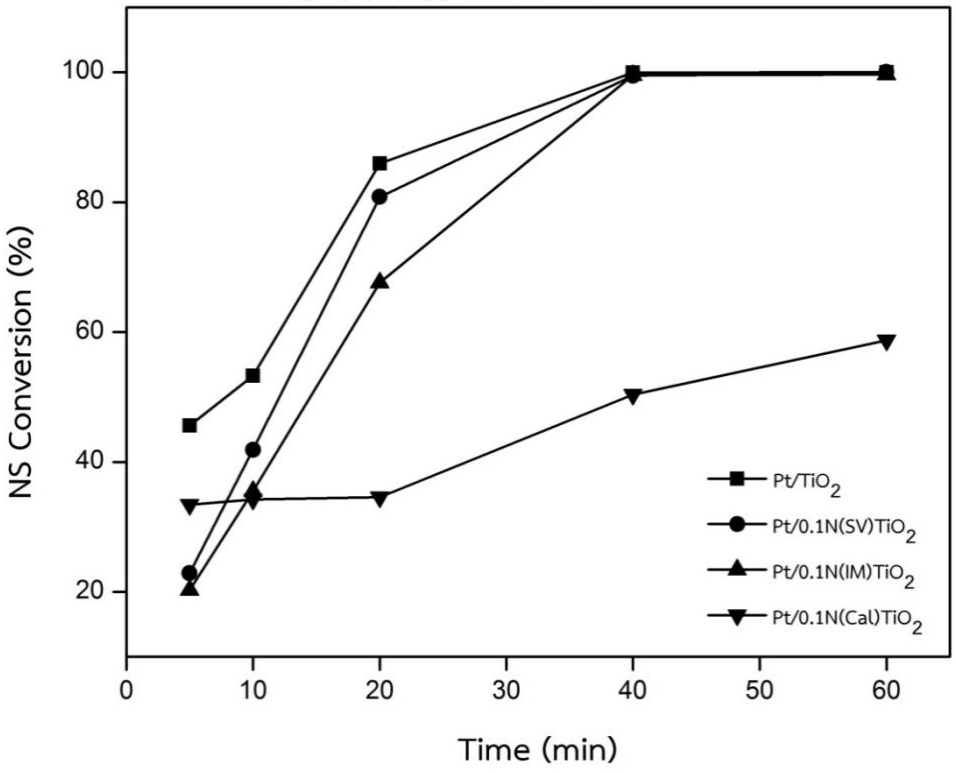

Figure 5.15 Conversion of 3-nitrostyrene of Pt catalysts with different N-doped TiO_2 supports synthesis

Under the reaction conditions used, the products of the NS hydrogenation were VA as a design product, ENB, EA, and other intermediate products such as N-hydroxylamines. Hydrogenation of NS occurs via two reaction pathways from hydrogenation of the C=C double bond and the nitro group N=O. The catalytic performances of Pt catalysts with different N-doped TiO_2 supports in the liquid phase hydrogenation of NS at 40 ^{o}C, 2 MPa, using 50 ml stainless steel autoclave reactor and various reaction time (5, 10 20, 40, and 60 min) are reported.

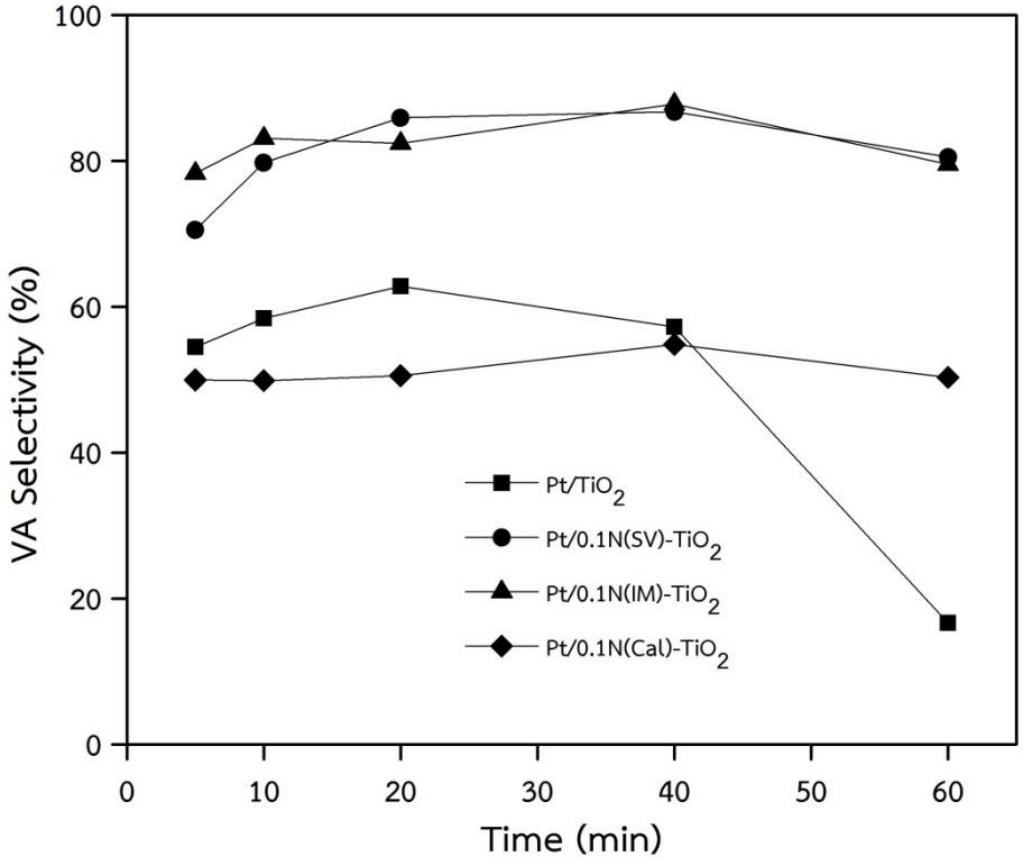

Figure 5.16 Selectivity of 3-vinylaniline of Pt catalysts with different N-doped TiO_2 supports synthesis

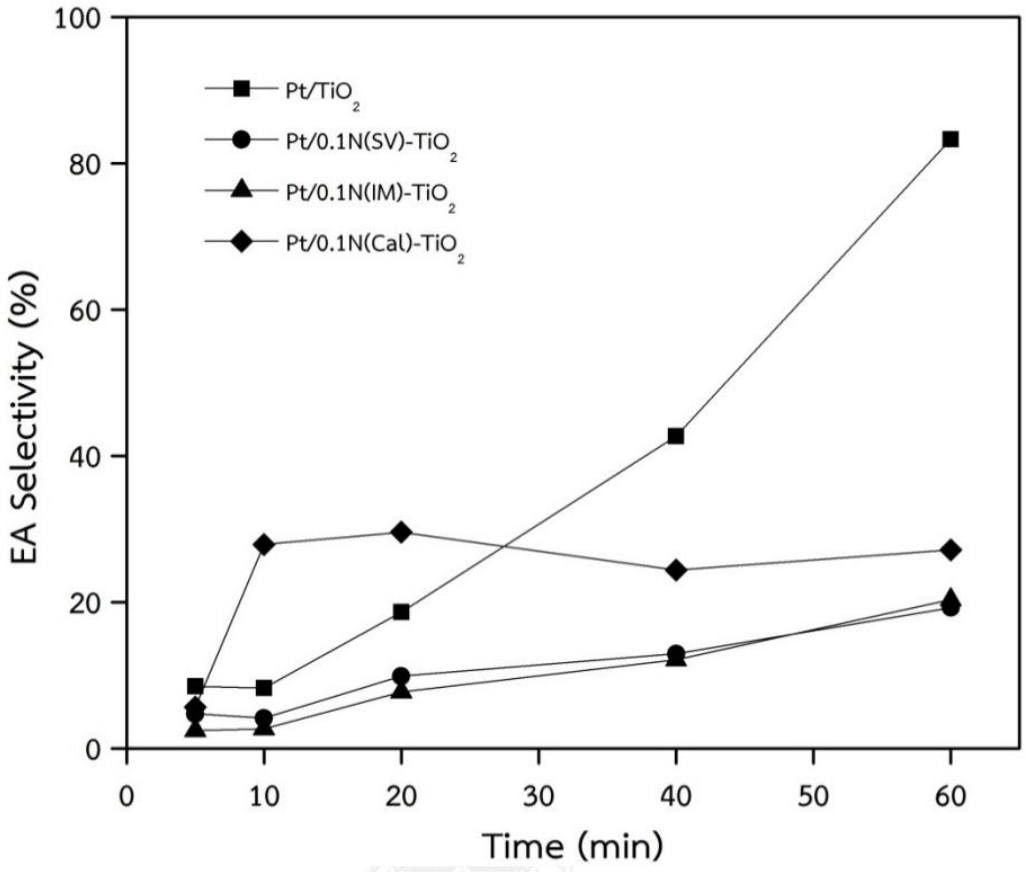

Figure 5.17 Selectivity of 3-ethylaniline of Pt catalysts with different N-doped TiO_2 supports synthesis

จุฬาลงกรณ์มหาวิทยาลัย
Chulalongkorn University

The catalytic performance of 3-nitrostyrene in liquid phase hydrogenation as a function of reaction time with different N-doped TiO_2 supports synthesis are illustrated in **Figure 5.15 – Figure 5.20**. The highest NS conversion in **Figure 5.15** was obtained over the Pt/TiO_2 catalyst which corresponded to the highest Pt dispersion and H_2 TPR profile that suggested that lowest reduction temperature than other catalysts. For the Pt/N-doped on TiO_2 support, the Pt dispersion decreased so the NS conversion was slightly decreased from Pt/TiO_2. However, this was not the case for the Pt/0.1N(Cal)-TiO_2 which it had the lowest the Pt dispersion and NS conversion. The difference of N-doped TiO_2 supports synthesis affected to these results. The UV-visible results indicated amount of nitrogen on the samples and inserted into TiO_2 lattice as follows Pt/0.1N(Cal)-TiO_2 > Pt/0.1N(IM)-TiO_2 > Pt/0.1N(SV)-TiO_2. And the TEM micrographs in

Figure 5.14 (IV) not showed Pt particles on the TiO_2 support. Therefore, it could be implied that the N-doped TiO_2 inhibited Pt metal attached on support surface. However, complete conversion of NS can be obtained on the Pt/TiO_2, Pt/0.1N(SV)-TiO_2, and Pt/0.1N(IM)-TiO_2 at 40 minutes. It was associated to small Pt particles with linear-type adsorbed CO formed on samples.

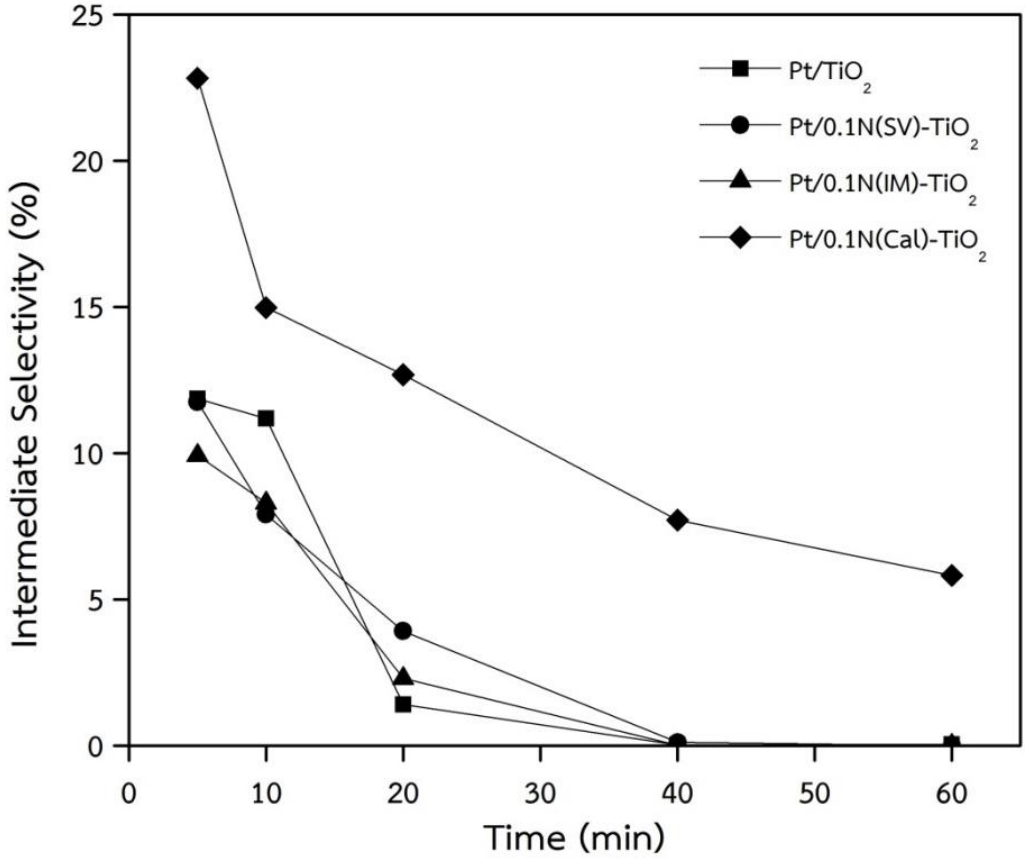

Figure 5.18 Selectivity of intermediate of Pt catalysts with different N-doped TiO_2 supports synthesis

Figure 5.16 shows the selectivity of 3-vinylaniline of catalysts as a function of reaction time. The selectivity of VA was significantly improved on the Pt/N(SV)-TiO_2 and Pt/N(IM)-TiO_2 which showed similar performances, regardless of the amount of NMP added or the preparation method used. The performance of Pt/0.1N-TiO_2 as a function of reaction time is shown in **Figure 5.16**. It can be seen that VA selectivity of Pt/N(SV)-TiO_2 and Pt/N(IM)-TiO_2 even after complete conversion of NS at 40 min reaction time

was maintained at around 87 and 88%, respectively. As observed in **Figure 5.15,** when prolonging the reaction time to 60 min, a slight decrease in VA selectivity to 81 and 80% were observed, respectively. The Pt/TiO_2 and $Pt/N(Cal)-TiO_2$ showed rather similar performances with low VA selectivity. For the Pt/TiO_2 after complete conversion of NS, the VA selectivity dropped drastically from 57% to 17%.

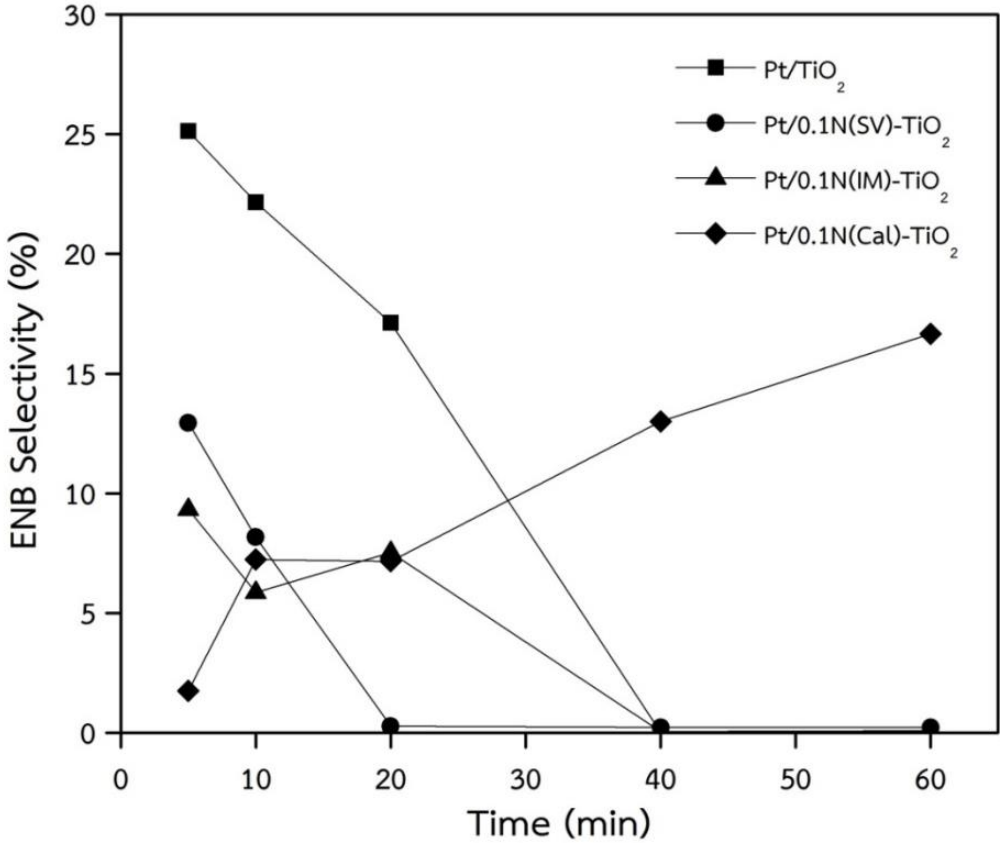

Figure 5.19 Selectivity of 3-ethylnitrobenzene of Pt catalysts with different N-doped TiO_2 supports synthesis

The results from **Figure 5.16 – 5.19** confirmed that the $Pt/N-TiO_2$ was more selective to VA than the Pt/TiO_2. The VA selectivity was stable while ENB, EA, and intermediate selectivity of $Pt/N-TiO_2$ catalyst were decreased or low selective. Nevertheless, the ENB and EA selectivity of Pt/TiO_2 was increased and was high intermediate selectivity than $Pt/N-TiO_2$ catalyst. Overall, the N-doped method can improve the catalyst performances of Pt/TiO_2 in the NS hydrogenation towards VA selectivity.

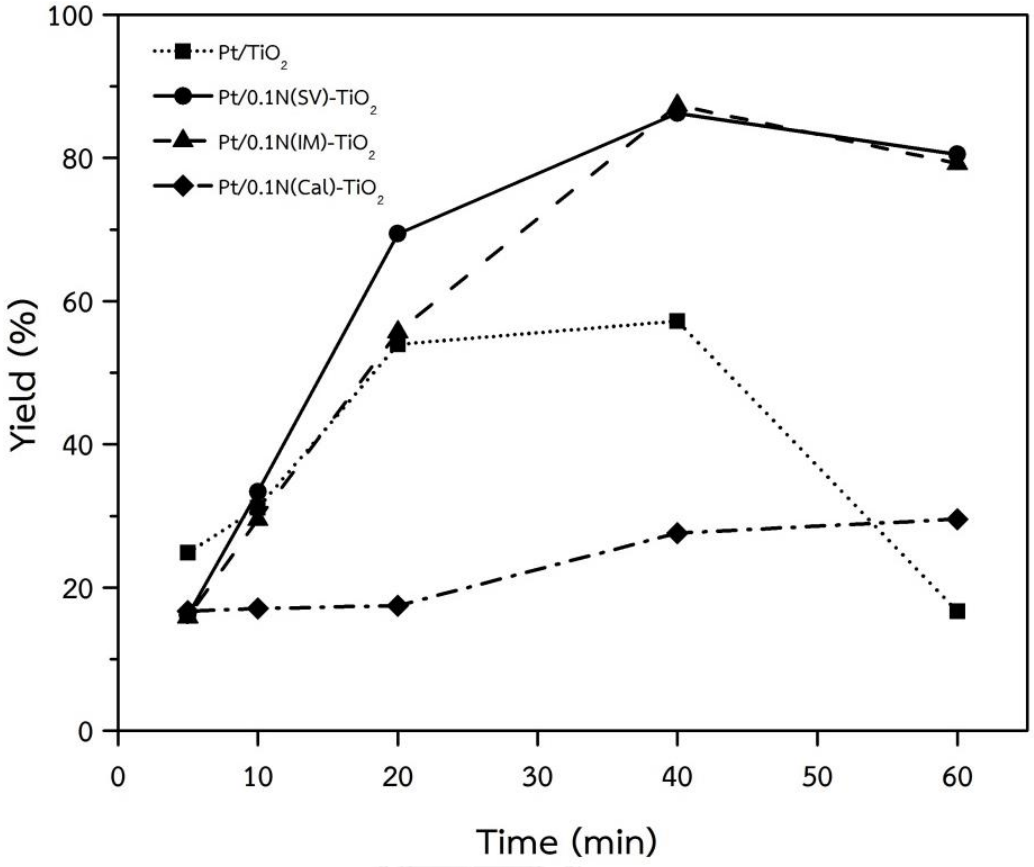

Figure 5.20 VA yield of Pt catalysts with different N-doped TiO_2 supports synthesis

Them the catalyst characterization results and the catalytic performances it is suggested that high performance was related to the strong interaction of Pt–TiO_x and some coverage of Pt active sites by TiO_x species, low-coordination Pt atom, as well as the presence of small Pt nanoparticles, and amount of N-doped on the catalysts [3, 35, 36]. The results from FT-IR, XPS, and UV-visible of the samples confirmed the presence of N species and the effect of the amount of nitrogen on the catalyst performances. It is also possible that the N-doped TiO_2 can trap electron from the support and transfer it to the Pt metal. Moreover, the presence of nitrogen on support surface could inhibit the hydrogenation of VA to EA. The hydrogenation of the vinyl group became more difficult while promoted the hydrogenation of nitro group. The adsorption/desorption of VA on Pt metal was altered [50]. The Pt/0.1N-TiO_2 showed the best catalyst performance in terms of high NS conversion and VA selectivity. The

ENB selectivity at 20 minutes was closed to 0%, which was faster than the other catalysts as shown in **Figure 5.19** and indicated on higher yield as a function of time than other catalysts is in **Figure 5.20**.

5.2 The effect of various amounts of N-doped TiO_2 supports

5.2.1 Catalysts characterization

5.2.1.1 XRD

The chemical phase and crystal structure of Pt/N-TiO_2 catalysts prepared by various amount of nitrogen doped TiO_2 with different methods were characterized by X-ray diffraction technique and measured by carried out at the diffraction angles (2θ) between 20° and 80°. The crystallite size was determined from the diffraction peaks by using Scherrer Equation.

Figure 5.21, Figure 5.22, and Figure 5.3 shows the XRD patterns of Pt/N-TiO_2 catalysts prepared by different methods with various amounts of nitrogen. The anatase phase TiO_2 was confirmed by the XRD characteristic peaks at 25°, 36°, 49°, 54°, 63°, 69° and 75° without other phases of TiO_2. The crystallite size, peak position of anatase (101) TiO_2, d-spacing, and the lattice parameters for TiO_2 and N-doped TiO_2 supports are given in **Table 5.8 – 5.10**. The position peaks of anatase (101) of Pt/N-TiO_2 are shown at 2θ around 25.16° - 25.45°, indicating that increaseding N/Ti ratios did not change the lattice properties of Pt/N(SV)-TiO_2. The diffaction angle was not trened for Pt/N(IM)-TiO_2, and increased for the Pt/N(Cal)-TiO_2. It is suggested that impregnation method could dope nitrogen into the TiO_2 lattice more than solvothermal method. The d-spacing of Pt/N-TiO_2 were not trened with increasing amount of N/Ti ratio in solvothermal and impregnation without calcination method but it increasing in impregnation with calcination method, due to some part of nitrogen insert into TiO_2 lattice by calcination process. And the trend of crystallite size was increased with increasing amount of N/Ti ratio in Pt/N-TiO_2. which it is indicated of increasing N element in TiO_2 lattice. Therefore, all of the methods used could decorate N element on TiO_2 surface and the N/Ti ratio increased with increasing NMP amounts [42].

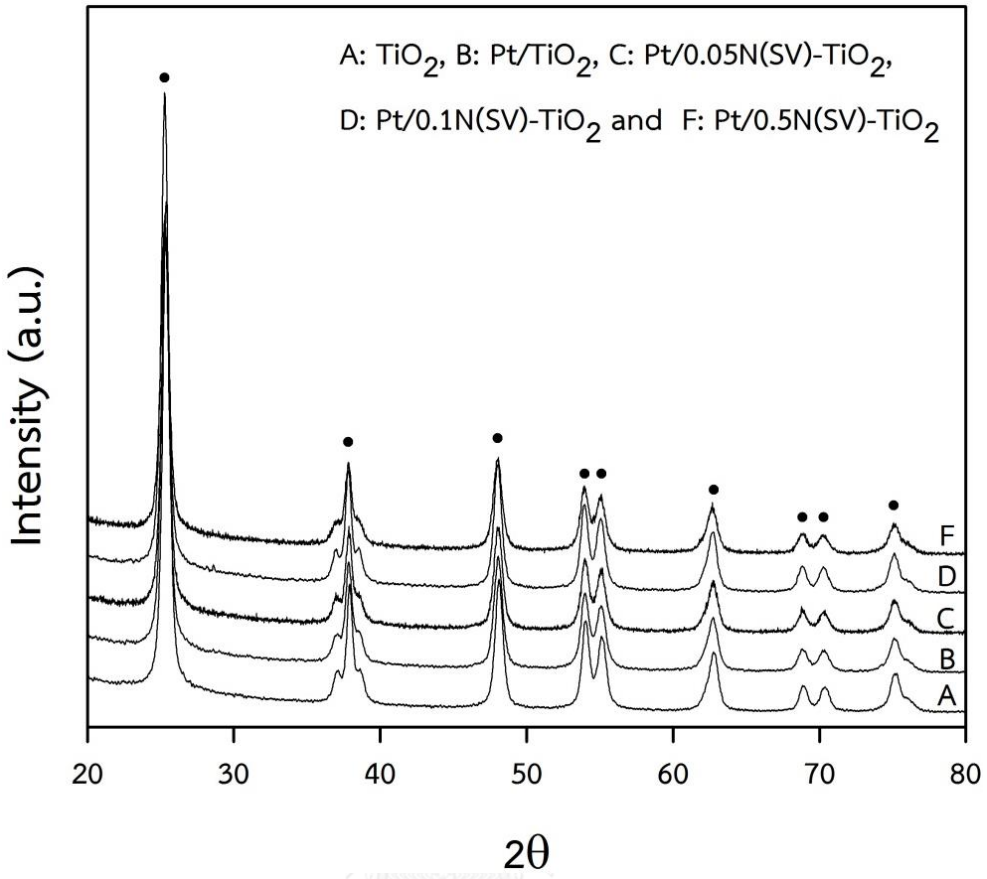

Figure 5.21 XRD patterns of Pt/N(SV)-TiO_2

Table 5.7 The peak position of anatase (101) TiO2, d-spacing and the lattice parameters of Pt/N(SV)-TiO_2

Catalysts	Crystallite size (nm)	Peak position of anatase (101) (2θ, degree)	d-spacing (nm)	Lattic parameter[a] (A^0)		
				a (=b)	c	c/a
Pt/0.05N(SV)-TiO_2	12.52	25.28	0.3519	3.7810	9.3534	2.47
Pt/0.1N(SV)-TiO_2	13.88	25.26	0.3522	3.7886	9.5068	2.51
Pt/0.5N(SV)-TiO_2	17.44	25.28	0.3519	3.7871	9.5874	2.53

[a] calculated from Bragg's law using the diffraction peaks of anatase (101) TiO_2.

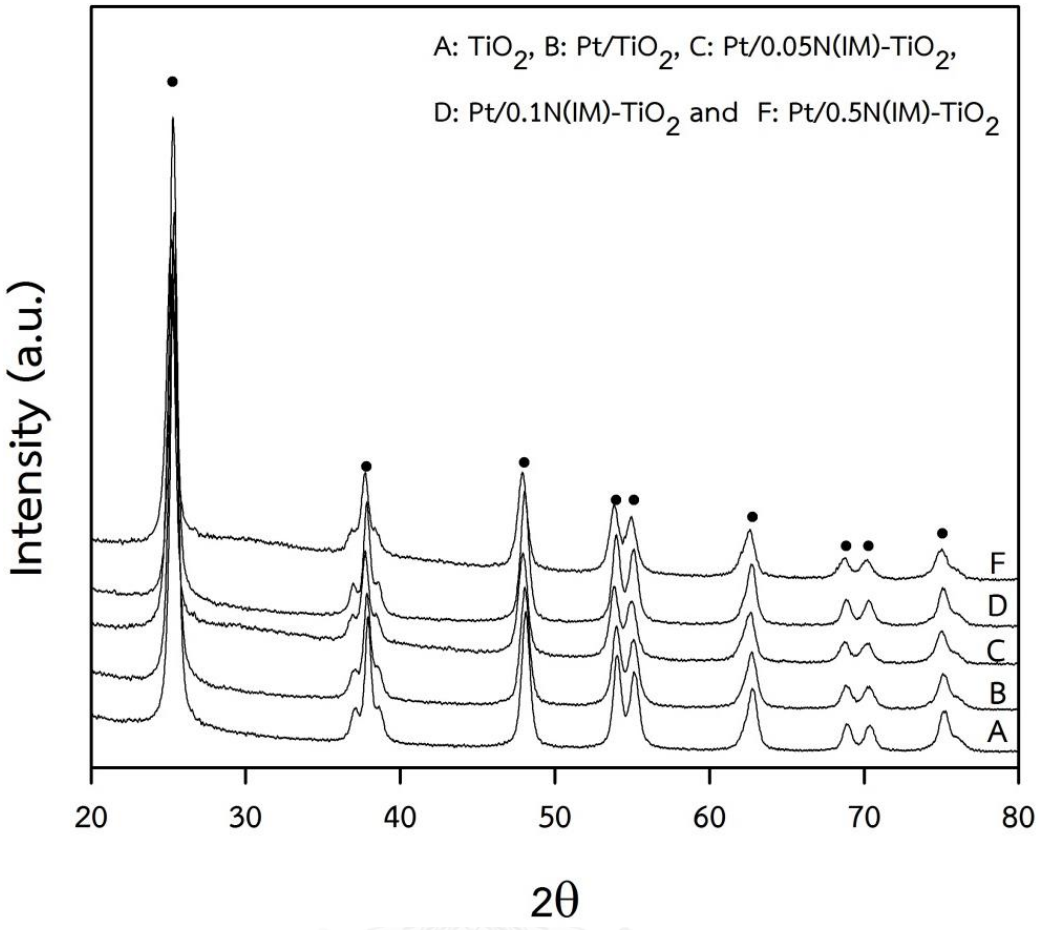

Figure 5.22 XRD patterns of Pt/N(IM)-TiO_2

Table 5.8 The peak position of anatase (101) TiO2, d-spacing and the lattice parameters of Pt/N(IM)-TiO_2

Catalysts	Crystallite size (nm)	Peak position of anatase (101) (2θ, degree)	d-spacing (nm)	Lattic parameter[a] (A^0)		
				a (=b)	c	c/a
Pt/0.05N(IM)-TiO_2	10.96	25.18	0.3534	3.7855	9.5555	2.52
Pt/0.1N(IM)-TiO_2	11.83	25.28	0.3519	3.7825	9.6049	2.54
Pt/0.5N(IM)-TiO_2	14.00	25.16	0.3536	3.7932	9.7282	2.56

[a] calculated from Bragg's law using the diffraction peaks of anatase (101) TiO_2.

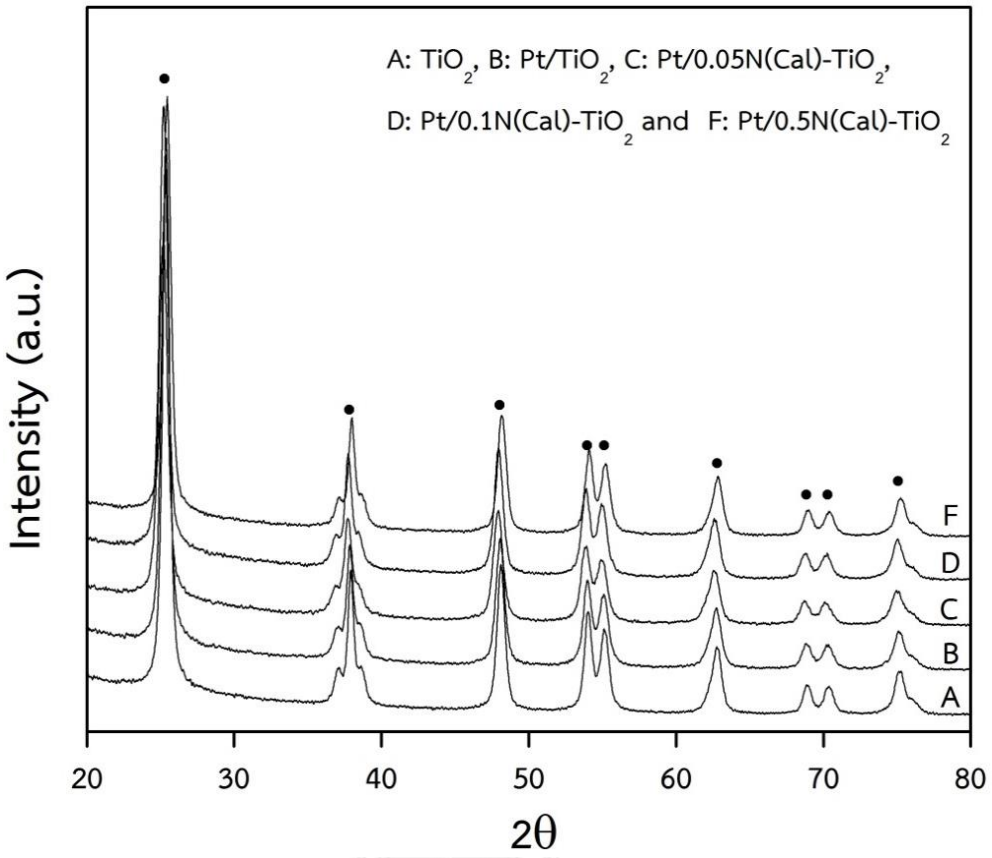

Figure 5.23 XRD patterns of Pt/N(Cal)-TiO_2

Table 5.9 The peak position of anatase (101) TiO2, d-spacing and the lattice parameters of Pt/N(Cal)-TiO_2

Catalysts	Crystallite size (nm)	Peak position of anatase (101) (2θ, degree)	d-spacing (nm)	Lattic parameter[a] (A^0)		
				a (=b)	c	c/a
Pt/0.05N(Cal)-TiO_2	10.37	25.20	0.3531	3.7963	9.7258	2.56
Pt/0.1N(Cal)-TiO_2	11.79	25.20	0.3531	3.7947	9.6345	2.54
Pt/0.5N(Cal)-TiO_2	12.41	25.45	0.3497	3.7901	9.7107	2.56

[a] calculated from Bragg's law using the diffraction peaks of anatase (101) TiO_2.

5.2.1.2 Fourier transforms infrared spectroscopy (FT-IR)

The FT-IR spectra of Pt/N-TiO_2 catalysts prepared by various amounts of nitrogen doped TiO_2 with different methods were investigated by Fourier transform infrared spectroscopy with a transmittance mode. The results are shown in **Figure 5.24 - 5.26**. According to respectively [21, 24, 38, 40-43] the Ti-O stretching vibration in the TiO_2 lattice was found at 710 cm^{-1} and the hydroxyl of Ti-OH bonds appeared as broad band around wavenumbers 3350 cm^{-1}. The bending vibration of O-H and N-H was found at 1640 cm^{-1}. The IR peaks corresponding to the C-H stretching, vibration of surface adsorbed NO_3 and Ti-N were indicated at 2350 cm^{-1}, 1420 cm^{-1} and 1280 cm^{-1}.

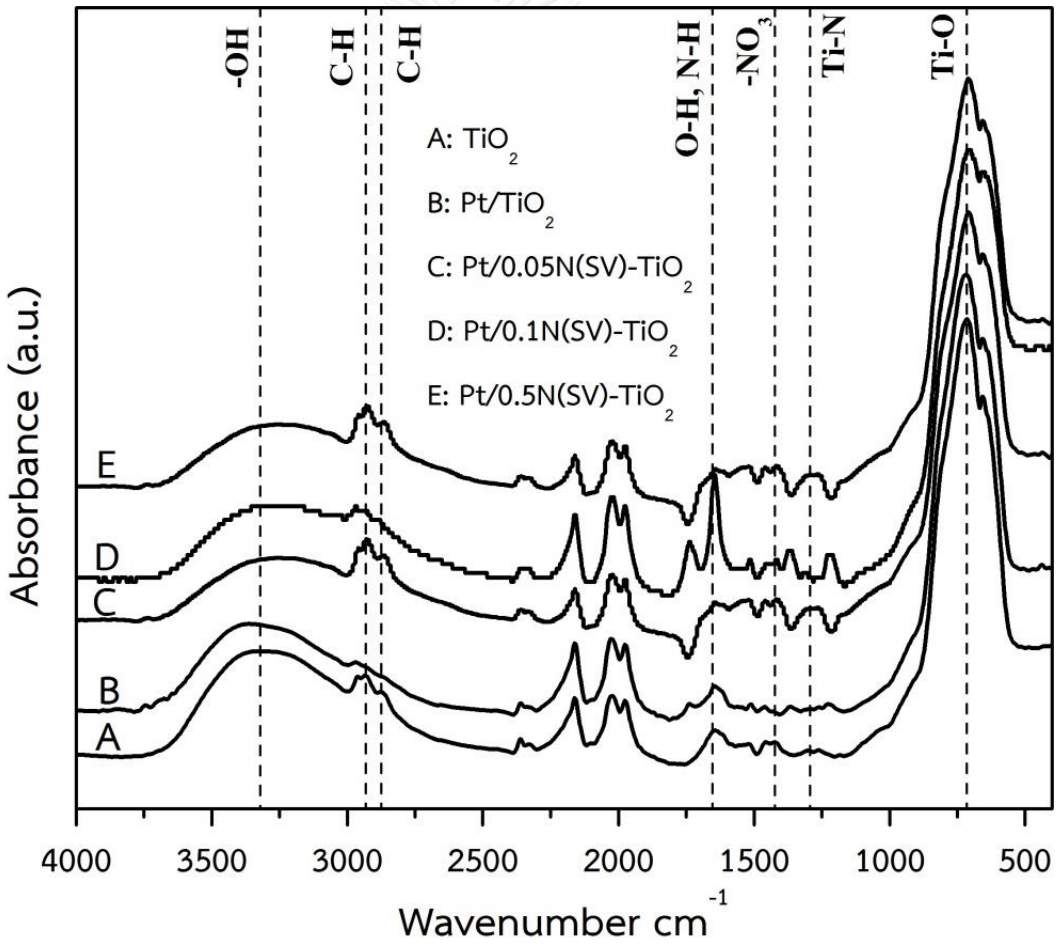

Figure 5.24 FT-IR spectra of Pt/N(SV)-TiO_2

The IR peaks at 2350 cm^{-1}, 1420 cm^{-1} and 1280 cm^{-1} with different support synthesis methods were detected and corresponded to the characteristics of the C-H stretching, vibration of surface adsorbed NO_3 and Ti-N. These bands were related to the incorporation of N-species in the N-doped TiO_2 samples. Considering the results of each method, Pt/N(SV)-TiO_2 and Pt/N(IM)-TiO_2 were not significant different when increased the amount of N/Ti ratio increased. The absorbance peaks were increased.

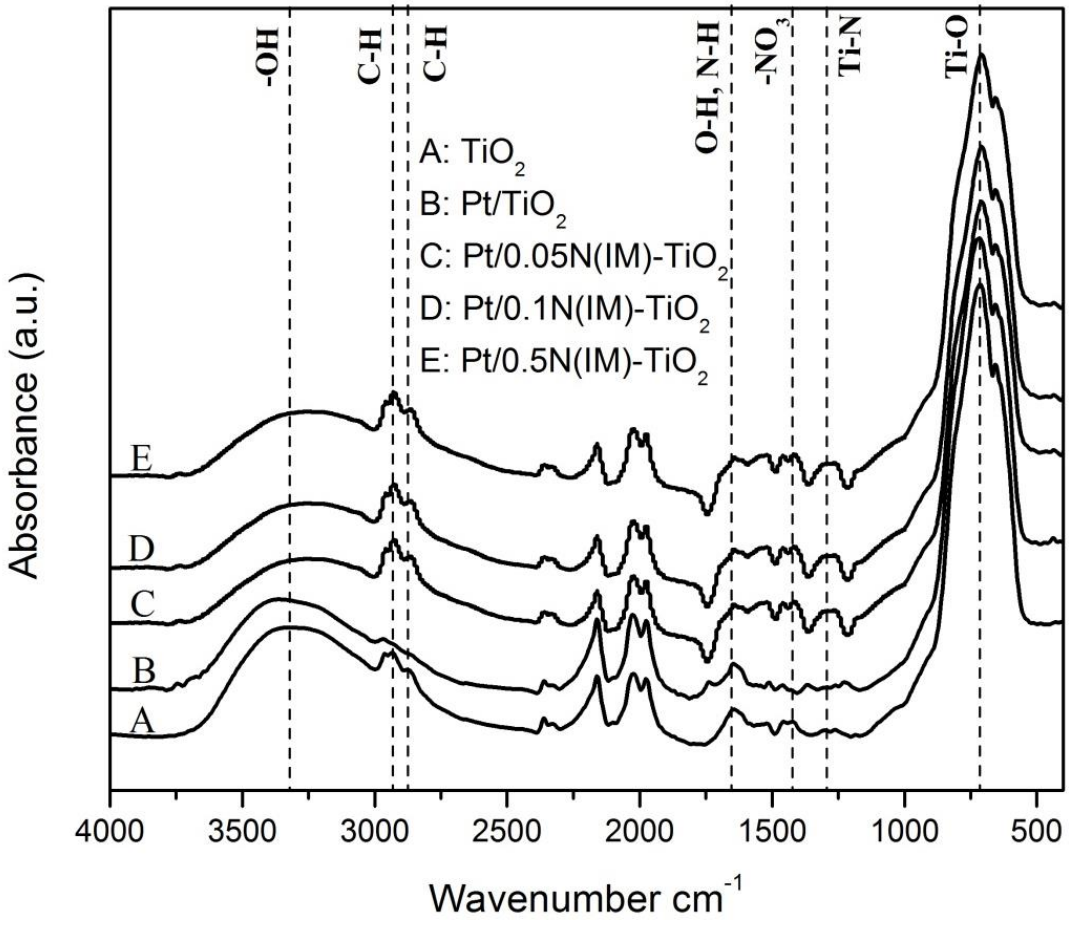

Figure 5.25 FT-IR spectra of Pt/N(IM)-TiO_2

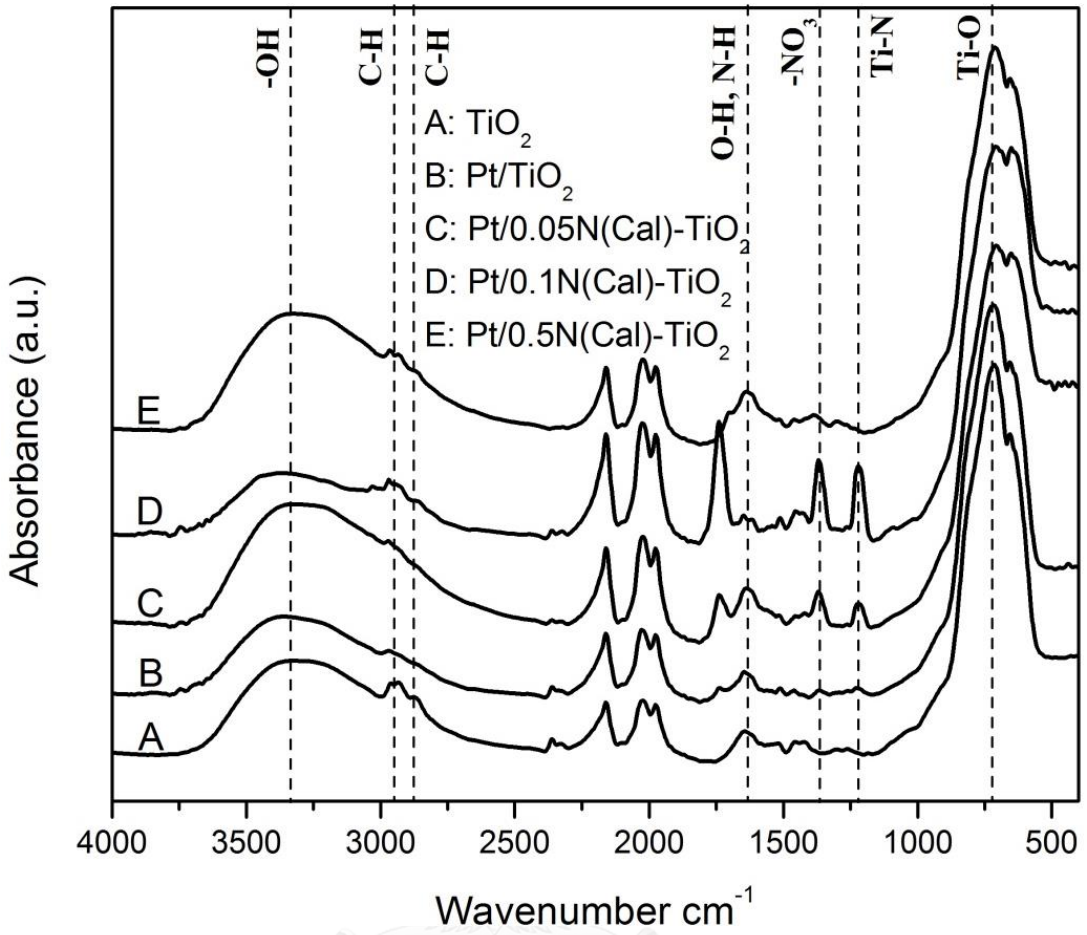

Figure 5.26 FT-IR spectra of Pt/N(Cal)-TiO_2

จุฬาลงกรณ์มหาวิทยาลัย
Chulalongkorn University

5.2.1.3 UV-Visible spectrophotometer (UV-Vis)

The N-doped TiO_2 structures were investigated by the UV-visible spectroscopy. The UV–visible spectra of the Pt/N-TiO_2 samples are presented in **Figure 5.27–5.29**. The UV–visible light absorption spectra results of Pt/N-TiO_2 catalysts with different of amount N-doping synthesis methods, the TiO_2 absorbance was in the region of 400-500 nm. A significant shift of the absorbance to the visible-light region implied that nitrogen was doped into the TiO_2 so that they exhibited the strong visible-light absorbance ability. The absorbance of visible light has been improved after the doping of the nitrogen in TiO_2, which is of great importance for its practical application [11-13, 17, 18, 23, 37, 38, 41, 43-45].

Considering the preparation methods, for the solvothermal method as shown in **Figure 5.27**, the results for Pt/0.05N(SV)-TiO_2 and Pt/0.1N(SV)-TiO_2 were similar to the Pt/TiO_2, owing to the low amount of N/Ti ratio of the N-doped samples and that solvothermal method may inhibit interaction of N-doped TiO_2. The absorbance of Pt/0.5N(SV)-TiO_2 was shifted compared to the Pt/0.05N(SV)-TiO_2 and Pt/0.1N(SV)-TiO_2. Thus, increasing the amount of N/Ti ratio in Pt/0.5N-TiO_2, significant affected visible-light adsorption and nitrogen inserted into TiO_2 structure.

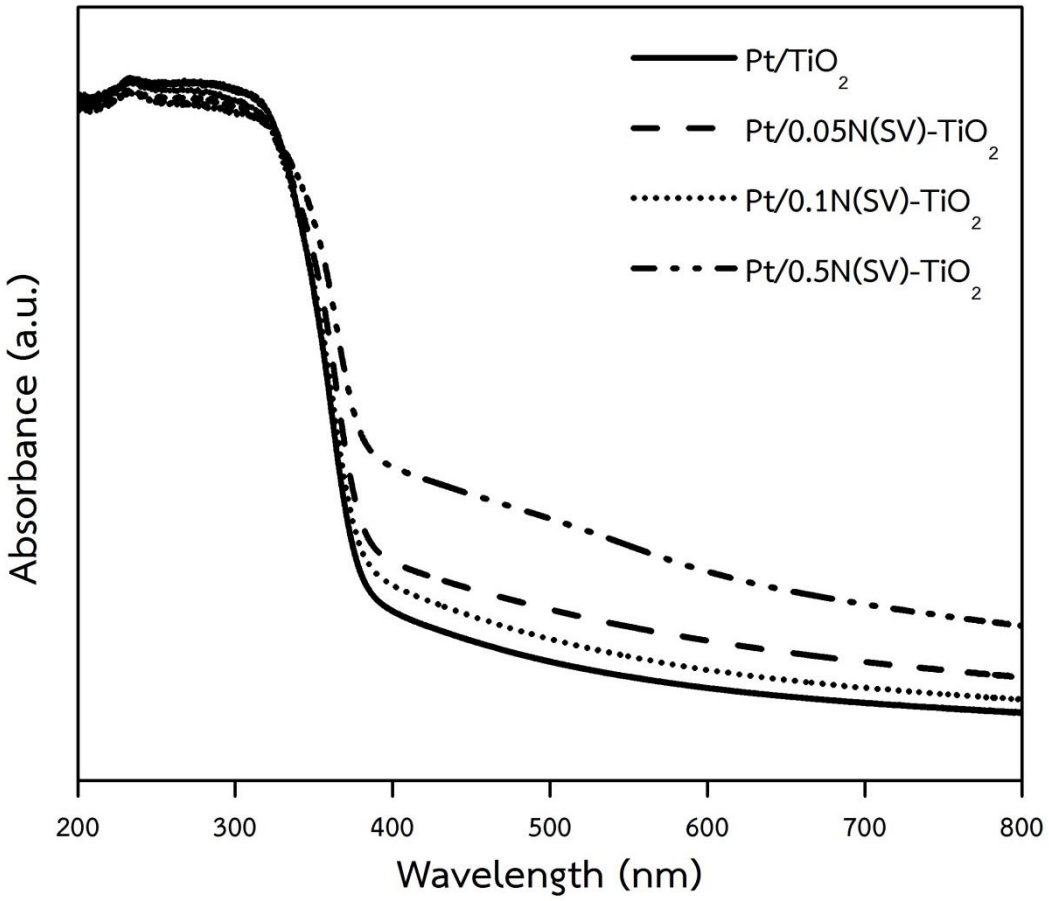

Figure 5.27 UV–visible of Pt/N(SV)-TiO_2

For the impregnation without calcination is in **Figure 5.28**. Although the visible-light adsorption was shifted but they were no significant differences among the samples with different N/Ti ratios. It could be implied that an appropriate amount of nitrogen could be doped on the support and inserted into TiO_2 lattice. For the impregnation with calcination, the results are shown in **Figure 5.29**. The absorbance was increased with increasing amount of N/Ti ratio. Thus, the results confirmed N-doed TiO_2 in catalyst particles and synthesis method has an effect to nitrogen doped into TiO_2 structure. The impregnation with calcination method shows more effect than the others.

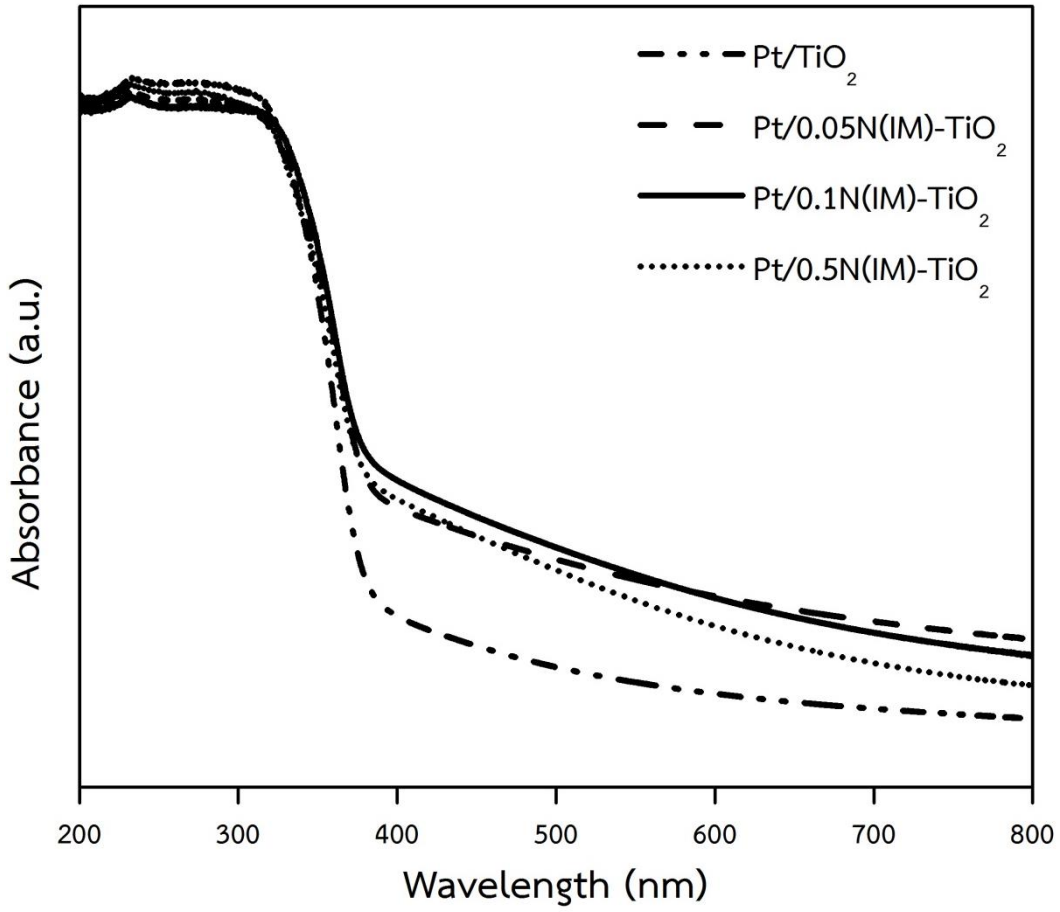

Figure 5.28 UV–visible of Pt/N(IM)-TiO_2

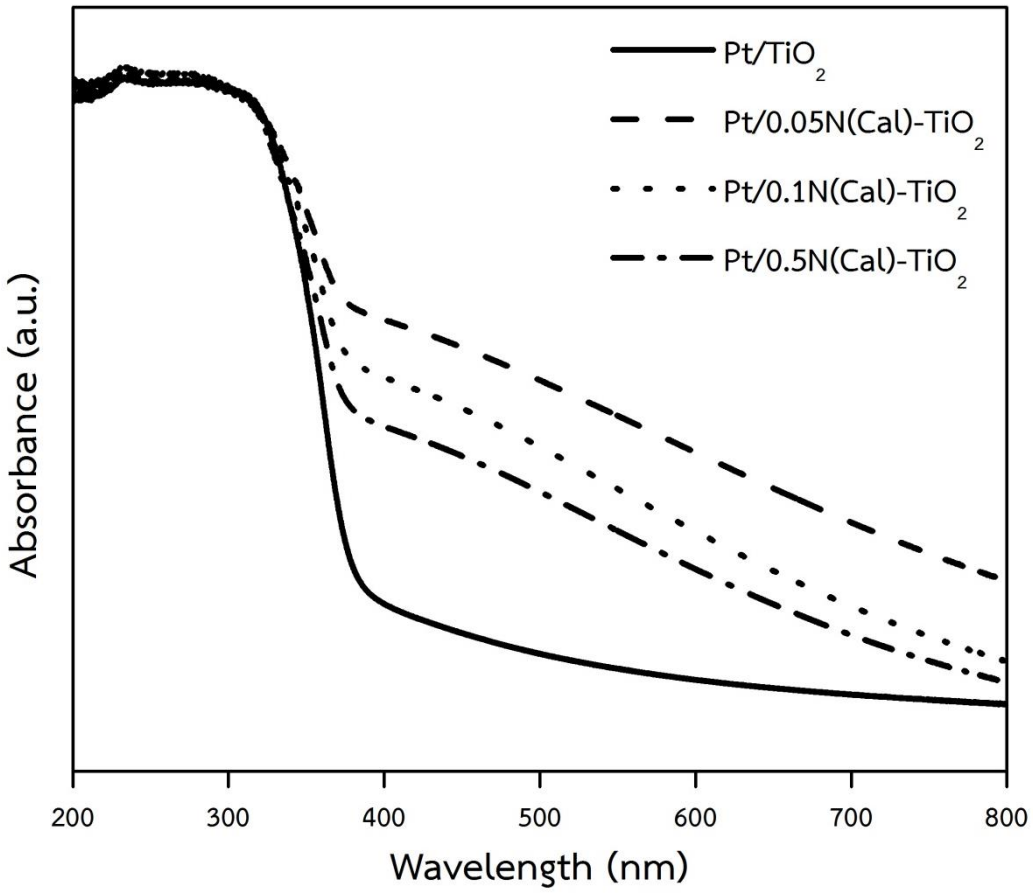

Figure 5.29 UV–visible of Pt/N(Cal)-TiO_2

จุฬาลงกรณ์มหาวิทยาลัย
Chulalongkorn University

5.2.1.4 X-ray photoelectron spectroscopy (XPS)

The chemical states of Pt/N-TiO_2 catalysts were examined by X-ray photoelectron spectroscopy to describe the relation between nitrogen and TiO_2 support and the characteristic of platinum and nitrogen species interaction with TiO_2 support on the samples. The XPS binding energy of N 1s peak is shown as a broad peak around 400 eV which could be originated from the nitrogen species bound to various surface oxygen sites [12, 14, 23, 26, 43, 45]. The first major peak around 400 eV was attributed to presence of interstitial N state and the oxidized nitrogen of Ti-O-N which were chemically adsorbed on the catalysts surface [12, 14, 23, 37, 43]. The second peak around 404-406 eV was assigned to nitrogen species bound to various

surface oxygen sites either NO or NO_2. And the broad peak around 396-397 eV can be attributed to N replacing oxygen in the TiO_2 to form Ti-N bond [24, 38, 40, 43].

The N 1s XPS spectra of Pt/N-TiO_2 were shown as two main peaks and are illustrated in **Figure 5.30 – 5.32**. The binding energies of Pt/N(SV)-TiO_2 appeared around 400 and 405 eV. The Pt/0.1N(SV)-TiO_2 showed the highest XPS intensity of N 1s species and was not found in Pt/0.05N(SV)-TiO_2. The Pt/TiO_2 showed the N 1s XPS spectra at 402 eV which it referred to the decomposition and oxidation of nitrogen precursor [46]. The Pt/0.05N(SV)-TiO_2 and Pt/0.5N(SV)-TiO_2 showed the binding energies around 396 eV. Moreover, the XPS spectra around 405 eV was corresponded to nitrogen species on surface oxygen sites which Pt/0.1N(SV)-TiO_2 represented higher XPS intensity than other catalyst in solvothermal method. These results were respected to Ti-O-N and Ti-N bond in Pt/0.1N(SV)-TiO_2 and both of Pt/0.05N(SV)-TiO_2 and Pt/0.5N(SV)-TiO_2, respectively. The various amount of nitrogen in solvothermal method did not significantly effect on catalyst. For Pt/N(IM)-TiO_2, the N 1s XPS spectra of Pt/0.05N(IM)-TiO_2 and Pt/0.5N(IM)-TiO_2 showed the highest intensity but there were not significant differences for Pt/0.1N(IM)-TiO_2. The Ti-N-O bond may be formed on Pt/0.05N(IM)-TiO_2 and Pt/0.5N(IM)-TiO_2. However, XPS spectra of Pt/0.1N(IM)-TiO_2 showed only Ti-N bond at 396 eV. Considering the Pt/N(Cal)-TiO_2, the highest XPS spectra of Pt/0.1N(Cal)-TiO_2 around 397 and 400 eV was appeared, showing the Ti-N and Ti-N-O bond, respectively. Pt/0.05N(Cal)-TiO_2 and Pt/0.5N(Cal)-TiO_2 showed all of three main peaks. But the XPS intensity of Pt/0.05N(Cal)-TiO_2 was not significant with Pt/TiO_2. Thus, all the methods with various amounts of nitrogen had no significant on the formation of Ti-N and Ti-O-N bond but they affected the nitrogen species on surface oxygen sites.

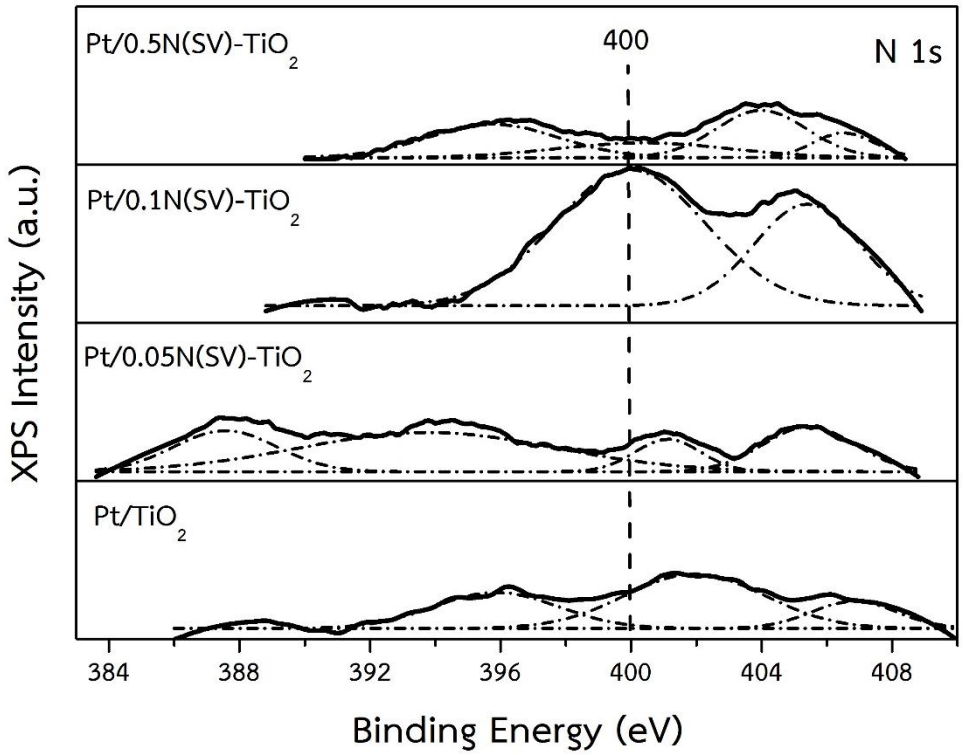

Figure 5.30 XPS spectra for N1s of Pt/N(SV)-TiO_2

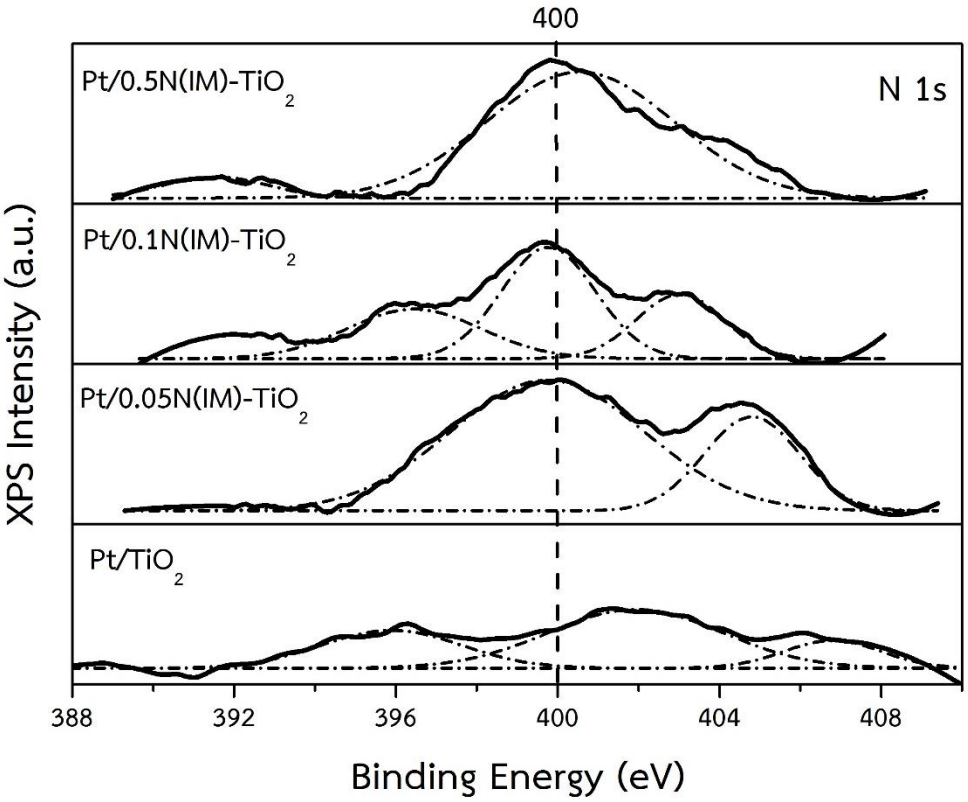

Figure 5.31 XPS spectra for N1s of Pt/N(IM)-TiO_2

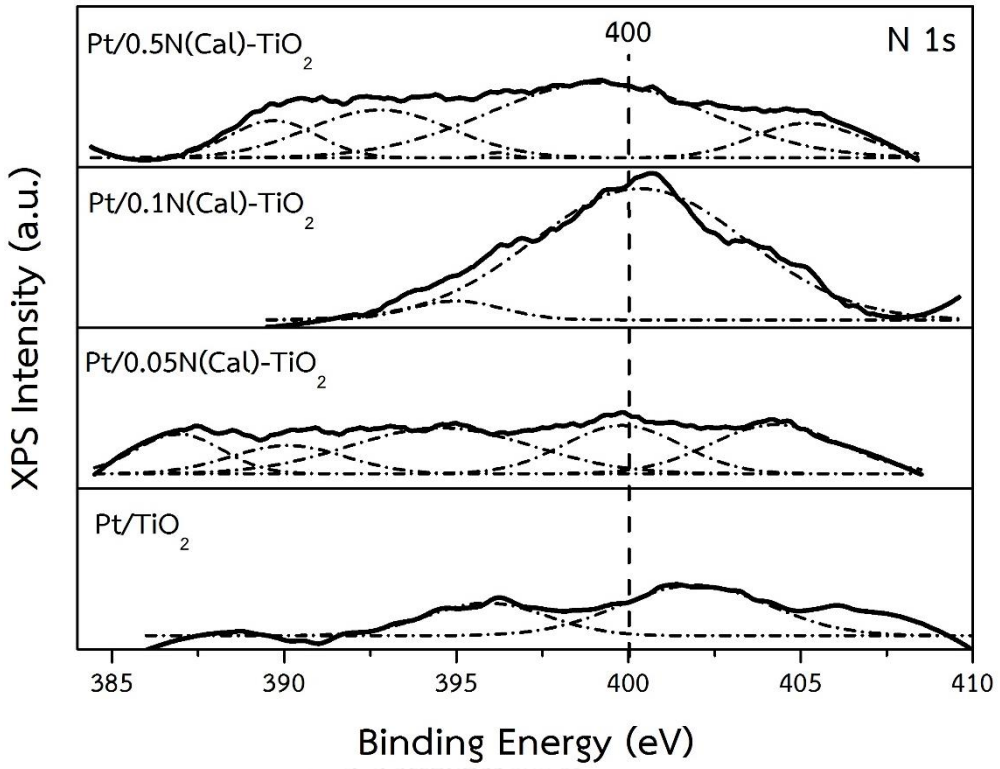

Figure 5.32 XPS spectra for N1s of Pt/N(Cal)-TiO_2

The oxidation state of platinum can be examined by XPS technique. Generally, the metallic platinum binding energies were consisted two main peaks which represented Pt^0, Pt^{2+}, and Pt^{4+} as follows by the first peak was assigned to $4f_{7/2}$ electrons around 70–71, 72–73 and 74–75 eV , respectively [12-14, 35]. The second peak was related to $4f_{5/2}$ electrons around 74, 76, and 77–78 eV, respectively. Pt/TiO2 showed the binding energy of platinum around 74 and 78 eV. All of Pt/N-TiO_2 oxidation states are shown in **Figure 5.33-5.35**. Two major peaks, the first around 73.1 - 73.9 eV and the second peak around 76.3 - 76.8 eV were attributed to oxidized platinum and Pt^{2+} species, respectively [14, 43, 47]. The Pt/N-TiO_2 was reduced with H_2 treatment so that Pt^{2+} was changed to Pt^0 species. At 0.1 N/Ti ratio, the highest XPS intensity for Pt 4f was observed, which related to more Pt particles on the catalyst surface.

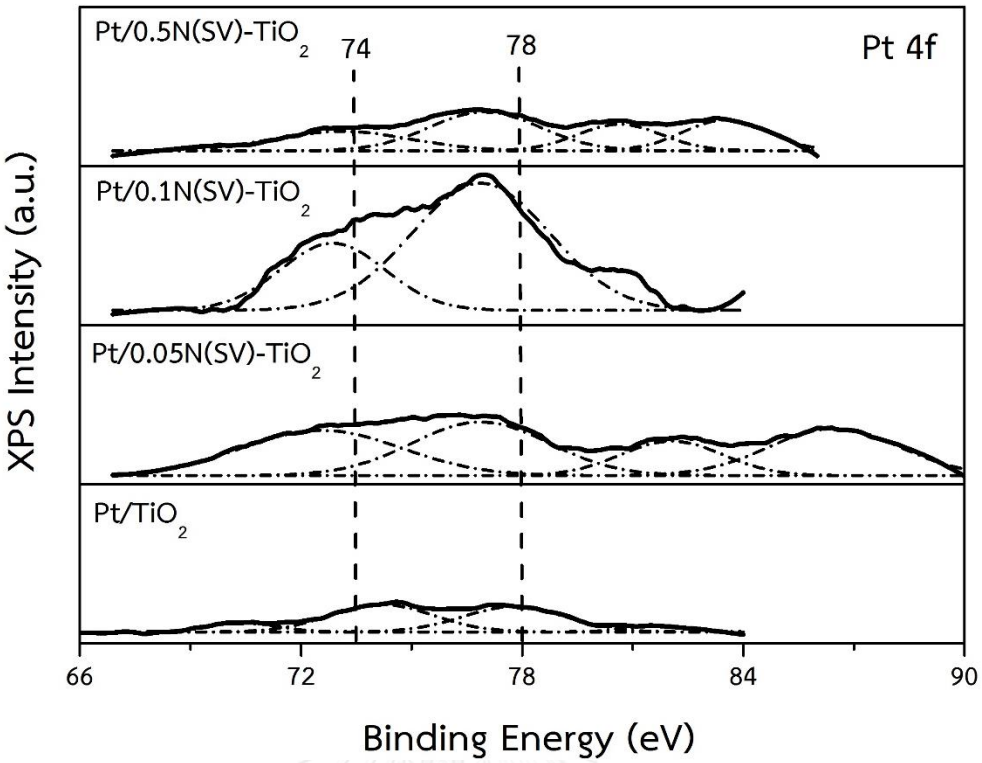

Figure 5.33 XPS spectra for Pt 4f of Pt/N(SV)-TiO_2

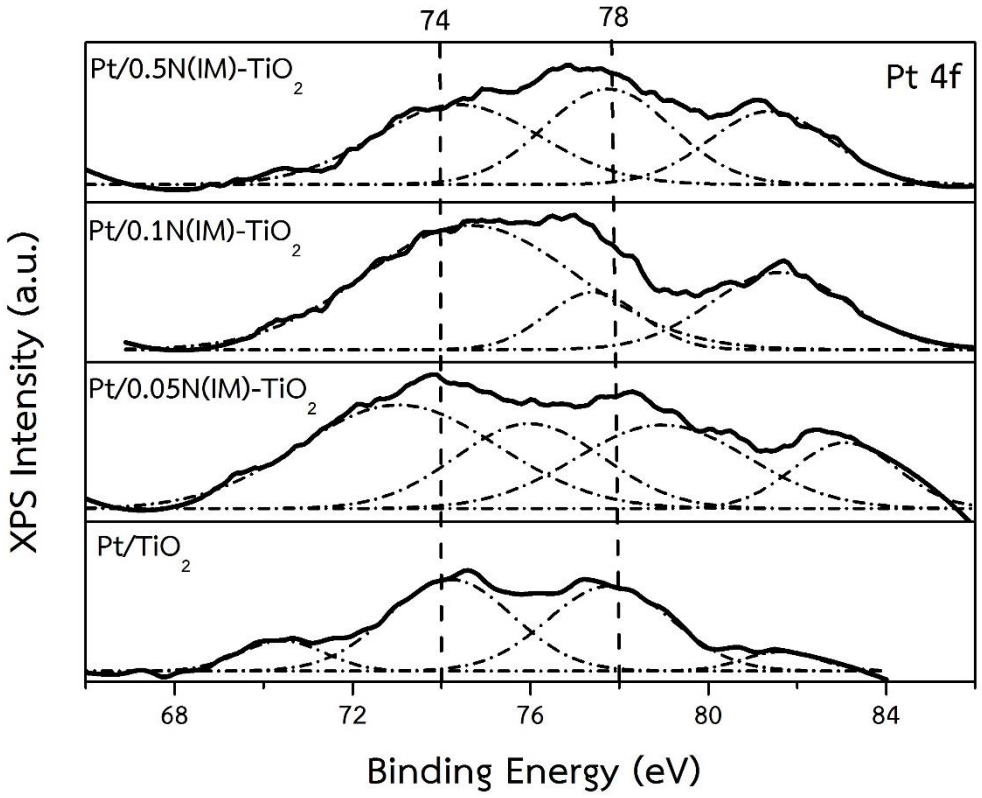

Figure 5.34 XPS spectra for Pt 4f of Pt/N(IM)-TiO_2

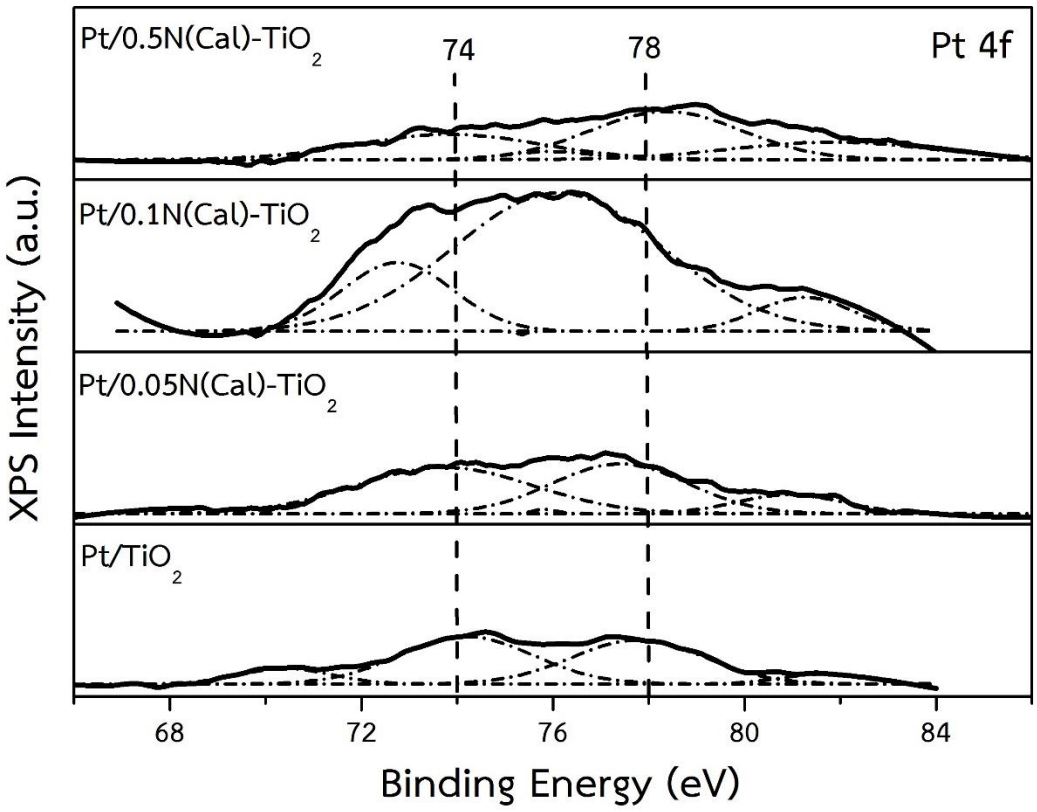

Figure 5.35 XPS spectra for Pt 4f of Pt/N(Cal)-TiO_2

5.2.1.5 H_2-temperature-programmedreduction (H_2-TPR)

The temperature-programmed reduction was investigated by H_2-TPR measurements. The catalysts exhibited two hydrogen consumption peaks around 350 and 450 °C. The first peak was the reduction of Pt oxide particles and the second peak was attributed to reduction of Pt species interacting with the TiO_2 support in the form of Pt-TiO_x interface sites [3, 27].

The reduction profiles of Pt/N(SV)-TiO_2 catalysts are shown in **Figure 5.36**. The reduction profiles showed a stronger metal-support interaction as they exhibited higher reduction temperature peaks compared to the reduction peak of Pt/TiO_2 at 435-463 °C. The reduction peak of Pt/N(SV)-TiO_2 also shifted toward higher temperature with increasing amount of N/Ti ratio. It is suggested that increasing amount of nitrogen on the TiO_2 resulted in the formation of more difficult to reduce Pt-TiO_x species. H_2 consumption of catalyst was calculated by ratio of main peak area and shown in **Table**

5.11. The Pt/Pt-TiO_x ratio was increased with increasing amount of N/Ti ratio. The lower reduction ratio of Pt oxide particle and lower H_2 consumption ratios of Pt/Pt–TiOx than other catalyst confirmed the stronger metal-support interaction of (Pt/0.05N(SV)-TiO_2 > Pt/0.1N(SV)-TiO_2 > Pt/0.5N(SV)-TiO_2). The catalysts with high reduction ratio of Pt oxide particle also showed high amount of Pt particles. Thus, solvothermal method was an affected of Pt species on on catalyst surface.

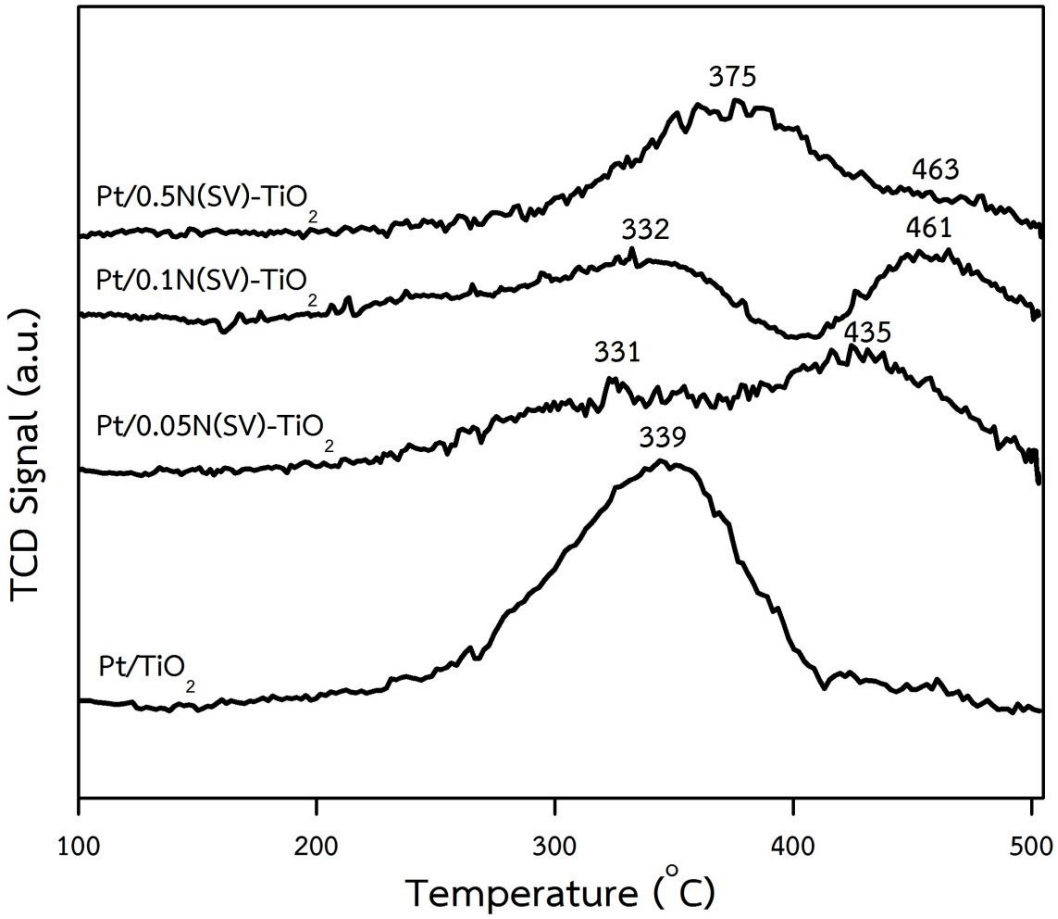

Figure 5.36 H_2-TPR profiles of Pt/N(SV)-TiO_2

Table 5.11 H_2 consumption ratios of Pt/Pt–TiO_x from H_2-TPR profiles of Pt/N(SV)-TiO_2

Catalysts	Reduction ratio of Pt oxide particle	Pt/Pt-TiOx
Pt/TiO_2	1.00	-
Pt/0.05N(SV)-TiO_2	0.47	1.41
Pt/0.1N(SV)-TiO_2	0.20	1.65
Pt/0.5N(SV)-TiO_2	0.35	3.28

The reduction profiles of Pt/N(IM)-TiO_2 catalysts are shown in **Figure 5.37**. The first reduction peak of Pt/N(IM)-TiO_2 was shifted toward higher temperature with increasing amount of N/Ti ratio. It is attributed to nitrogen formation on the TiO_2 more difficult to reduce Pt-TiO_x species. It was obviously observed for the Pt/0.1N(IM)-TiO_2. And the second peak at 443-463 °C indicated to stronger metal-support interaction of catalysts. H_2 consumption of catalyst was calculated by ratio of main peak area which illustrated in **Table 5.12**. It was determined by deconvoluted reduction peak. The reduction ratio of Pt oxide particle was increased with increasing amount of N/Ti ratio, showing higher amount of Pt particles on catalyst surface. However the Pt/Pt-TiO_x ratio was not same trend at low H_2 consumption ratios of Pt/Pt–TiO_x which showed stronger metal-support interaction.

The reduction profiles of Pt/N(Cal)-TiO_2 catalysts are shown in **Figure 5.38**. The reduction first peak of Pt/N(Cal)-TiO_2 was shifted toward higher temperature with increasing amount of N/Ti ratio but not for the Pt/0.5N(Cal)-TiO_2. It is attributed to nitrogen formation on the TiO_2 resulted in more difficult to reduce Pt-TiO_x species which was obviously observed for the Pt/0.1N(Cal)-TiO_2 and corresponded to more nitrogen element inhibited Pt particle attached on catalyst surface. The second reduction peak also indicated the same trend, corresponding to the stronger metal-support interaction of catalysts. H_2 consumption of catalyst was calculated by ratio of main peak area and illustrated in **Table 5.13**. It was determined by deconvoluted

reduction peak. The reduction ratio of Pt oxide particle was not significant different for the various amounts of N/Ti ratio. But the Pt/Pt-TiO_x ratio of Pt/0.05N(Cal)-TiO_2 and Pt/0.5N(Cal)-TiO_2, a similar trend was observed especially at low H_2 consumption ratios of Pt/Pt–TiO_x which showed a stronger metal-support interaction.

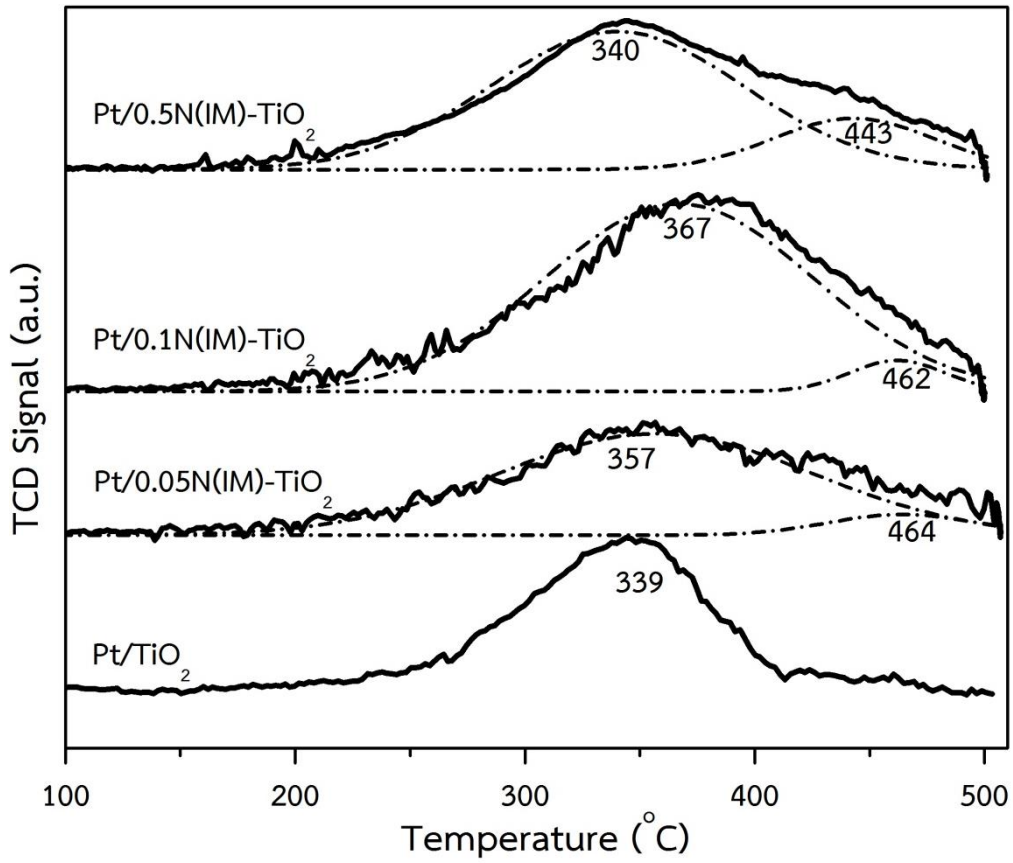

Figure 5.37 H_2-TPR profiles of Pt/N(IM)-TiO_2

Table 5.12 H_2 consumption ratios of Pt/Pt–TiO_x from H_2-TPR profiles of Pt/N(IM)-TiO_2

Catalysts	Reduction ratio of Pt oxide particle	Pt/Pt-TiOx
Pt/TiO_2	1.00	-
Pt/0.05N(IM)-TiO_2	1.13	10.77
Pt/0.1N(IM)-TiO_2	1.34	14.71
Pt/0.5N(IM)-TiO_2	1.39	9.70

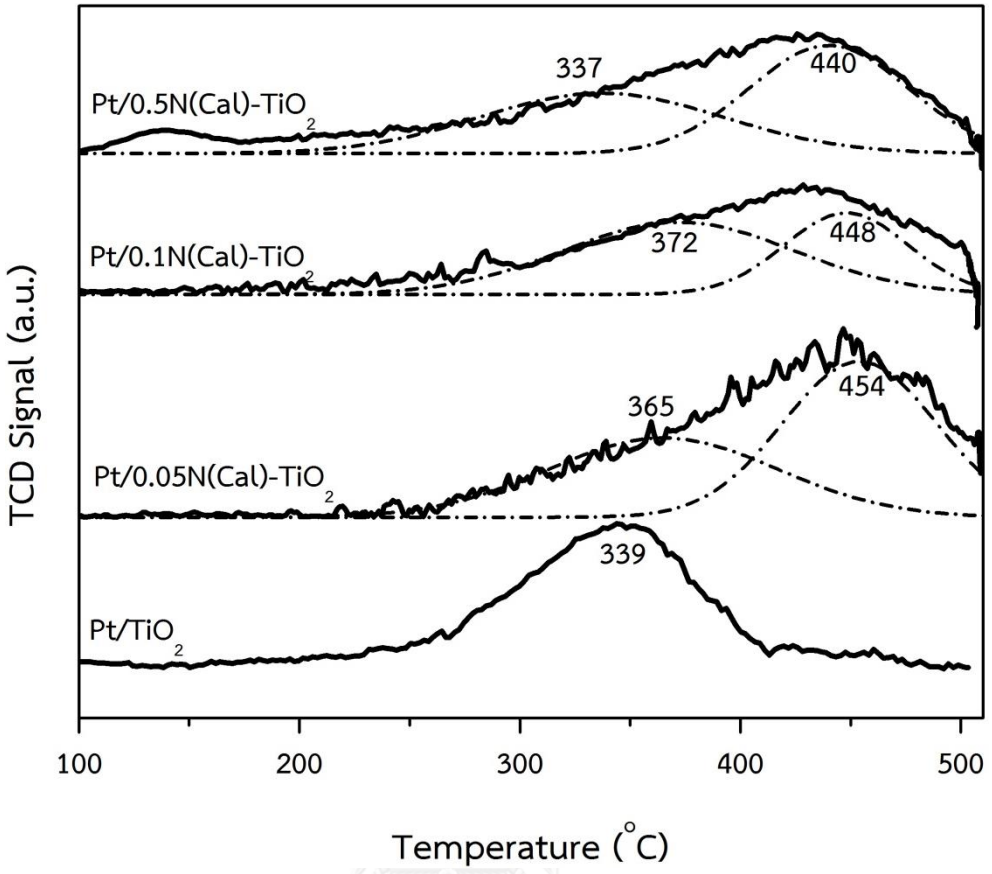

Figure 5.38 H_2-TPR profiles of Pt/N(Cal)-TiO_2

Table 5.13 H_2 consumption ratios of Pt/Pt–TiO_x from H_2-TPR profiles of Pt/N(Cal)-TiO_2

Catalysts	Reduction ratio of Pt oxide particle	Pt/Pt-TiOx
Pt/TiO_2	1.00	-
Pt/0.05N(Cal)-TiO_2	0.65	0.66
Pt/0.1N(Cal)-TiO_2	0.66	1.67
Pt/0.5N(Cal)-TiO_2	0.61	0.70

5.2.1.6 CO chemisorption

Table 5.14 Pt Dispersion (%) of Pt catalysts

Supports preparation	Catalysts	Pt Dispersion (%)
Solvothermal	Pt/TiO_2	68.5
	$Pt/0.05N(SV)-TiO_2$	53.3
	$Pt/0.1N(SV)-TiO_2$	64.1
	$Pt/0.5N(SV)-TiO_2$	47.7
Impregnation without calcination	$Pt/0.05N(IM)-TiO_2$	18.8
	$Pt/0.1N(IM)-TiO_2$	53.5
	$Pt/0.5N(IM)-TiO_2$	40.0
Impregnation with calcination	$Pt/0.05N(Cal)-TiO_2$	12.4
	$Pt/0.1N(Cal)-TiO_2$	13.5
	$Pt/0.5N(Cal)-TiO_2$	13.3

จุฬาลงกรณ์มหาวิทยาลัย
Chulalongkorn University

The amounts of active Pt particles in the present of $Pt/N-TiO_2$ catalysts surface with various amount of nitrogen and different of TiO_2 supports synthesis were based on the assumption that one carbon monoxide molecule adsorbs on one Pt site [3, 27]. The results are shown in **Table 5.14. T**he range of metal dispersion of 12-68 % as determined from CO chemisorption. For a synthesis method used similar trend of Pt dispersion was observed in the order: $Pt/0.1N-TiO_2 > Pt/0.5N-TiO_2 > Pt/0.05N-TiO_2$. The highest Pt dispersion suggested an appropriate amount of N/Ti ratio on catalyst surface

that provided the highest Pt dispersion. And the solvothermal method had higher Pt dispersion than the other methods. However, nitrogen covered on support surface that it was suppressed interaction of Pt particle with N-doped TiO_2. This effect resulted in 0.5 N/Ti ratio and impregnation method.

5.2.2 Catalytic activity

Table 5.15 The catalytic performance of Pt/N(SV)-TiO_2 at reaction conditions: 40 °C, 2 MPa, and 20 minutes

Catalysts	NS conversion	VA selectivity	ENB selectivity	EA selectivity	Intermediate selectivity
Pt/TiO_2	85.9	62.8	17.1	18.7	1.4
Pt/0.05N(SV) - TiO_2	62.0	87.9	4.3	4.7	3.1
Pt/0.1N(SV) - TiO_2	80.8	85.9	0.3	9.9	3.9
Pt/0.5N(SV) - TiO_2	57.5	87.4	4.7	4.8	3.1

จุฬาลงกรณ์มหาวิทยาลัย
Chulalongkorn University

Table 5.16 The catalytic performance of Pt/N(IM)-TiO_2 at reaction conditions: 40 °C, 2 MPa, and 20 minutes

Catalysts	NS conversion	VA selectivity	ENB selectivity	EA selectivity	Intermediate selectivity
Pt/TiO_2	85.9	62.8	17.1	18.7	1.4
Pt/0.05N(IM)-TiO_2	65.2	83.5	5.8	8.1	2.6
Pt/0.1N(IM)-TiO_2	67.6	82.4	7.5	7.8	2.3
Pt/0.5N(IM)-TiO_2	46.7	82.5	6.6	6.9	4.0

Table 5.17 The catalytic performance of Pt/N(Cal)-TiO_2 at reaction conditions: 40 °C, 2 MPa, and 20 minutes

Catalysts	NS conversion	VA selectivity	ENB selectivity	EA selectivity	Intermediate selectivity
Pt/TiO_2	85.9	62.8	17.1	18.7	1.4
Pt/0.05N(Cal)-TiO_2	32.0	39.3	10.3	40.0	10.4
Pt/0.1N(Cal)-TiO_2	34.6	50.6	7.2	29.6	12.7
Pt/0.5N(Cal)-TiO_2	44.3	32.6	9.8	49.0	8.6

Table 5.18 VA yield of Pt/N-TiO_2 prepared by different method with various amount of nitrogen

Catalysts	VA Yield (%)
Pt/TiO_2	54.0
Pt/0.05N(SV)-TiO_2	54.5
Pt/0.1N(SV)-TiO_2	69.4
Pt/0.5N(SV)-TiO_2	50.2
Pt/0.05N(IM)-TiO_2	54.4
Pt/0.1N(IM)-TiO_2	55.7
Pt/0.5N(IM)-TiO_2	38.5
Pt/0.05N(Cal)-TiO_2	12.6
Pt/0.1N(Cal)-TiO_2	17.5
Pt/0.5N(Cal)-TiO_2	14.5

จุฬาลงกรณ์มหาวิทยาลัย
Chulalongkorn University

The catalytic performances of Pt/N-TiO_2 catalysts with different N-doped TiO_2 supports and various amounts of N/Ti ratio in the liquid phase hydrogenation of NS at 40 °C, 2 MPa, and 20 minutes using 50 ml stainless steel autoclave reactor are reported and shown in **Table 5.15 – 5.18**. When considering Pt/N(SV)-TiO_2 catalysts (**Table 5.15**), the highest NS conversion was obtained over the Pt/0.1N(SV)-TiO_2 catalyst which corresponded to the highest Pt dispersion. The highest yield of VA was obtained at this N/Ti ratio. The H_2 TPR profile of Pt/0.1N-TiO_2 indicated that this catalyst reduced at lower temperature and showed strongly interaction of Pt-TiO_x species with the highest peak area at higher temperature, corresponding to the stronger metal-support interaction. Furthermore, the XPS spectra of N and Pt peak showed more Ti-N-O and Pt^{2+} that confirmed the highest NS conversion because nitrogen on support surface could help the hydrogenation of nitro groups and inhibited the hydrogenation of VA to EA. The VA selectivity were not significant different for the other N/Ti ratios. The ENB selectivity of Pt/0.1N(SV)-TiO_2 was lower but the EA selectivity and intermediate selectivity of Pt/0.1N(SV)-TiO_2 were higher than the other N/Ti ratio. These results were related to the NS hydrogenation pathway in as shown **Figure 2.2** that shows Pt/0.1N(SV)-TiO_2 was more selected to VA than ENB. And Pt/0.5N(SV)-TiO_2 shown lowest NS conversion owing to the cover of N-doped inhibited Pt particle attached on support surface which confirm by increasing of the d-spacing in XRD reported and high absorbance of UV-visible.

The catalytic performances of Pt/N(IM)-TiO_2 are in **Table 5.16 and 5.18**. The NS conversion and VA yield showed similar trend as that of Pt/N(SV)-TiO_2 with the Pt/0.1N(IM)-TiO_2 exhibited the highest performance, corresponding to high Pt dispersion from CO-chemisorption. In addition, high Pt oxide particles reduced higher reduction temperature from H_2 –TPR profile. And the XPS spectra at 71.7 eV indicated the Pt^0 species on catalyst surface. These results implied that the higher performance was related to the higher Pt dispersion and the presence of Pt-TiO_x species. The VA selectivity was not significant different due to similar amount of Ti-N-O bond as shown by XPS spectra of N 1s. Nevertheless, the catalytic performance as a NS conversion and VA yield of Pt/0.05N(IM)-TiO_2 were not significant different with Pt/0.1N(IM)-TiO_2 because both could be reduced at low temperature and high Ti-N-O species were

obtained in XPS spectra. The low selectivity of ENB, intermediate, and VA suggest that the presence of nitrogen suppressed hydrogenation of vinyl groups and improved hydrogenation of nitro groups, so that the formation of NS to VA increased. From the H_2 –TPR profile showing the shift of reduction peaks to high temperature, it is suggested that more difficult to catalyst reduction and Pt/Ti-O_x was highly presented.

The catalytic performances of Pt/N(Cal)-TiO_2 are shown in **Table 5.17 and 5.18**. The NS conversion was enhanced which was attributed to increasing amount of nitrogen with increasing N/Ti ratio. It is also confirmed by increasing of crystallite size and UV-visible absorbance of Pt/N(Cal)-TiO_2. The highest selectivity and yield of VA were found for Pt/0.1N(Cal)-TiO_2, corresponding to the highest XPS spectra of N 1s and Pt $4f_{7/2}$ peaks which showed the presence of Ti-N-O bond and more Pt^{2+} species. The Pt/N(Cal)-TiO_2 showed the lowest activity which attributed to low Pt dispersion. From the H_2-TPR profile was reported that the reduction temperature was shifted to high temperature with increasing N/Ti ratio by this method. It could be implied that more difficult to catalyst reduction. When the Pt/N(Cal)-TiO_2 compared with the other methods, the ENB selectivity was not significantly changed. And the VA selectivity decreased but the intermediate selectivity and the EA selectivity were increased. These results suggested that impregnation with calcination method had an effect on the hydrogenation of nitro groups as well as hydrogenation of vinyl groups and amount of Pt particle attached on support surface which indicating not significant difference in Pt dispersion.

CHAPTER 6

CONCLUSIONS AND RECOMMENDATIONS

The effects of the synthesis methods of the N-doped TiO_2 supports and the amounts of NMP in the N-doped TiO_2 were investigated in the liquid-phase selective hydrogenation of 3-nitrostyrene to 3-vinylaniline. The conclusions and recommendations are given below.

6.1 Conclusions

Based on the XPS results, adding NMP on TiO_2 during the solvothermal or impregnation resulted in the formation of Ti-O-N. The H_2-TPR results suggest presence of the strong metal-support interaction and the Pt-TiO_x species. The higher amount of N was obtained by impregnation method, compared to the solvothermal synthesis. The UV-visible and FT-IR spectroscopy results also confirmed the incorporation of N in the TiO_2 lattice. The catalysts exhibited higher reduction temperature with increased amounts of N/Ti ratio. The CO-IR adsorption band showed the CO linearly absorbance on low-coordination Pt atom on edge site. TEM micrographs indicated small Pt particles and Pt oxidation state of Pt^{2+} species.

The Pt/N-TiO_2 exhibited higher selectivity of VA in the hydrogenation of NS due to the stronger metal-support interaction and probably the promotion of electron transfer from TiO_2 support to Pt metal, which improved the hydrogenation of the NO_2 group. Increasing the amount of N/Ti ratio did not significantly affect the performance of catalysts. The Pt/N(SV)-TiO_2 catalyst showed the best catalyst performance in the liquid phase hydrogenation of NS with high catalytic activity and high VA selectivity.

6.2 Recommendations

1) The nitrogen doping using another solution such as NH_3, NH_4NO_3 and NH_4Cl as nitrogen source via the solvothermal method and/or impregnation should be studied.

2) The electron transfer from N to Pt and the changes of polar when presented of N-doped TiO_2 was presented should be investigated.

3) The catalysts could be reduced at 300-500 ^{o}C in order investigate the effect of strong metal support interaction on the catalytic behavior of the Pt/N-doped TiO_2 catalyst comparing to the Pt/TiO_2 catalyst in the liquid phase selective hydrogenation of NS.

จุฬาลงกรณ์มหาวิทยาลัย
Chulalongkorn University

REFERENCES

[1] Boronat, M., Concepcio, P., Corma, A., Gonza, S., Illas, F., and Serna, P. A Molecular Mechanism for the Chemoselective Hydrogenation of Substituted Nitroaromatics with Nanoparticles of Gold on TiO_2 Catalysts: A Cooperative Effect between Gold and the Support. J. AM. CHEM. SOC 129 (2007): 16230-16237.

[2] Makosch, M., et al. Organic Thiol Modified Pt/TiO_2 Catalysts to Control Chemoselective Hydrogenation of Substituted Nitroarenes. ACS Catal. 2 (2012): 2079–2081.

[3] Pisduangdaw, S., Mekasuwandumrong, O., Yoshida, H., Fujita, S.-I., Arai, M., and Panpranot, J. Flame-made Pt/TiO_2 catalysts for the liquid-phase selective hydrogenation of 3-nitrostyrene. Applied Catalysis A: General 490 (2015): 193-200.

[4] Serna, P., Concepción, P., and Corma, A. Design of highly active and chemoselective bimetallic gold–platinum hydrogenation catalysts through kinetic and isotopic studies. Journal of Catalysis 265 (2009): 19-25.

[5] Shimizu, K.-i., Miyamoto, Y., Kawasaki, T., Tanji, T., Tai, Y., and Satsuma, A. Chemoselective Hydrogenation of Nitroaromatics by Supported Gold Catalysts: Mechanistic Reasons of Size- and Support-Dependent Activity and Selectivity. J. Phys. Chem. C 113(41) (2009): 17803–17810.

[6] Yoshida, H., et al. Hydrogenation of Nitrostyrene with a Pt/TiO_2 Catalyst in CO_2-Dissolved Expanded Polar and Nonpolar Organic Liquids: Their Macroscopic and Microscopic Features. J. Phys. Chem. C 115 (2011): 2257–2267.

[7] Beier, M.J., Andanson, J.-M., and Baiker, A. Tuning the Chemoselective Hydrogenation of Nitrostyrenes Catalyzed by Ionic Liquid-Supported Platinum Nanoparticles. ACS Catalysis 2(12) (2012): 2587-2595.

[8] Furukawa, S., Yoshida, Y., and Komatsu, T. Chemoselective Hydrogenation of Nitrostyrene to Aminostyrene over Pd- and Rh-Based Intermetallic Compounds. ACS Catal. 4 (2014): 1441–1450.

[9] Comsup, N., Panpranot, J., and Praserthdam, P. The effect of phosphorous precursor on the CO oxidation activity of P-modified TiO_2 supported Ag catalysts. Catalysis Communications 11(15) (2010): 1238-1243.

[10] Comsup, N., Panpranot, J., and Praserthdam, P. The influence of Si-modified TiO_2 on the activity of Ag/TiO_2 in CO oxidation. Journal of Industrial and Engineering Chemistry 16(5) (2010): 703-707.

[11] Higashimoto, S., Takamatsu, K., Azuma, M., Kitano, M., Matsuoka, M., and Anpo, M. Enhancement of the Photocatalytic Activity Under Visible-Light Irradiation over N-doped TiO_2 Modified by Platinum Chloride. Catalysis Letters 122(1-2) (2007): 33-36.

[12] Higashimoto, S., Ushiroda, Y., Azuma, M., and Ohue, H. Synthesis, characterization and photocatalytic activity of N-doped TiO_2 modified by platinum chloride. Catalysis Today 132(1-4) (2008): 165-169.

[13] Morikawa, T., Ohwaki, T., Suzuki, K.-i., Moribe, S., and Tero-Kubota, S. Visible-light-induced photocatalytic oxidation of carboxylic acids and aldehydes over N-doped TiO_2 loaded with Fe, Cu or Pt. Applied Catalysis B: Environmental 83(1-2) (2008): 56-62.

[14] Sreethawong, T., Laehsalee, S., and Chavadej, S. Use of Pt/N-doped mesoporous-assembled nanocrystalline TiO_2 for photocatalytic H_2 production under visible light irradiation. Catalysis Communications 10(5) (2009): 538-543.

[15] Weerachawanasak, P., Praserthdam, P., Arai, M., and Panpranot, J. A comparative study of strong metal–support interaction and catalytic behavior of Pd catalysts supported on micron- and nano-sized TiO2 in liquid-phase selective hydrogenation of phenylacetylene. Journal of Molecular Catalysis A: Chemical 279(1) (2008): 133-139.

[16] Fujishima, A., N. Rao, T., and Tryk, D.A. Titanium dioxide photocatalysis. Photochemistry and Photobiology C: Photochemistry Reviews 1 (2000): 1-21.

[17] Hashimoto, K., Irie, H., and Fujishima, A. TiO_2 Photocatalysis: A Historical Overview and Future Prospects. Japanese Journal of Applied Physics 44(12) (2005): 8269-8285.

[18] Sathish, M., Viswanathan, B., Viswanath, R.P., and S. Gopinath, C. Synthesis, Characterization, Electronic Structure, and Photocatalytic Activity of Nitrogen-Doped TiO_2 Nanocatalyst. Chem. Mater. 2 17 (2005): 6349-6353.

[19] TAUST, S.J. Strong Metal-Support Interactions. Journal of Catalysis 55(1) (1987): 29-35.

[20] Akira Fujishima, T.N.R., Donald A. Tryk. Titanium dioxide photocatalysis. Journal of Photochemistry and Photobiology C Photochemistry Reviews 1 (2000): 1–21.

[21] C. Martin, V.R., V. Sanchez-Escbano. Surface reactivity and morphology of vanadia-titania catalysts. Surface Science 251(252) (1991): 825-830.

[22] Chen, X. and S. Mao, S. Titanium Dioxide Nanomaterials: Synthesis, Properties, Modifications, and Applications. Chemical Reviews 107 (2007): 2891-2959.

[23] Du, J., et al. A facile method for synthesis of N-doped TiO2 nanooctahedra, nanoparticles, and nanospheres and enhanced photocatalytic activity. Applied Surface Science 273 (2013): 278-286.

[24] Jagadale, T.C., et al. N-Doped TiO_2 Nanoparticle Based Visible Light Photocatalyst by Modified Peroxide Sol-Gel Method. J. Phys. Chem. C 112 (2008): 14595–14602.

[25] Yin, S., Liu, B., Zhang, P., Morikawa, T., Yamanaka, K.-i., and Sato, T. Photocatalytic Oxidation of NOx under Visible LED Light Irradiation over Nitrogen-Doped Titania Particles with Iron or Platinum Loading. J. Phys. Chem. C 112 (2008): 12425–12431.

[26] Zhang, X., et al. Photocatalytic and photoelectrochemical studies on N-doped TiO_2 photocatalyst. Journal of Photochemistry and Photobiology A: Chemistry 202(1) (2009): 39-47.

[27] Pisduangdawa, S., Mekasuwandumrong, O., Fujita, S.-I., Arai, M., Yoshida, H., and Panpranot, J. One step synthesis of Pt–Co/TiO_2 catalysts by flame spray

pyrolysis for the hydrogenation of 3-nitrostyrene. Catalysis Communications 61 (2015): 11-15.

[28] Yoshida, H., Igarashi, N., Fujita, S.-i., Panpranot, J., and Arai, M. Influence of Crystallite Size of TiO_2 Supports on the Activity of Dispersed Pt Catalysts in Liquid-Phase Selective Hydrogenation of 3-Nitrostyrene, Nitrobenzene, and Styrene. Catalysis Letters 145(2) (2014): 606-611.

[29] Ramsurn, H. and Gupta, R.B. Hydrogenation by Nanoparticle Catalysts. (2013): 347-374.

[30] Ishida, T., et al. Preparation of microporous polymer-encapsulated Pd nanoparticles and their catalytic performance for hydrogenation and oxidation. Tetrahedron 70(36) (2014): 6150-6155.

[31] Blaser, H.U.S., U.; Steiner, H. . Aromatic Nitro Compounds: Fine Chemicals through Heterogeneous Catalysis. WileyVCH: Weinheim, 2001.

[32] Shimizu, K.-i., Miyamoto, Y., and Satsuma, A. Size- and support-dependent silver cluster catalysis for chemoselective hydrogenation of nitroaromatics. Journal of Catalysis 270(1) (2010): 86-94.

[33] Serna, P., Boronat, M., and Corma, A. Tuning the Behavior of Au and Pt Catalysts for the Chemoselective Hydrogenation of Nitroaromatic Compounds. Topics in Catalysis 54(5-7) (2011): 439-446.

[34] Campos, C., Torres, C., Oportus, M., Peña, M.A., Fierro, J.L.G., and Reyes, P. Hydrogenation of substituted aromatic nitrobenzenes over 1% 1.0wt.%Ir/ZrO_2 catalyst: Effect of meta position and catalytic performance. Catalysis Today 213 (2013): 93-100.

[35] Yarulin, A., Berguerand, C., Alonso, A.O., Yuranov, I., and Kiwi-Minsker, L. Increasing Pt selectivity to vinylaniline by alloying with Zn via reactive metal–support interaction. Catalysis Today (2015).

[36] Yarulin, A., Berguerand, C., Yuranov, I., Cárdenas-Lizana, F., Prokopyeva, I., and Kiwi-Minsker, L. Pt–Zn nanoparticles supported on porous polymeric matrix for selective 3-nitrostyrene hydrogenation. Journal of Catalysis 321 (2015): 7-12.

[37] M. Sathish, B.V., †R. P. Viswanath, and Chinnakonda S. Gopinath. Synthesis, Characterization, Electronic Structure, and Photocatalytic Activity of Nitrogen-Doped TiO2 Nanocatalyst. American Chemical Society 17(25) (2005): 6349-6353.

[38] Cheng, X., Yu, X., and Xing, Z. Characterization and mechanism analysis of N doped TiO2 with visible light response and its enhanced visible activity. Applied Surface Science 258(7) (2012): 3244-3248.

[39] Weerachawanasak, P., Mekasuwandumrong, O., Arai, M., Fujita, S.-I., Praserthdam, P., and Panpranot, J. Effect of strong metal–support interaction on the catalytic performance of Pd/TiO2 in the liquid-phase semihydrogenation of phenylacetylene. Journal of Catalysis 262(2) (2009): 199-205.

[40] Asahi, R., Morikawa, T., Ohwaki, T., Aoki, K., and Taga, Y. Visible-light photocatalysis in nitrogen-doped titanium oxides. Science 293(5528) (2001): 269-71.

[41] Ilinoiu, E.C., et al. Photocatalytic activity of a nitrogen-doped TiO2 modified zeolite in the degradation of Reactive Yellow 125 azo dye. Journal of the Taiwan Institute of Chemical Engineers 44(2) (2013): 270-278.

[42] Weerachawanasak, P., et al. Surface functionalized TiO2 supported Pd catalysts for solvent-free selective oxidation of benzyl alcohol. Catalysis Today 250 (2015): 218-225.

[43] Yang, G., Jiang, Z., Shi, H., Xiao, T., and Yan, Z. Preparation of highly visible-light active N-doped TiO_2 photocatalyst. Journal of Materials Chemistry 20(25) (2010): 5301.

[44] Jiang, Z., et al. Solvothermal synthesis of N-doped TiO_2 nanotubes for visible-light-responsive photocatalysis. Chem Commun (Camb) (47) (2008): 6372-4.

[45] Yu, X., Wang, Y., Meng, X., and Yang, J. Preparation and characterization of Pd/N codoped TiO_2 photocatalysts with high visible light photocatalytic activity. Chinese Journal of Catalysis 34(7) (2013): 1418-1428.

[46] Wang, Q., Yang, X., Wang, X., Huang, M., and Hou, J. Synthesis of N-doped TiO2 mesosponge by solvothermal transformation of anodic TiO2 nanotubes

and enhanced photoelectrochemical performance. Electrochimica Acta 62 (2012): 158-162.

[47] Silvestre-Albero, J. Influence of Zn on the characteristics and catalytic behavior of TiO2-supported Pt catalysts. Journal of Catalysis 223(1) (2004): 179-190.

[48] Ramosfernandez, E., Ferreira, A., Sepulvedaescribano, A., Kapteijn, F., and Rodriguezreinoso, F. Enhancing the catalytic performance of Pt/ZnO in the selective hydrogenation of cinnamaldehyde by Cr addition to the support. Journal of Catalysis 258(1) (2008): 52-60.

[49] Brent Fultz, J.H. Transmission lectron Microscopy and Diffractometry of Materials. 2001, S.-V.B.H., Editor. 2002.

[50] Fujita, S.-i., Watanabe, H., Katagiri, A., Yoshida, H., and Arai, M. Nitrogen and oxygen-doped metal-free carbon catalysts for chemoselective transfer hydrogenation of nitrobenzene, styrene, and 3-nitrostyrene with hydrazine. Journal of Molecular Catalysis A : Chemical 393 (2014): 257–262.

จุฬาลงกรณ์มหาวิทยาลัย
Chulalongkorn University

APPENDIX A

CALCULATION FOR ALL THE CATALYSTS PREPARATION

Preparation of 0.5 wt% catalysts by incipient wetness impregnation method were follows by

- Chloroplatinic acid hexahydrate 37.5% ($H_2PtCl_6 6H_2O$) , MW = 517.90 g/mol
- Titanium dioxide (TiO_2)

Example calculation based on 100 g of catalyst used and the composition of the catalyst was follows by

Platinum = 0.5 g

Then, TiO_2 = (100 – 0.5) g

So, TiO_2 = 99.5 g

For TiO_2 = 1 g

Then, Platinum required = $\frac{(1\,g)\times(0.5\,g)}{(99.5\,g)}$

So, Platinum required = 5.021×10^{-3} g

Platinum 5.021×10^{-3} g was prepared from $H_2PtCl_6 6H_2O$ and molecular weight of Pt is 195.08

$H_2PtCl_6 6H_2O$ required = $\frac{H_2PtCl_6\,6H_2O \times \text{Pt required}}{\text{MW of Pt}}$

Then, $H_2PtCl_6 6H_2O$ required = $\frac{(5.0251\times10^{-3}\,g)\times(517.90\,g/mol)}{(195.08\,g/mol)}$

So, $H_2PtCl_6 6H_2O$ required = 0.0133 g

APPENDIX B

CALCULATION OF NITROGEN DOPED TITANIA

Preparation of N-doped TiO_2 by sovothermal and incipient wetness impregnation method were follows by

- Titanium (IV) n-butoxide 97% (97% $Ti(OCH_2CH_2\ CH_2CH_3)_4$), MW = 340.32 g/mol and density = 1.00 g/ml
- N-metylpyrrolidone 99.5% (99.5% C_5H_9NO), MW = 99.13 g/mol mol and density = 1.03 g/ml

Example calculation based on 0.1 molar ratios of N and Ti

Molar of Titanium (IV) n-butoxide 25 g = $\frac{25\,g}{340.32\,g/mol}$

Molar of Titanium (IV) n-butoxide 25 g = 0.0735 mol

Then, N-metylpyrrolidone 1 mol = 99.13 g

N-metylpyrrolidone 0.0735 mol = 0.7282 g

So, Volume = $\frac{Mass}{Density}$

Volume of N-metylpyrrolidone required = $\frac{0.7282\,g}{1.03\,g/ml}$

Volume of N-metylpyrrolidone required = 0.71 ml

จุฬาลงกรณ์มหาวิทยาลัย
Chulalongkorn University

APPENDIX C

CALCULATION OF CO CHEMISORPTION

The platinum metal active sites and the catalyst dispersion measured by CO adsorption and calculations were follows by

Calculation of the platinum metal active sites

Let the weight of catalyst used	=	W	g
Integral area of CO peak after adsorption	=	A	unit
Integral area of 20 µl of standard CO peak	=	B	unit
Amounts of CO adsorbed on catalyst	=	B-A	unit
Volume of CO adsorbed on catalyst	=	20 [(B-A)/B]	µl
Volume of 1 mole of CO at 30°C	=	24.86×10^{6}	µl

Mole of CO adsorbed on catalyst = $\left[\frac{B - A}{B}\right] \times \left[\frac{20}{24.86 \times 10^{6}}\right]$ mole

Molecule of CO adsorbed on catalyst = $\frac{[8.05 \times 10^{-7}] \times [6.02 \times 10^{23}] \times [B - A]}{B}$

molecules Metal active sites = $4.84 \times 10^{16} \times \left[\frac{B - A}{B}\right] \times \left[\frac{1}{W}\right]$ molecules of CO/g of catalyst

Calculation of metal dispersion

$$\text{Metal dispersion (\%)} = 100 \times \frac{\text{molecule of Pt from CO adsorption}}{\text{molecule of Pt loaded}}$$

Thus, the formula of metal dispersion

$$\%D = S_f \times \frac{V_{ads}}{V_g} \times \frac{M.W.}{\%M} \times 100\,\% \times 100\,\% \qquad (1)$$

Where $\%D$ = % Pt metal dispersion

S_f = stoichiometry factor, (CO : Pt = 1)

V_{ads} = volume of chemisorbed (cm^3/g)

V_g = molar volume of gas at STP = 22,414 (cm^3/mol)

M.W. = molecular weight of platinum (a.m.u.)

$\%M$ = weight percent platinum loading

Calculation of Volume chemisorbed

$$V_{ads} = \frac{V_{inj}}{M} \times \sum_{i=1}^{n} \left(1 - \frac{A_i}{A_f}\right) \quad (2)$$

Where V_{ads} = volume of chemisorbed (cm^3)

V_{inj} = volume injected = 0.02 cm^3

M = mass of catalyst sample (g)

A_f = area of peak last peak

A_i = area of peak i

i = start at this value

n = go to this value

จุฬาลงกรณ์มหาวิทยาลัย
Chulalongkorn University

For example: Pt/TiO_2

Where V_{inj} = 20 µl

M = 0.0516 g

i = 1

n = 8

No. peak	A_i	$\frac{A_i}{A_f}$	$1 - \frac{A_i}{A_f}$
1	0.015	0.43	0.57
2	0.026	0.74	0.26
3	0.030	0.85	0.15
4	0.033	0.93	0.07
5	0.033	0.97	0.03
6	0.035	0.98	0.02
7	0.035	0.99	0.01
8	0.035	1	0
Sum			1.11

Thus, $\sum_{i=1}^{8}\left(1 - \frac{A_i}{A_f}\right) = 1.11$

Replaced the values into equation (1) and (2)

Eq. (2)

$$V_{ads} = \frac{0.02}{0.055\ g} \times 1.11$$

$$V_{ads} = 0.40\ cm^3$$

Eq. (1)

$$\%\ D = 1 \times \frac{0.40\ cm^3}{22{,}414\ cm^3/mole} \times \frac{195.08\ g/mole}{0.5\ \%} \times 100\ \% \times 100\ \%$$

So, $\%\ D = 68.53\ \%$

APPENDIX D

CALCULATION OF THE 3-NITROSTYRENE CONVERSION, PRODUCT SELECTIVITY AND YIELD

Calculation of 3-nitrostyrene conversion, 3-vinylaniline selectivity, 3-vinylaniline yield and are defined as follow by

$$\%\ \text{conversion of 3 - NS} = \frac{(\text{mole of 3 - NS in feed}) - (\text{mole of 3 - NS in product})}{\text{mole of 3 - NS in feed}} \times 100$$

$$\%\ \text{selectivity of 3 - VA} = \frac{\text{mole of 3 - VA}}{\text{total mole of products}} \times 100$$

$$\%\ \text{Yield of 3 - VA} = \frac{\%\ \text{conversion of 3 - NS x \% selectivity of 3 - VA}}{100}$$

จุฬาลงกรณ์มหาวิทยาลัย
Chulalongkorn University

APPENDIX E

CALCULATION OF THE CRYSTALLITE SIZE

Calculation of the crystallite size was from the half-height width of the diffraction peak of XRD pattern using the Debye-Scherrer equation.

$$D = \frac{\kappa\lambda}{\beta \cos\theta}$$

Where D = Crystallite size, Å

κ = Crystallite-shape factor = 0.9

λ = X-ray wavelength, 1.54056 Å for CuKα

θ = Observed peak angle

β = X-ray diffraction broadening, radian

The X-ray diffraction broadening is the pure width of powder diffraction free from all broadening due to the experimental equipment. Corundum was used as a standard sample to observe the instrumental broadening [42]. The X-ray diffraction broadening can be followed by using Warren's formula.

$$\beta = \sqrt{B_M^2 - B_S^2}$$

Where B_M = The measured peak width in radians at half peak height

B_S = The corresponding width of the standard material

Example

The half-height width of peak = 0.66° (from figure D.1)

= $(2\pi \times 0.66)/360$

= 0.01152 radian

The corresponding half-height width of peak of corundum = 0.000915 radian

Replaced the values into Warren's formula equation

$$\beta = \sqrt{B_M^2 - B_S^2}$$

$$\beta = \sqrt{0.01152_M^2 - 0.000915_S^2}$$

β = 0.0115 radian

Replaced the values into the Debye-Scherrer equation

$$D = \frac{0.9 \times 1.54056}{0.0115 \cos 12.66}$$

$$D = 123.37 \text{ Å}$$

$$D = 12.4 \text{ nm}$$

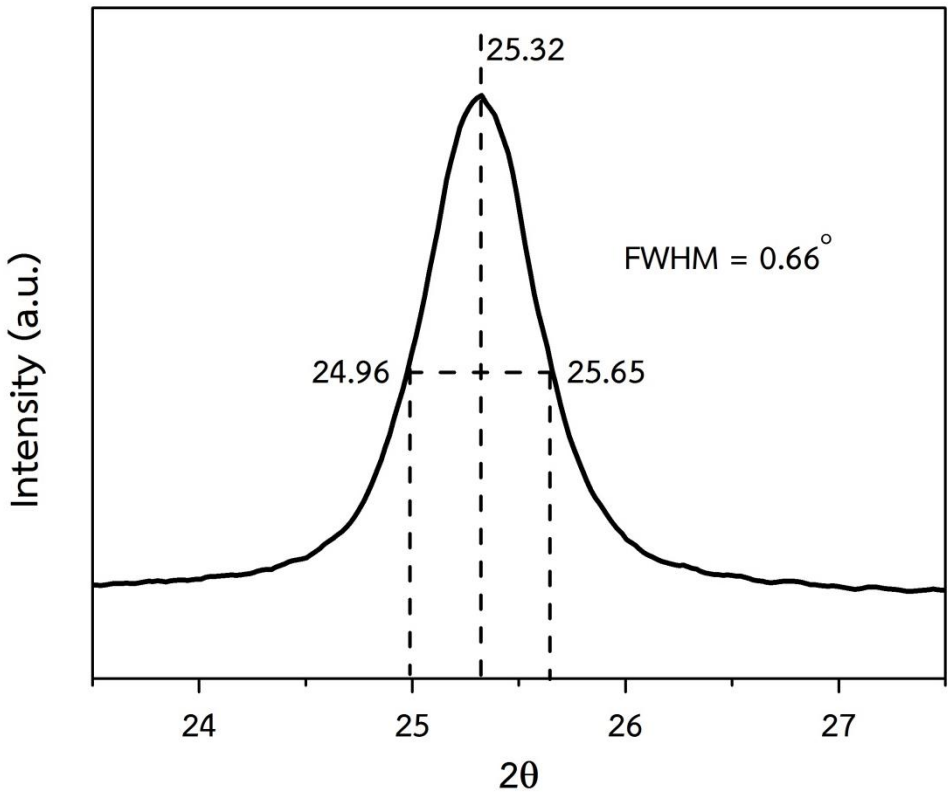

Figure E.1 The measured peak of TiO_2 for calculation the crystallite size

APPENDIX F

CALCULATION FOR OF THE PARTICLE SIZE FROM TEM MICROGRAPHS

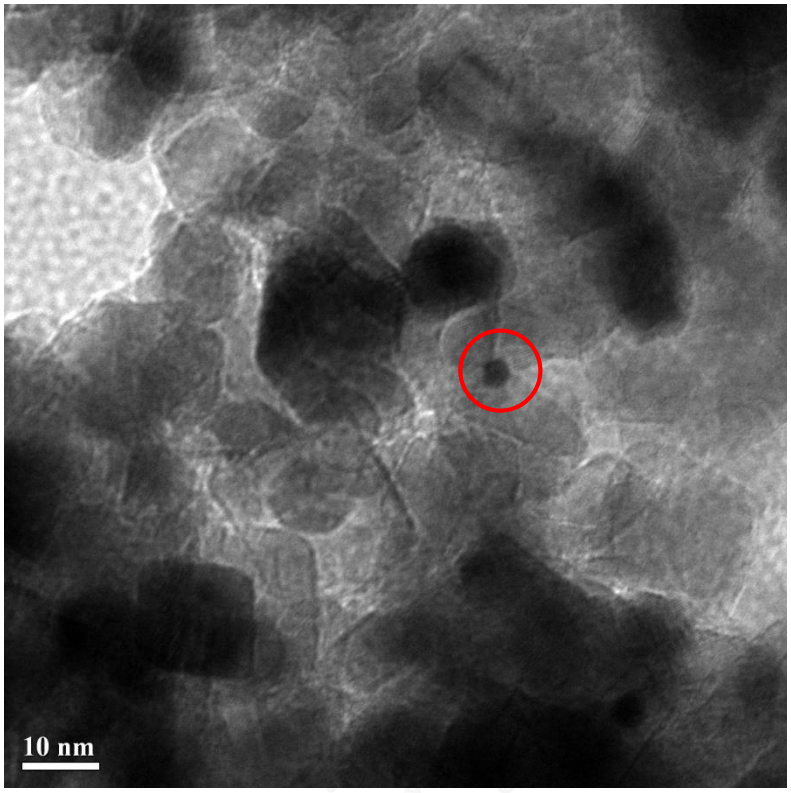

จุฬาลงกรณ์มหาวิทยาลัย
Chulalongkorn University

Figure F.1 TEM micrographs of Pt/TiO_2 catalyst

Example

Calculation of the particle size was determined by calibrated the object and scale bar from TEM micrographs in same unit (cm). Then the value of calibration was substituted in the equation as a follows by

$$\text{Particle size (nm)} = \frac{\text{Object scale (cm)} \times \text{Magnification of TEM (nm)}}{\text{Scale bar (cm)}}$$

$$\text{Particle size (nm)} = \frac{0.30\,\text{(cm)} \times 10\,\text{(nm)}}{0.95\,\text{(cm)}}$$

$$\text{Particle size (nm)} = 3.16\,\text{nm}$$

VITA

Mr. Kampanat Nuttabat was born on 28th November 1990, in Loei, Thailand. He graduated Bachelor degree of Chemical Engineering from Silpakorn University, Thailand in May 2013. Since June 2013, he studied Master degree of Engineering from the department of Chemical Engineering, Chulalongkorn University.

The publication of research, characteristics and catalytic properties of Pt/N-doped Titanium dioxide in the liquid-phase selective hydrogenation of 3-nitrostyrene was presented in the 25th TIChE Conference 2015 Pattaya, Thailand, November 8-10, 2015 by oral presentation and "Creating Green Society through Green Process Engineering" as the main topic.

จุฬาลงกรณ์มหาวิทยาลัย
Chulalongkorn University